The Semiconductor Drift Detector (SDD)

The Concept of Semiconductor Drift Detector
History of the development

Transport of charged carriers in thin fully depleted semiconductor detectors in direction parallel to the large surface of the detector.

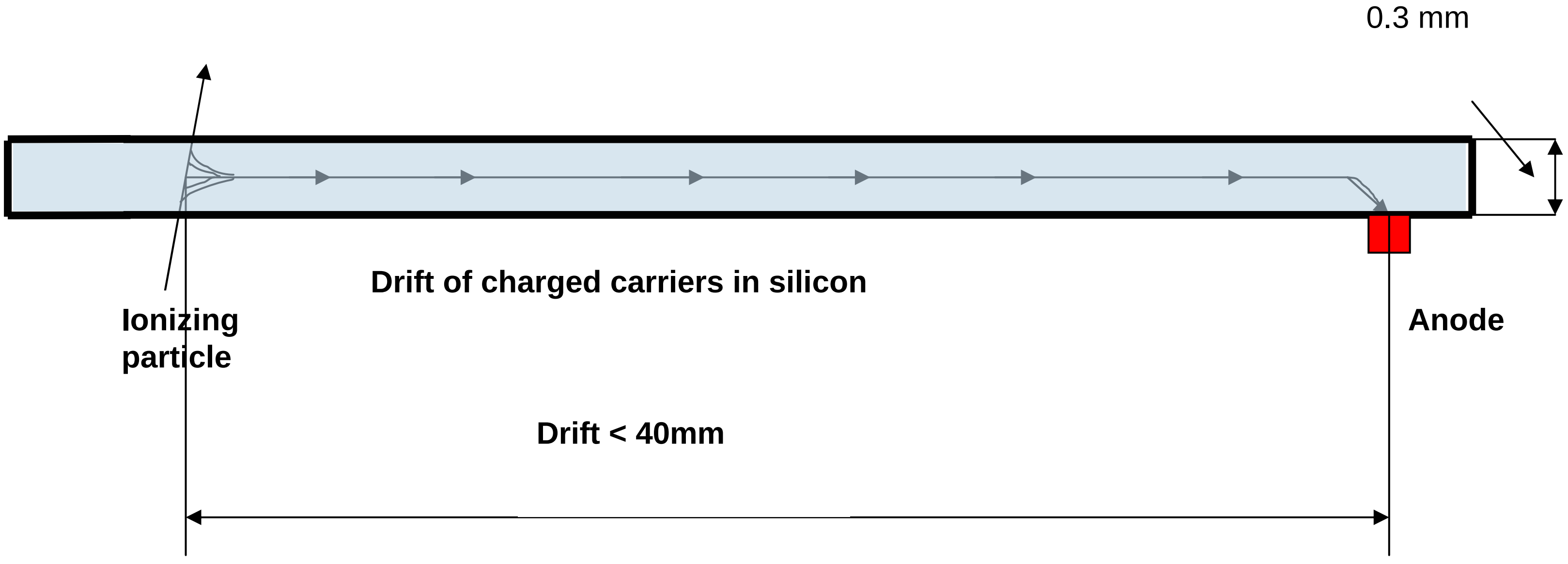

Reverse-biased one sided step p-n junction in 1dimension

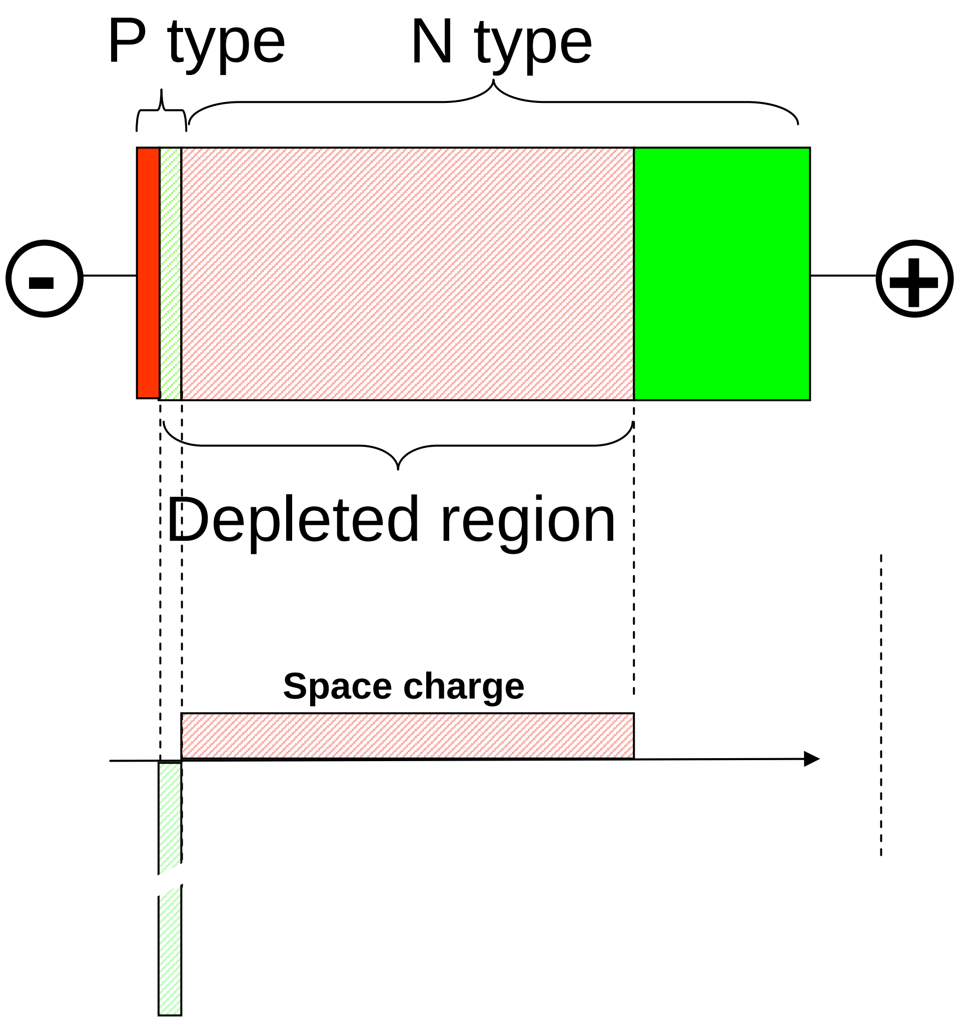

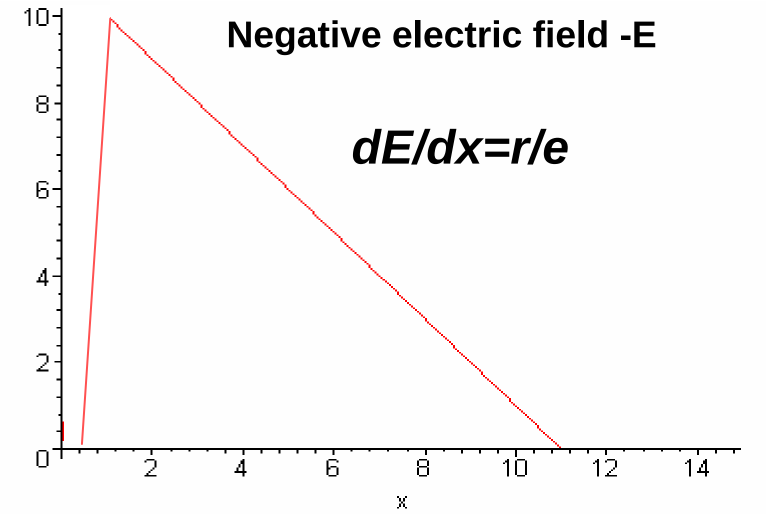

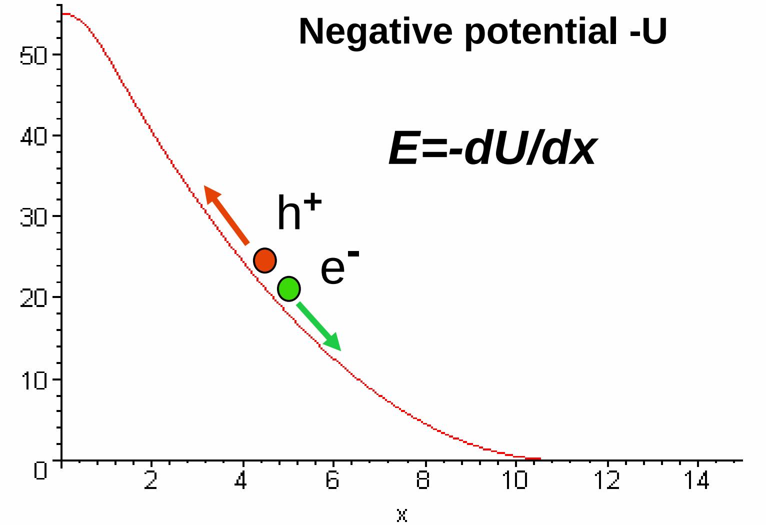

Depletion from two sides

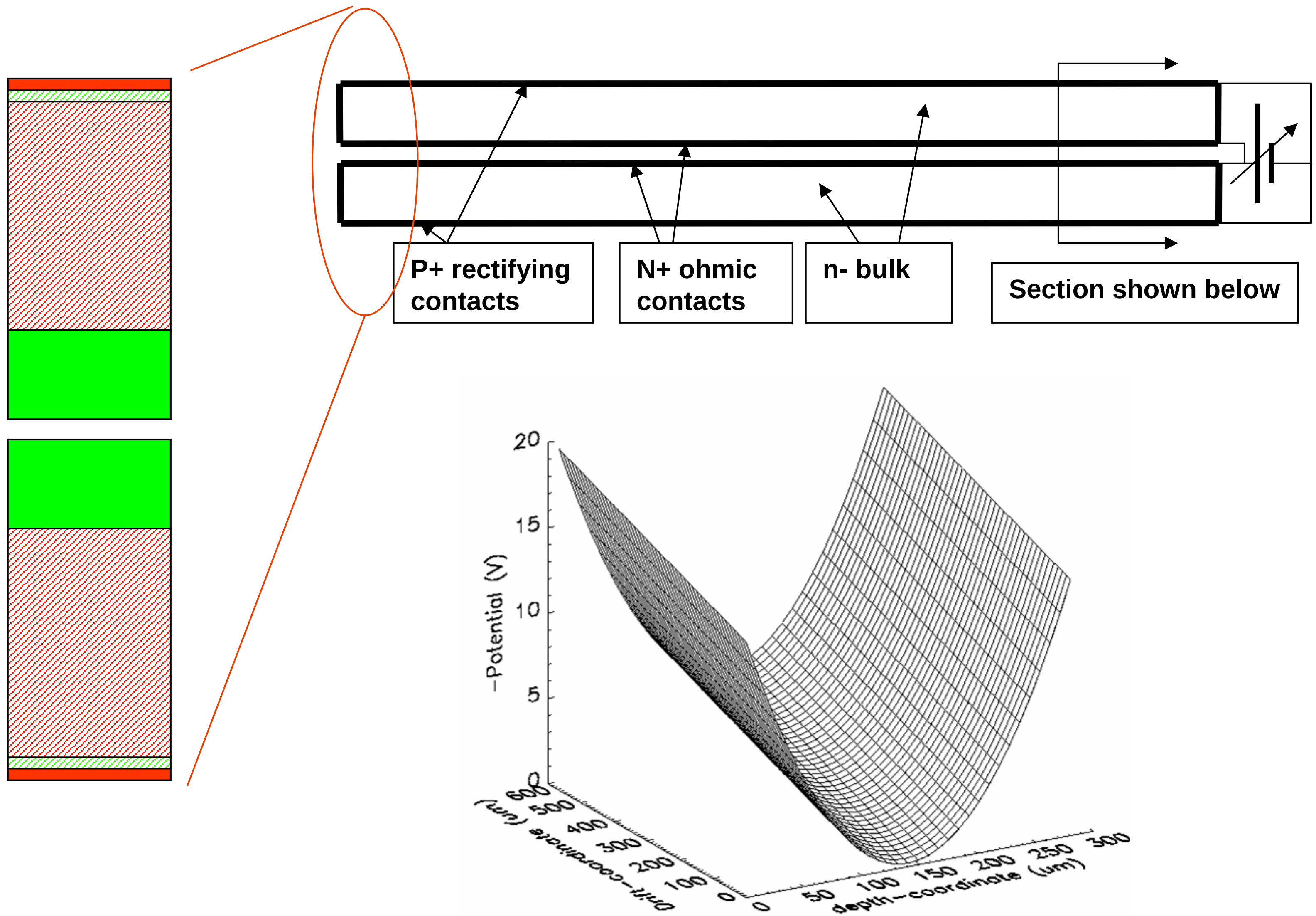

SDD principle

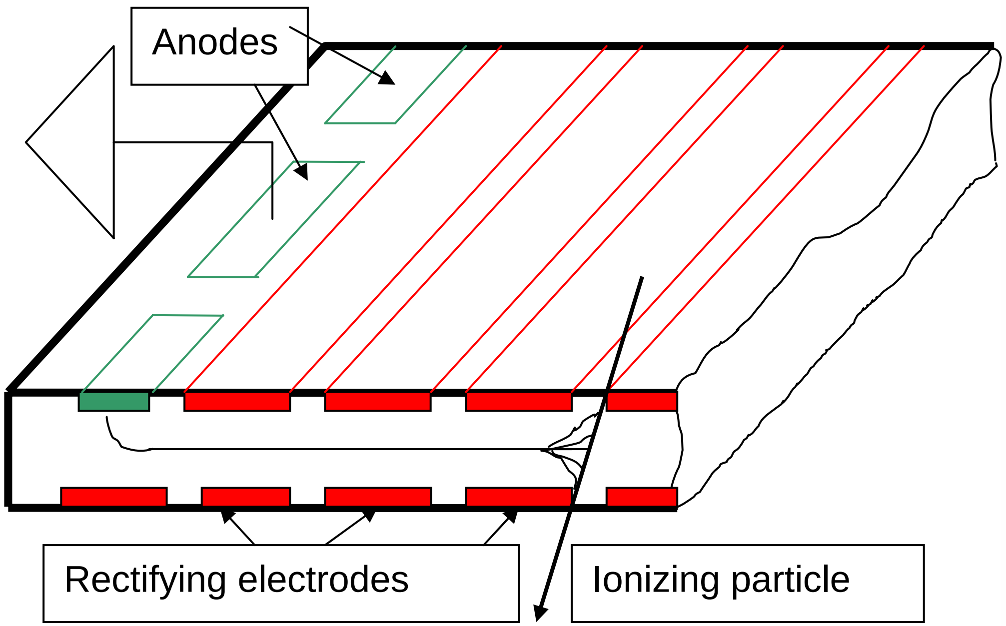

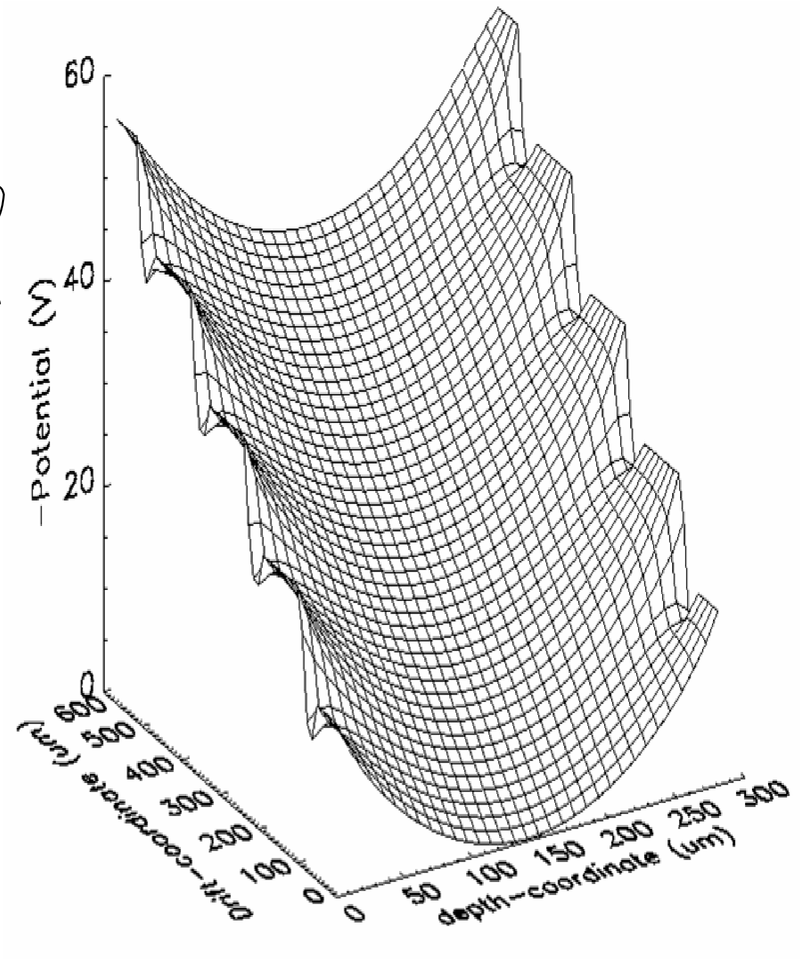

* M f PR t

Low capacitance anode

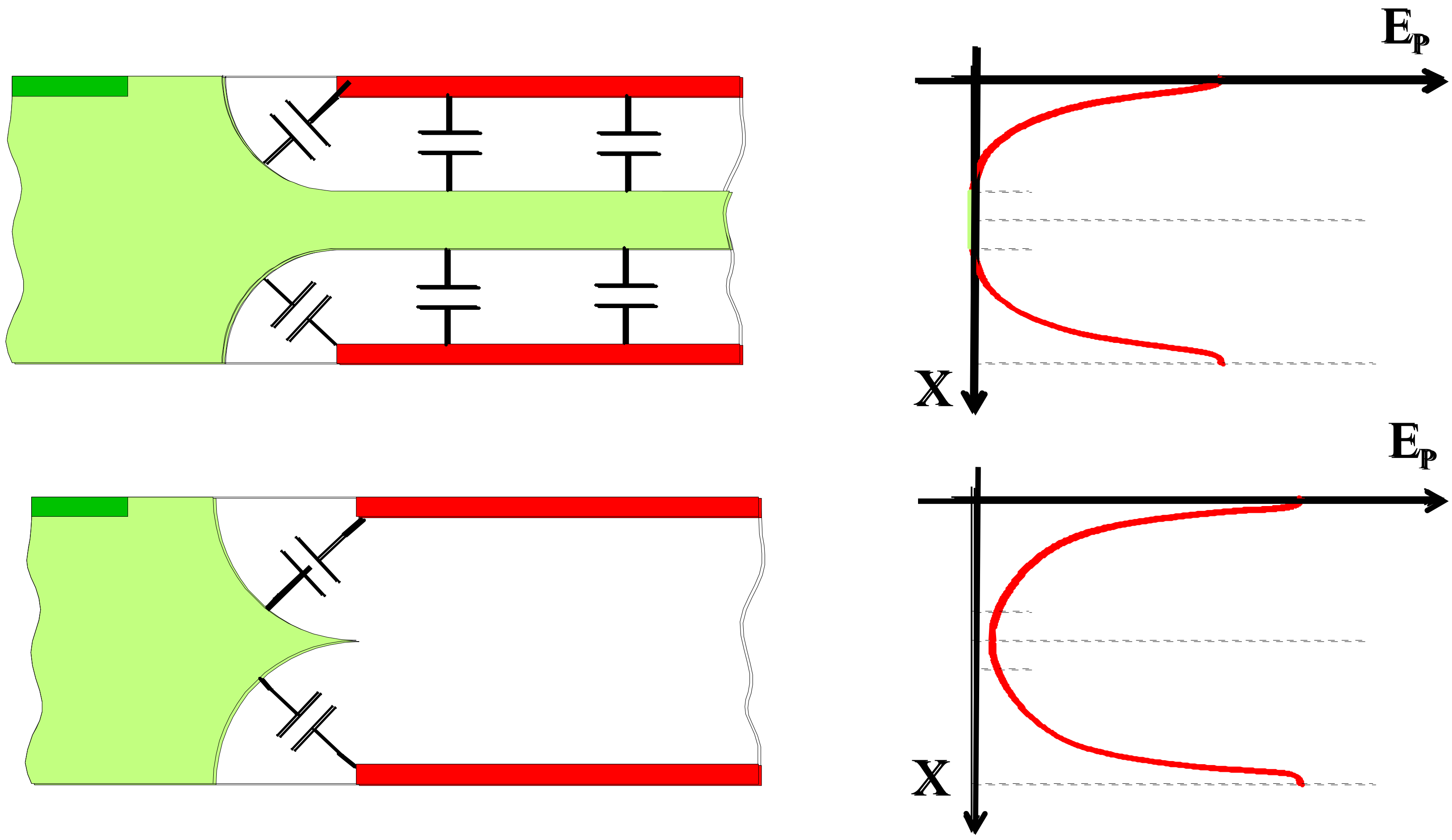

The first signals from a SDD

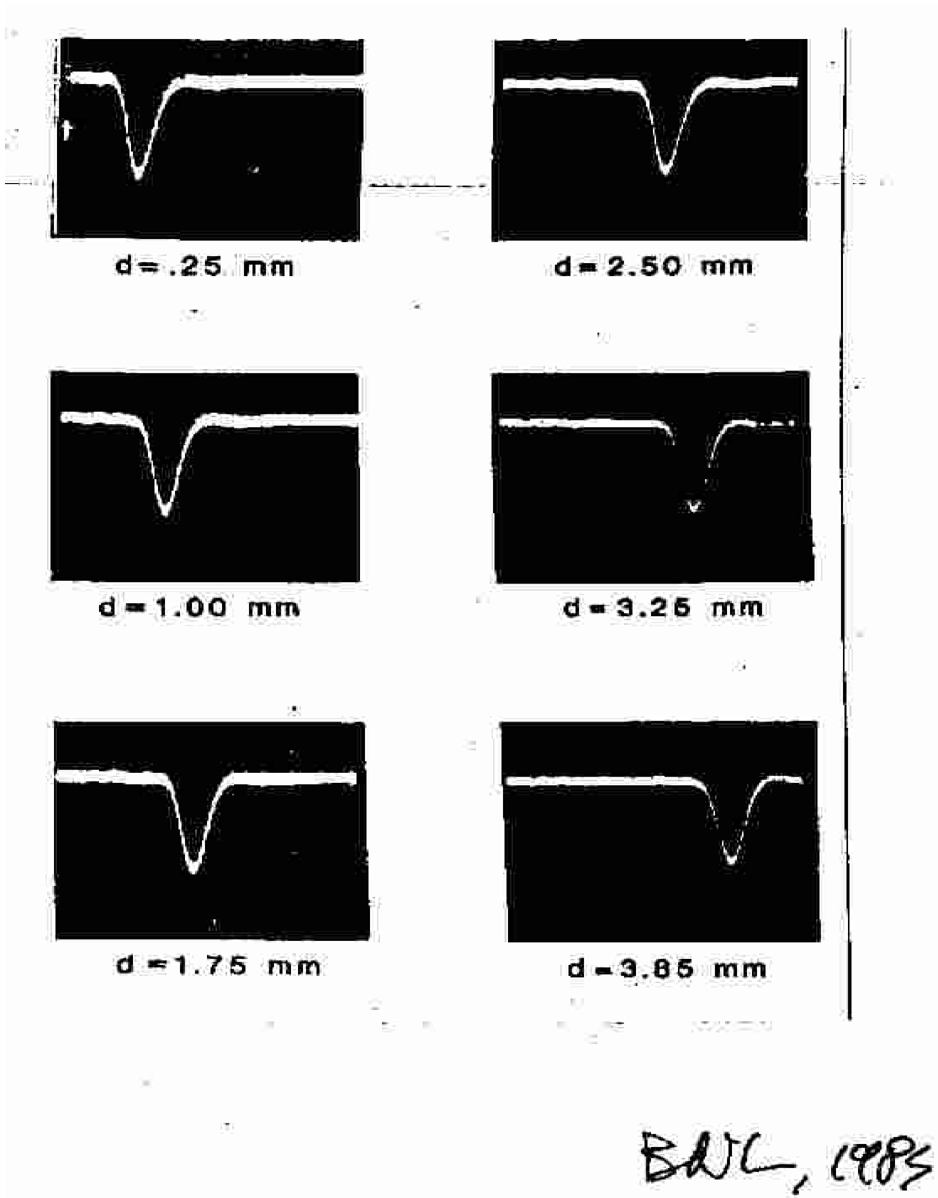

The classical PIN diode detector

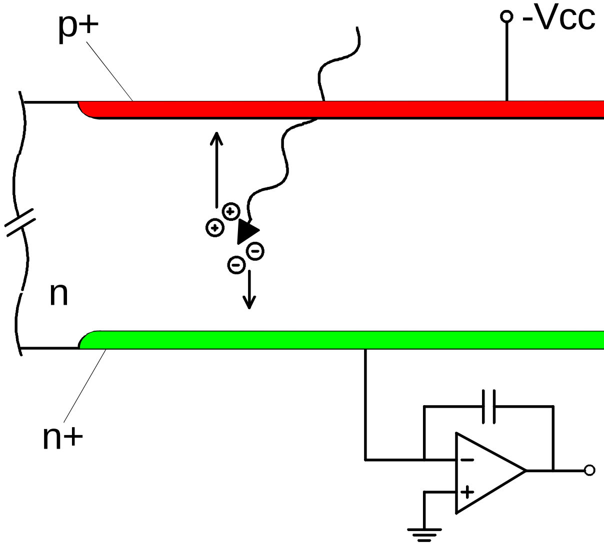

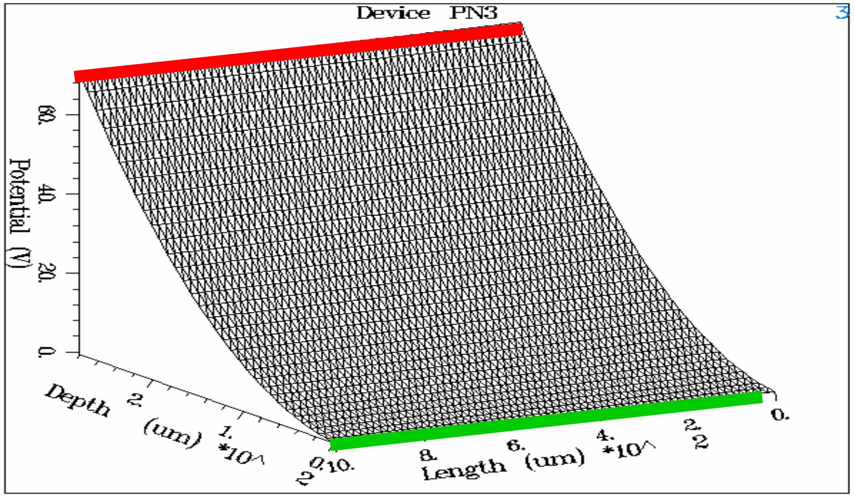

The anode capacitance is proportional to the detector active area

The SDD for X-ray spectroscopy

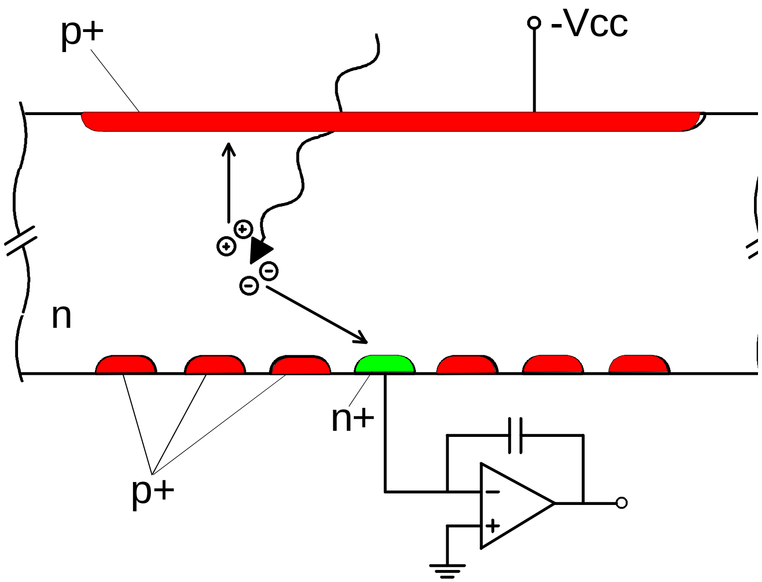

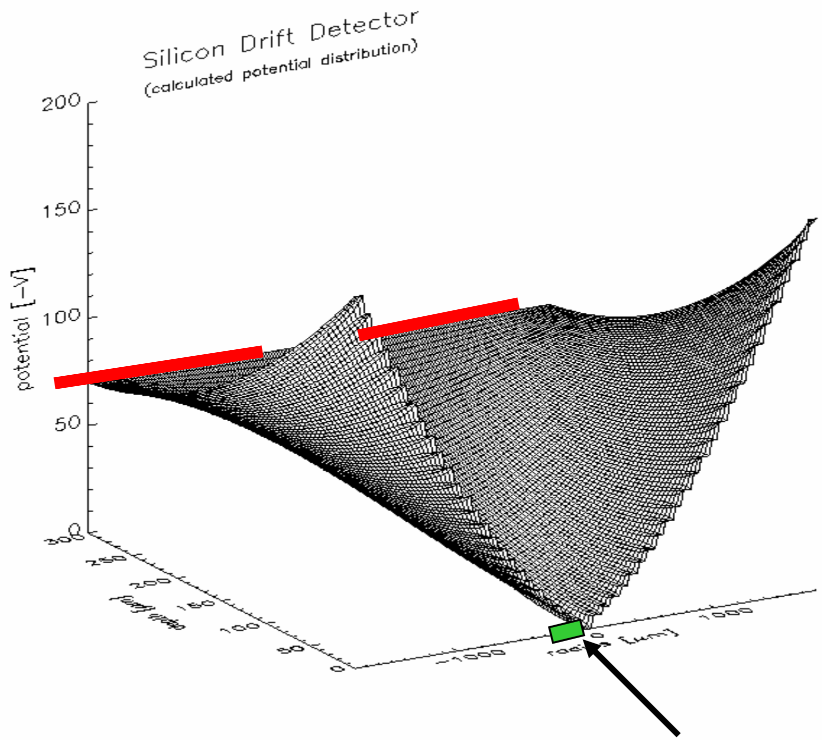

The electrons are collected by the small anode, characterised by a **low output capacitance** which is **independent on the active area of the detector**.

The SDD structure

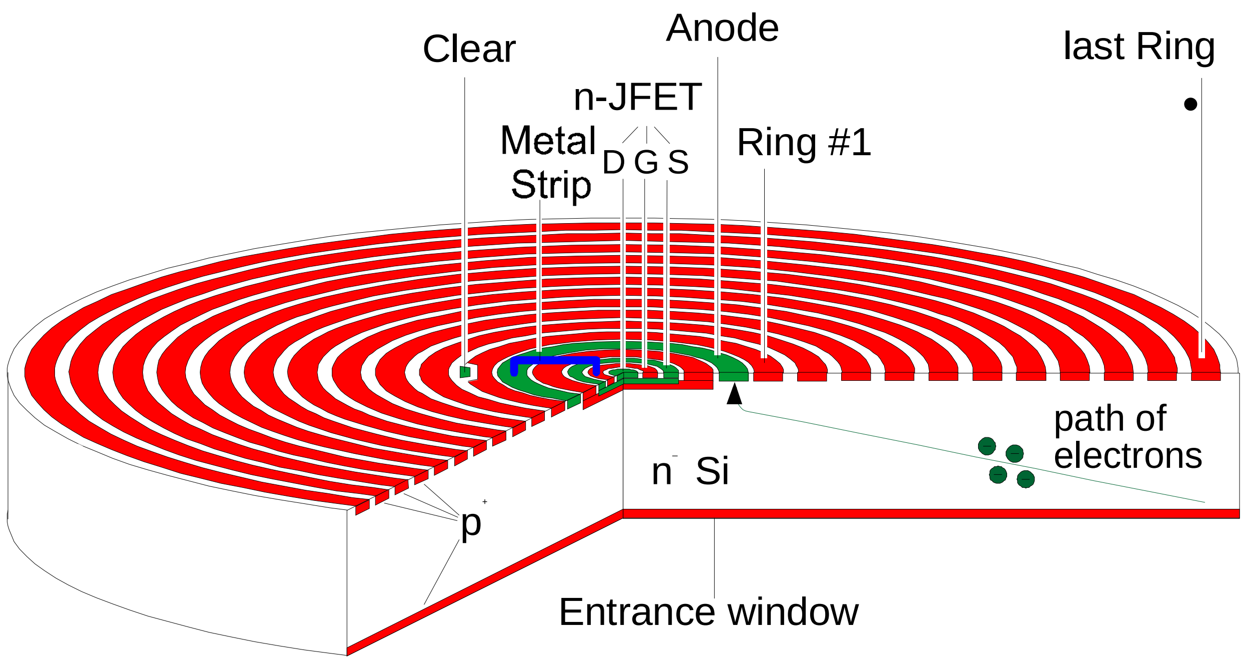

- The electrons, generated in the fully depleted silicon by the X-ray photons, are collected by the small anode (having a very low capacitance, **Cdet=150fF**).

The integrated front-end transistor (n-JFET) allows the capacitive matching between detector and amplifier(Cdet≈Cgate)

Advantages: very high energy resolution at fast shaping times, due to the small anode capacitance, independent of the active area of the detector

The integrated JFET

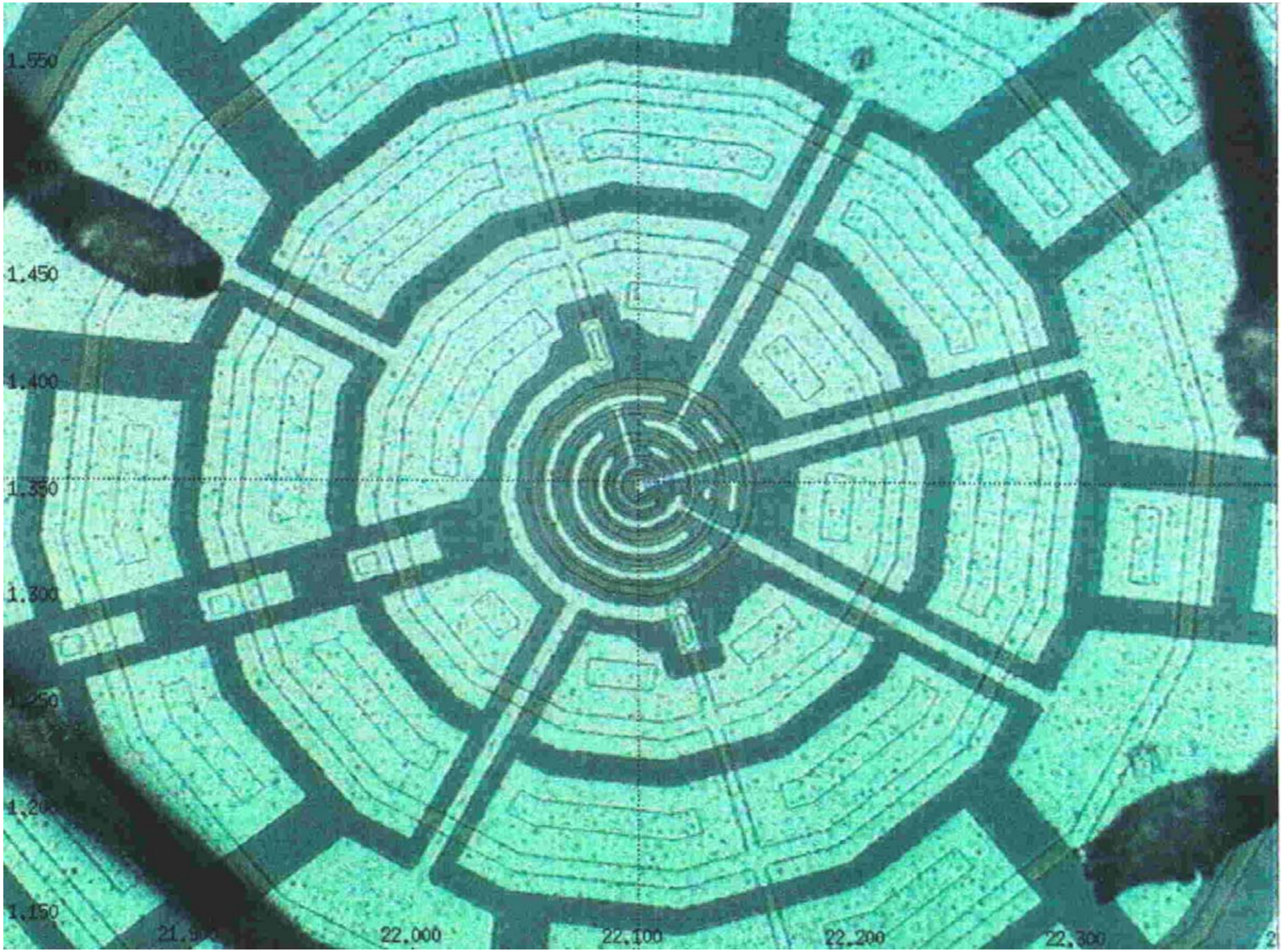

Detector produced at the MPI Halbleiterlabor, Munich, Germany

SDD performances

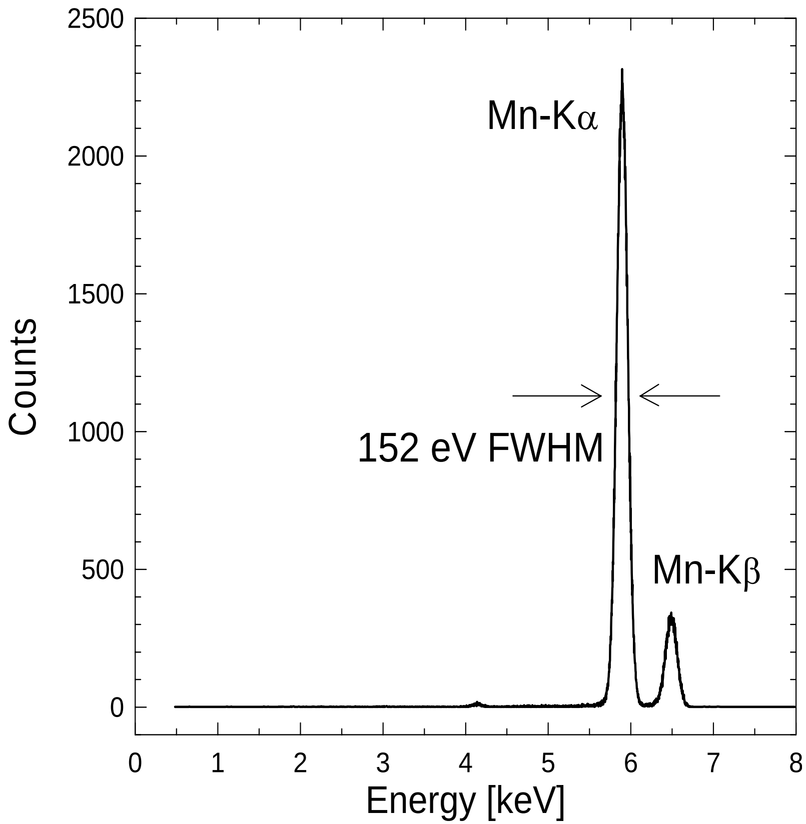

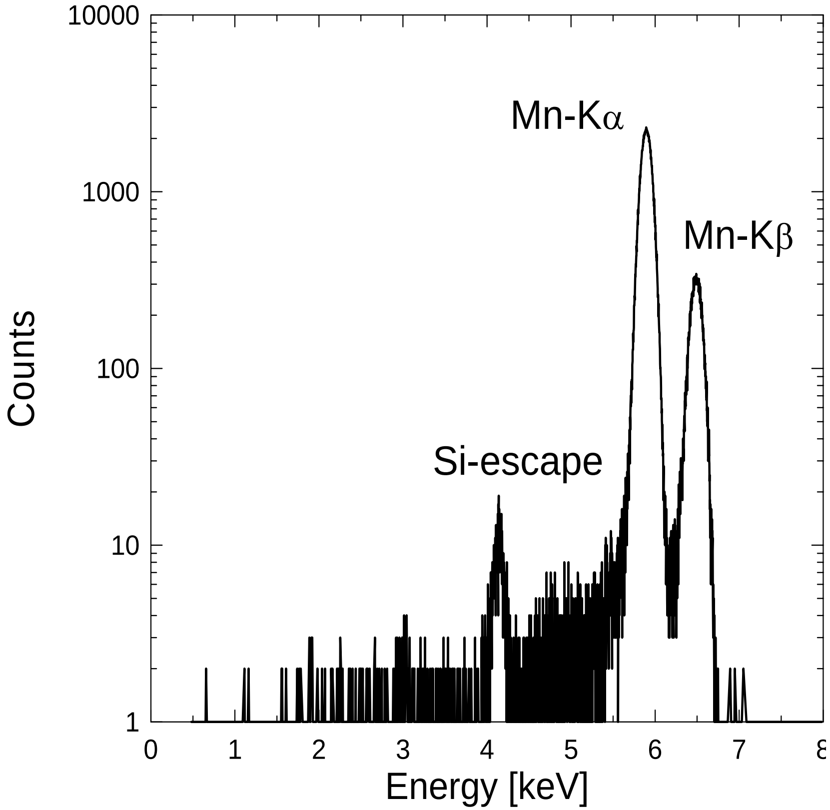

- ^{55}Fe spectrum measured with the SDD module at T= -8°C and a shaping time of 0.5 μs.

The integrated JFET

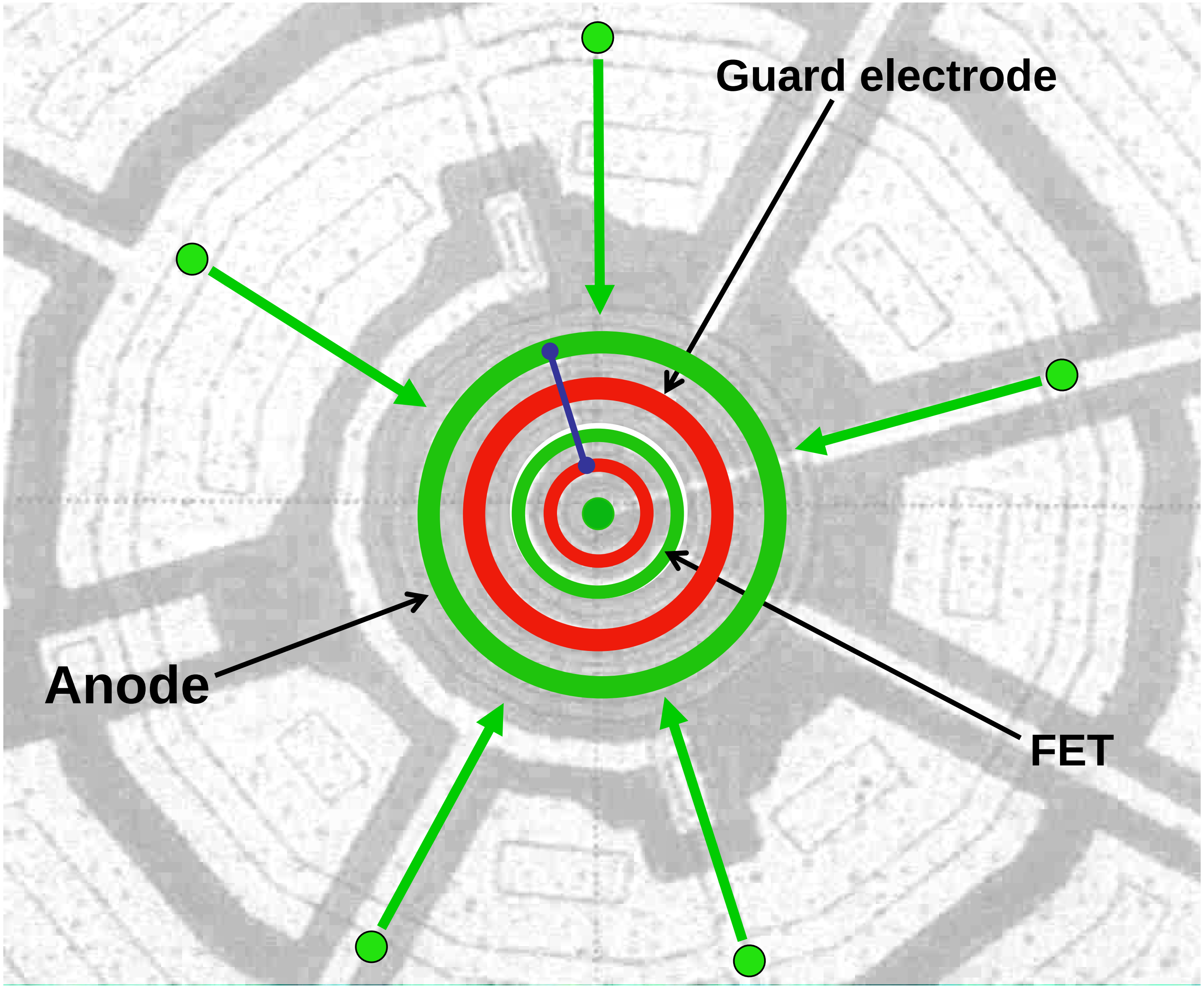

The “conventional” central anode containing the FET

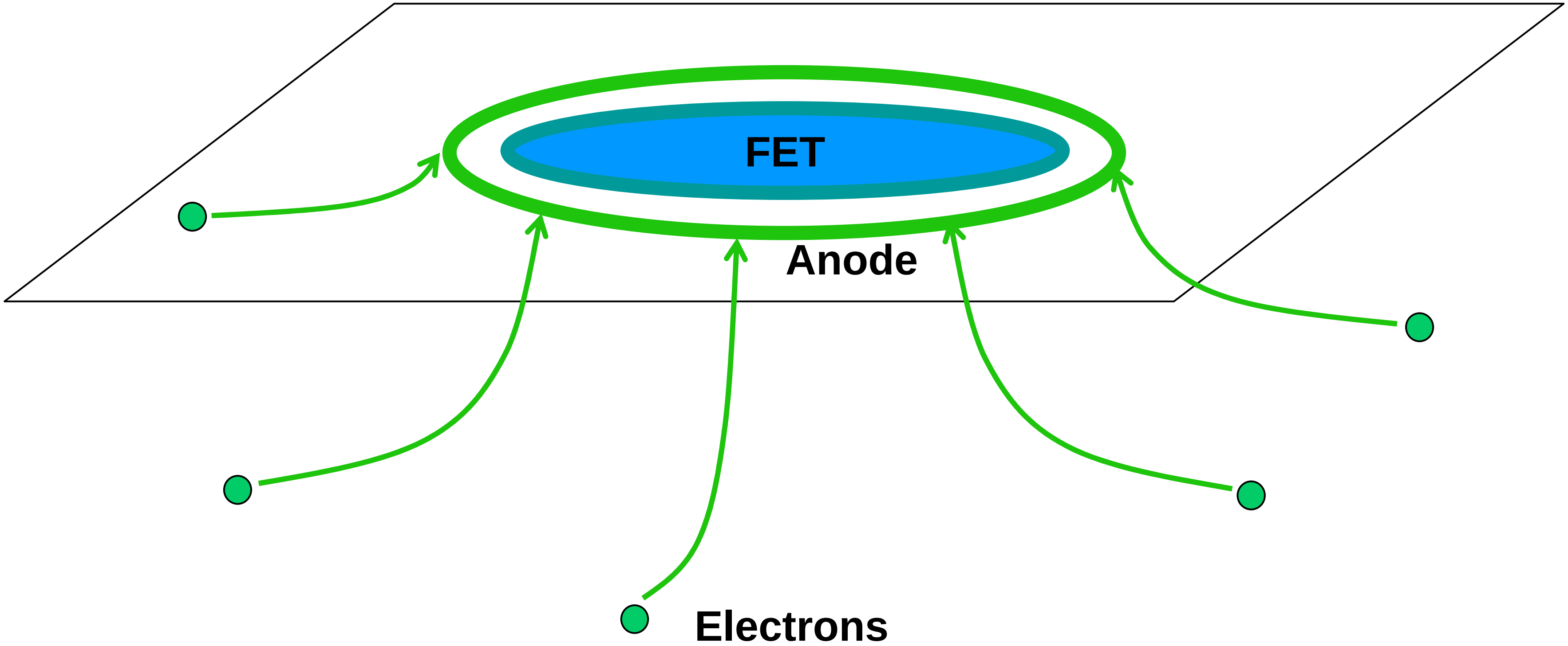

The "lateral" anode with side FET

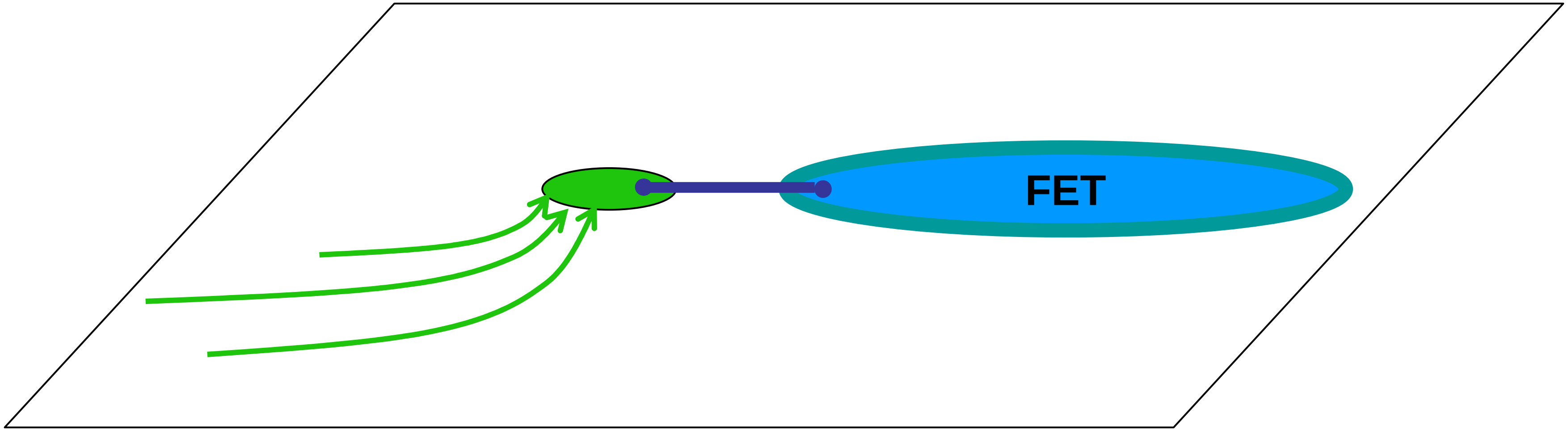

The new Silicon Drift Detector Droplet (SD³)

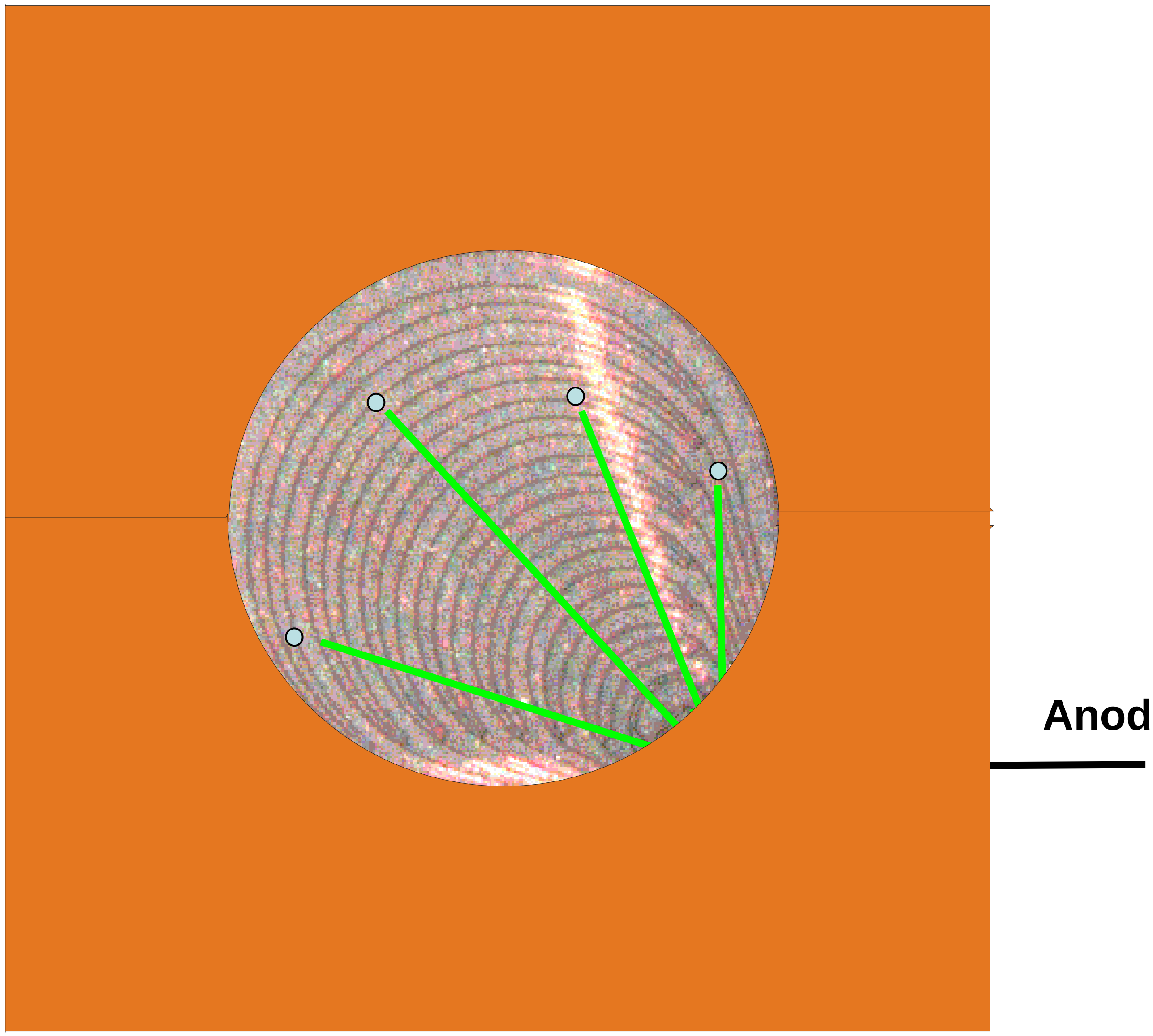

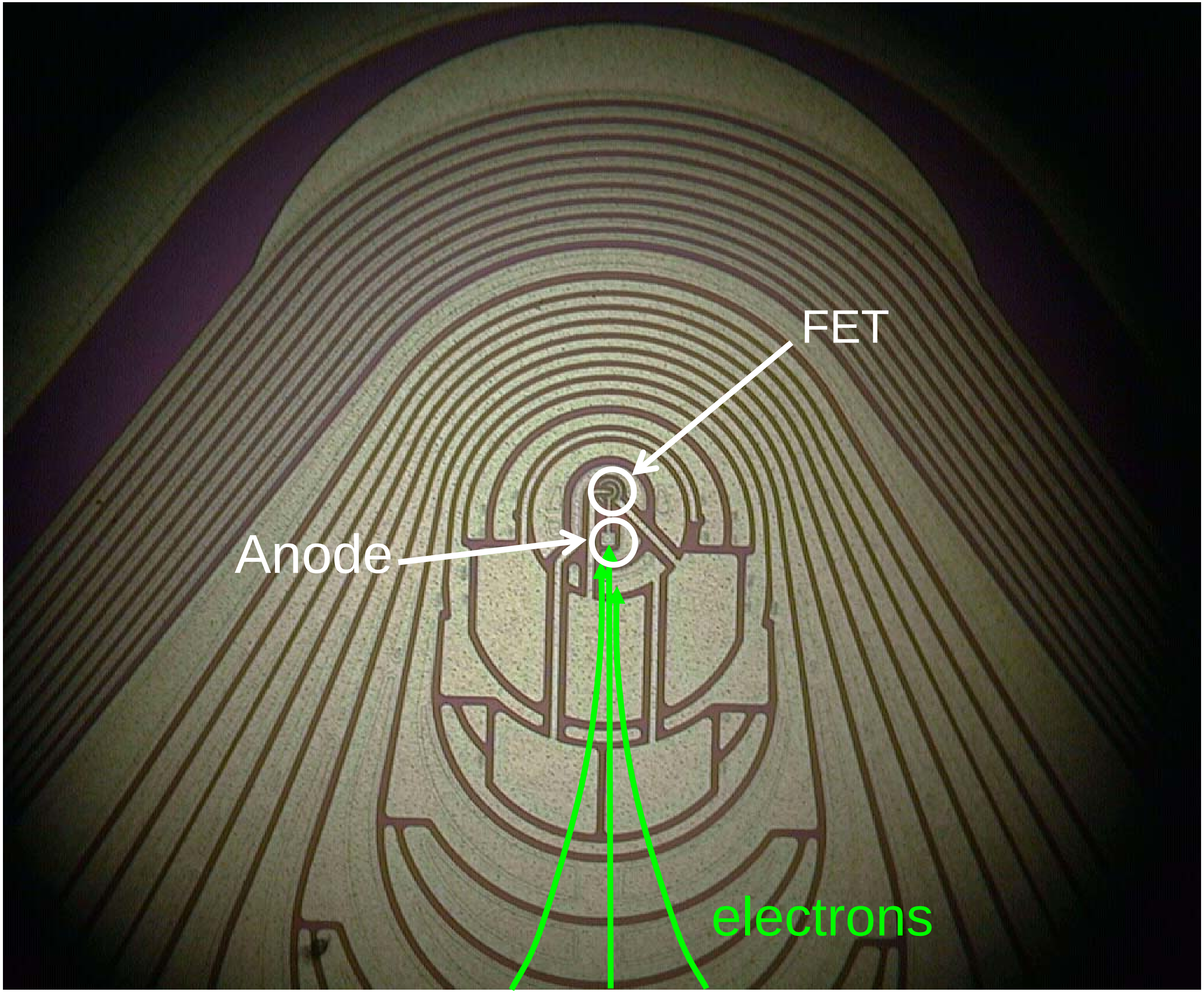
FET
Anode
electrons

The resolution of the new SD^3

STANDARD SDD

Anode capacitance = 150 fF

FWHM= 150 eV (typ)
at T= -10°C

DROPLET SDD

Anode capacitance = 50 fF

FWHM= 130 eV (typ)
at T= -20°C

Peak/Background > 5000

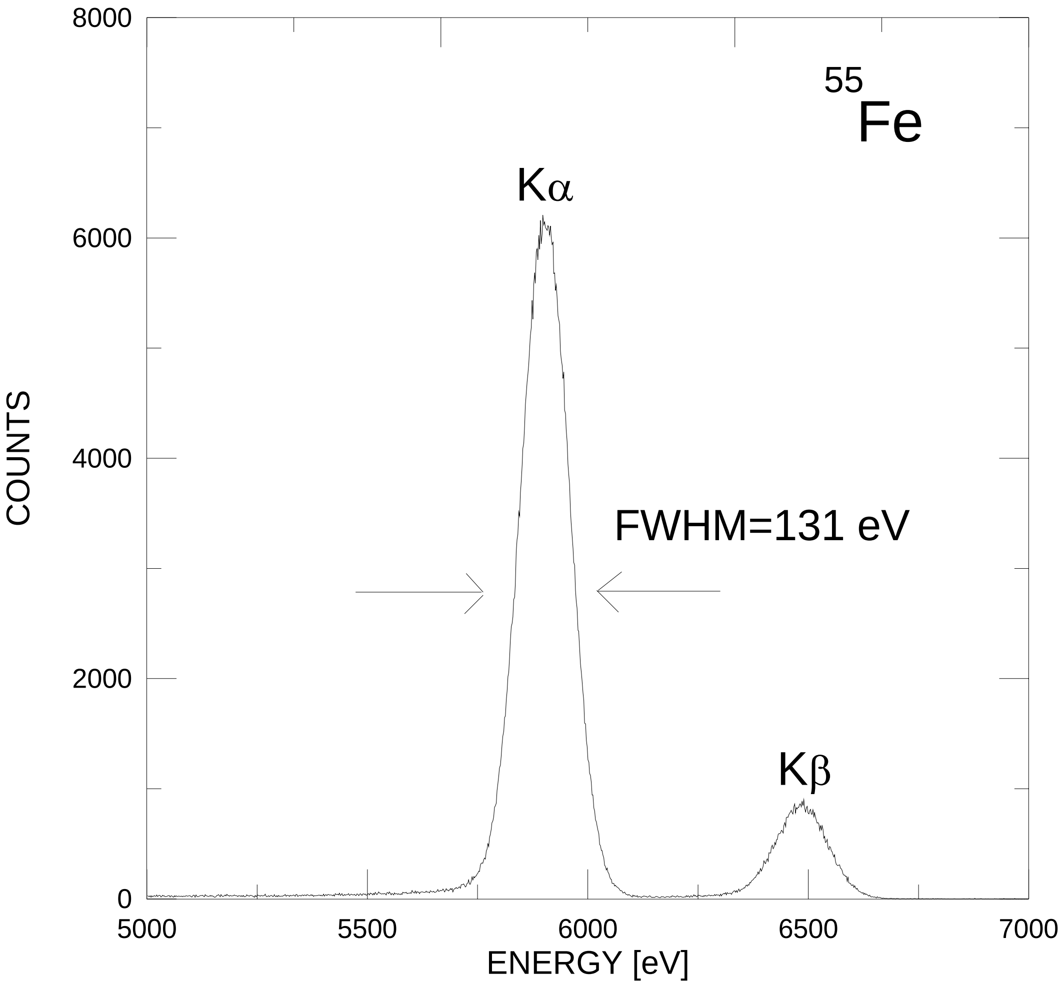

Performances with soft X-ray

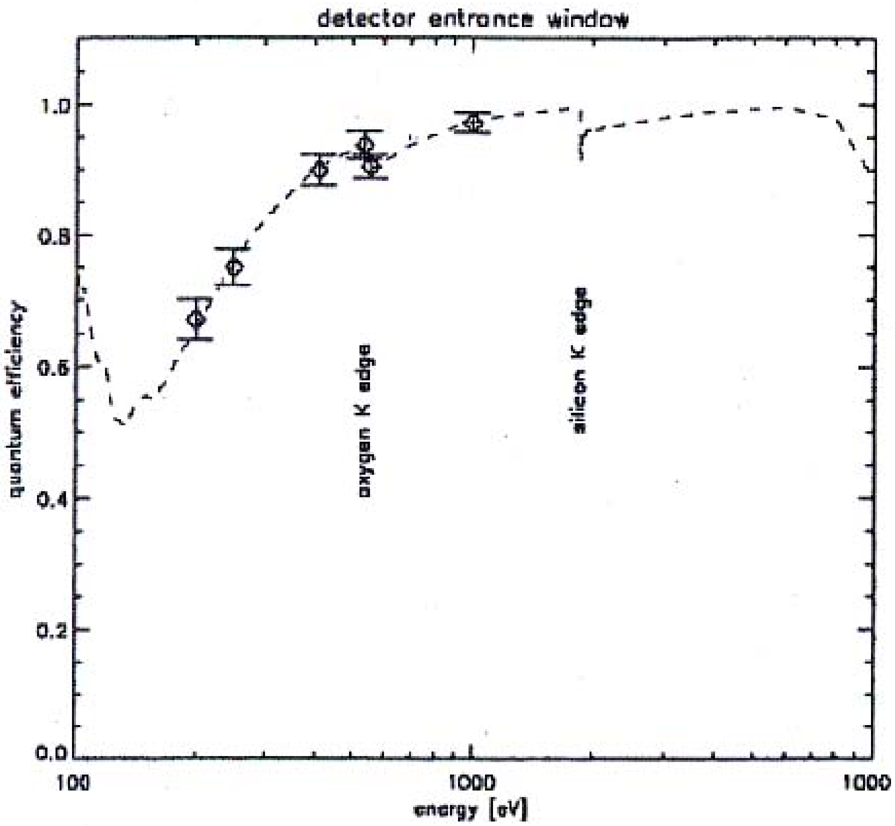

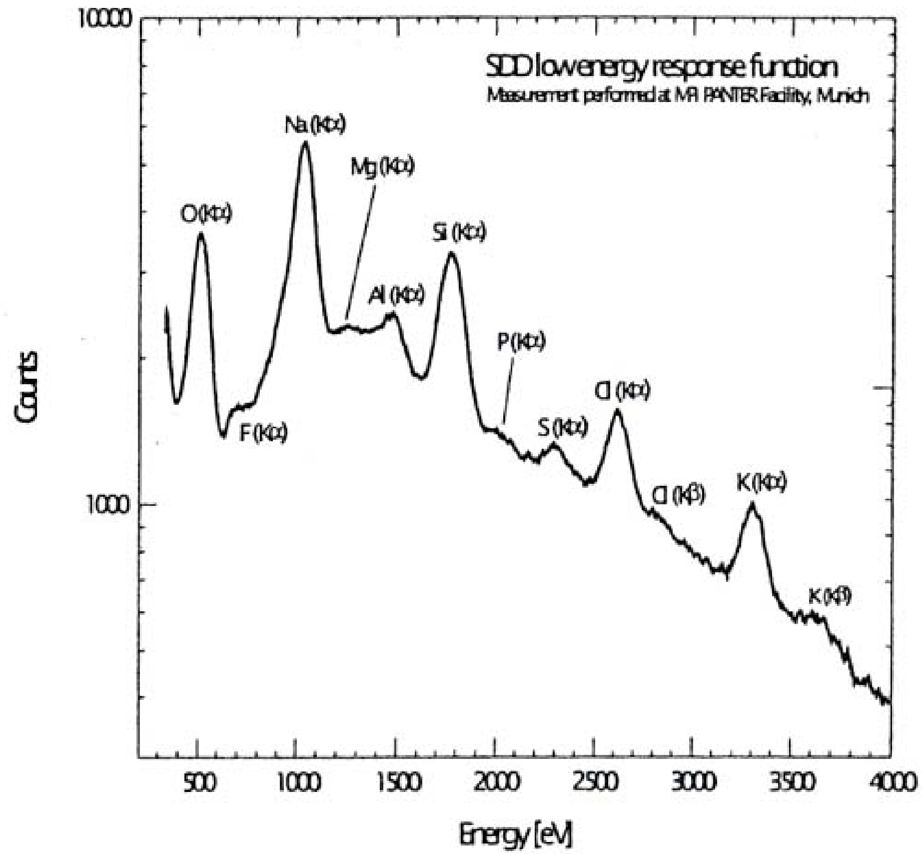

Some applications of the single-element SDDs in X-ray spectroscopy

Analysis of the alloy composition of the 'Lupa Capitolina'

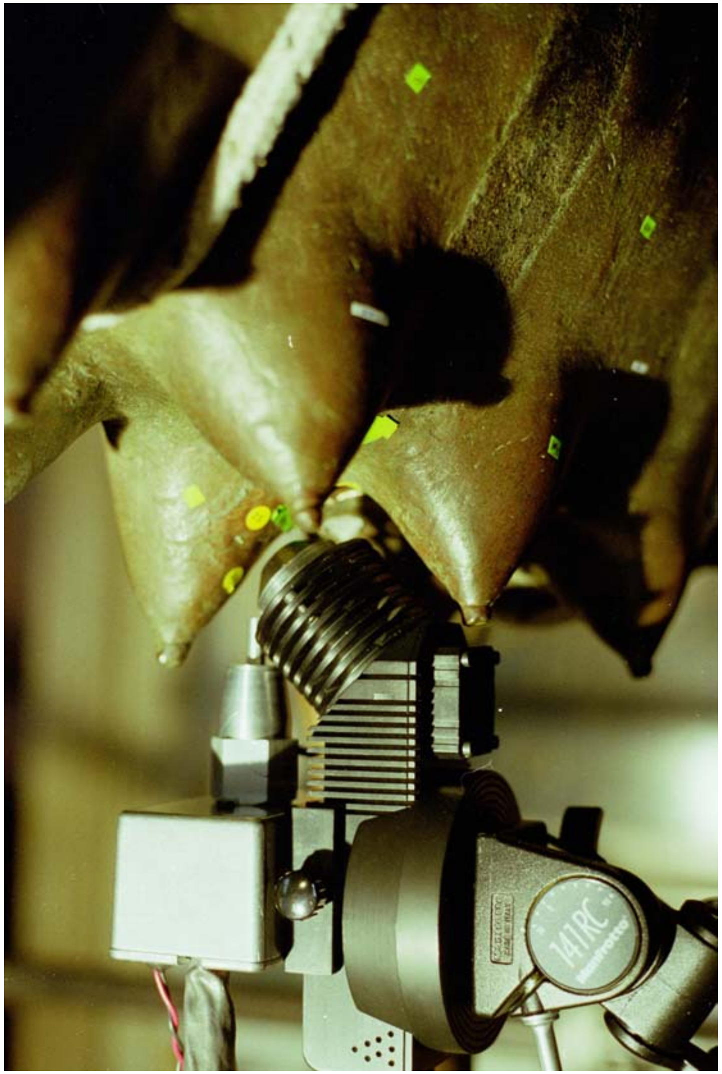

Musei Capitolini, Roma

XRF spectrum of the bronze alloy of the 'Lupa'

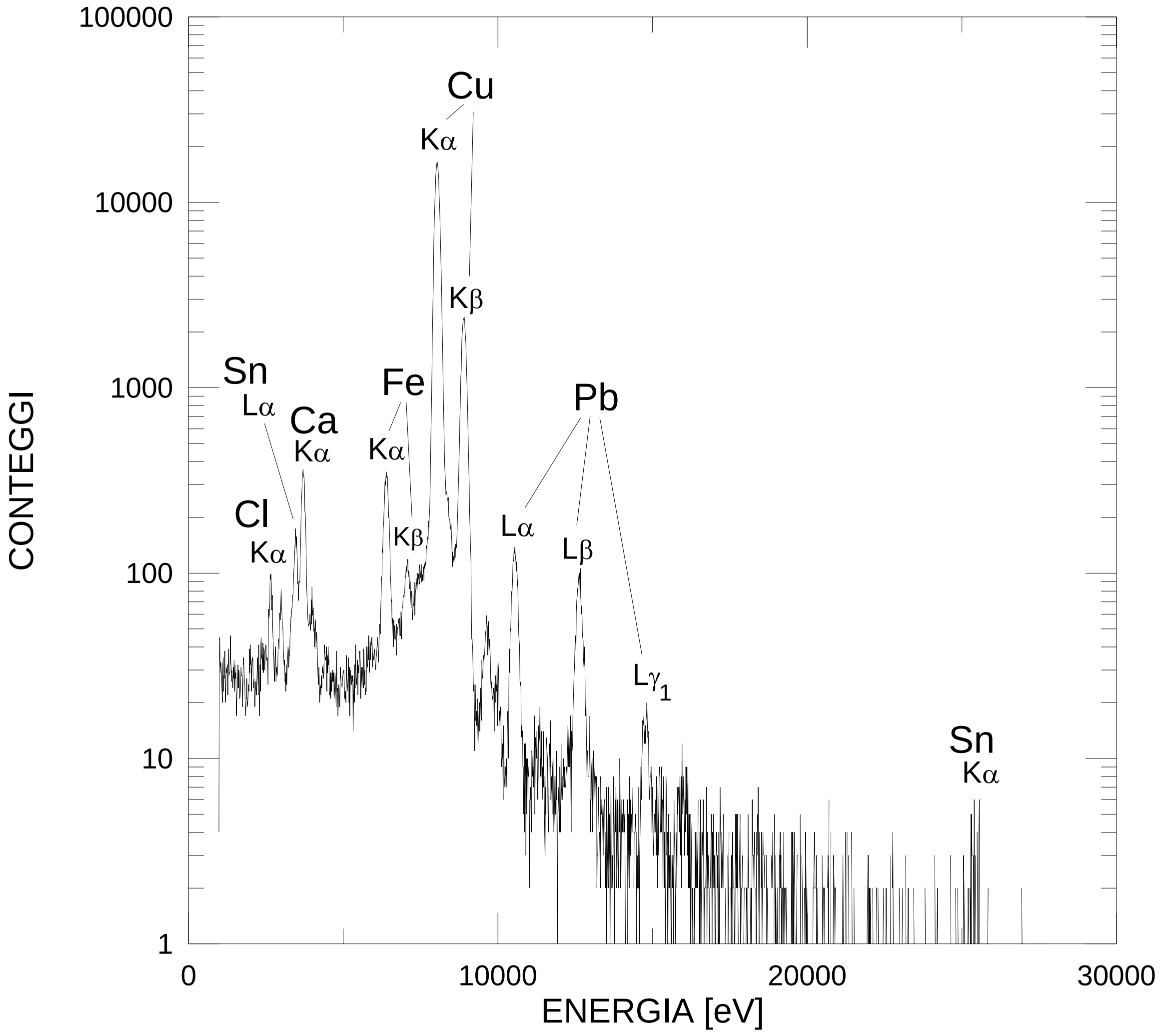

Element distribution on the 'Lupa' body

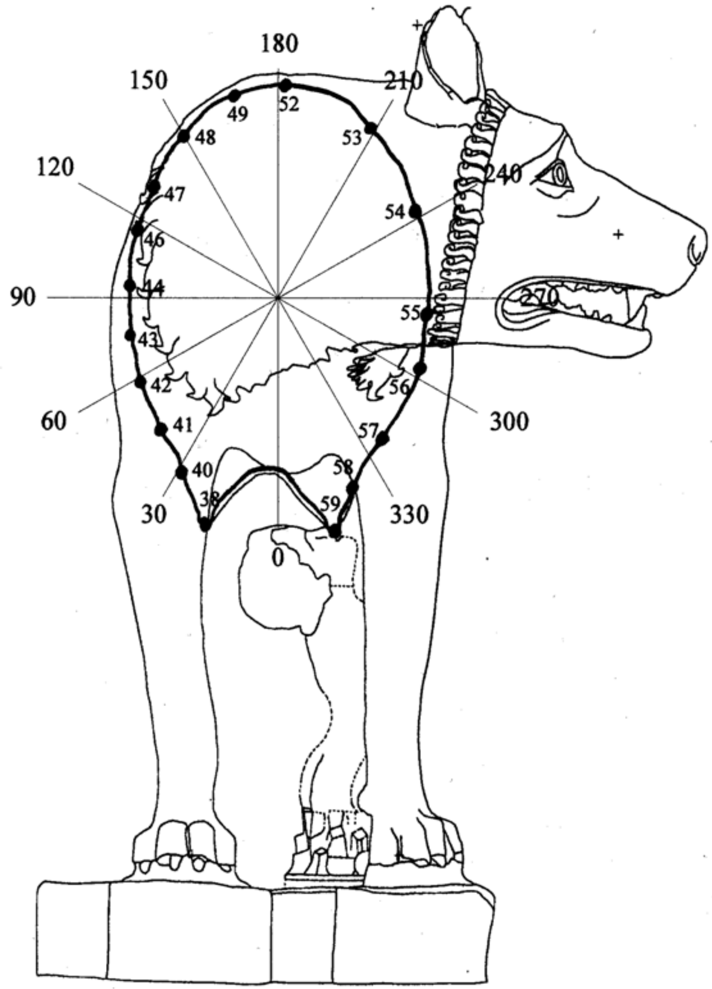

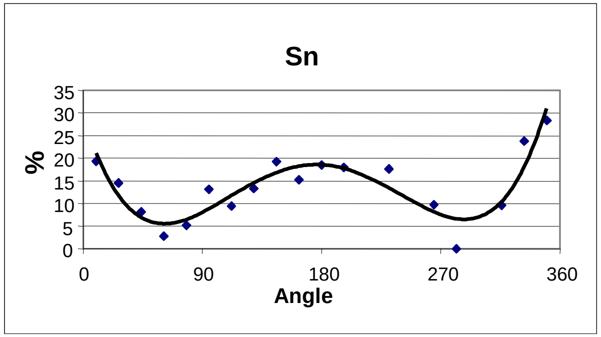

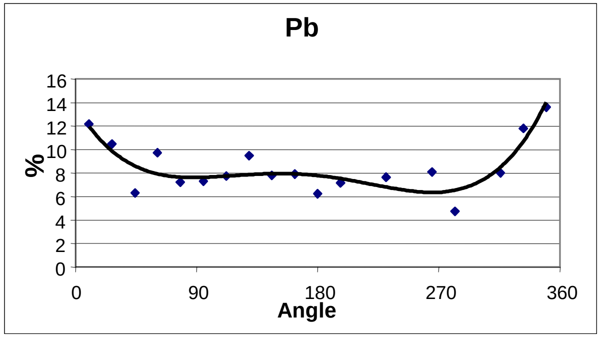

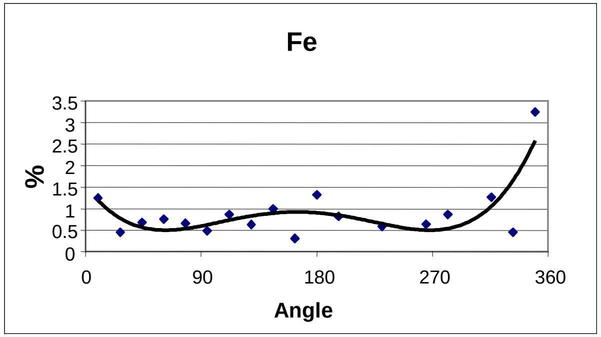

Analysis of the alloy composition of the “Spinario”

Musei Capitolini, Roma

Analysis of a bronze roman sculpture

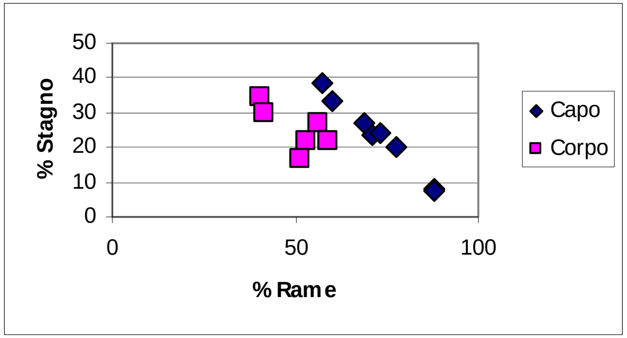

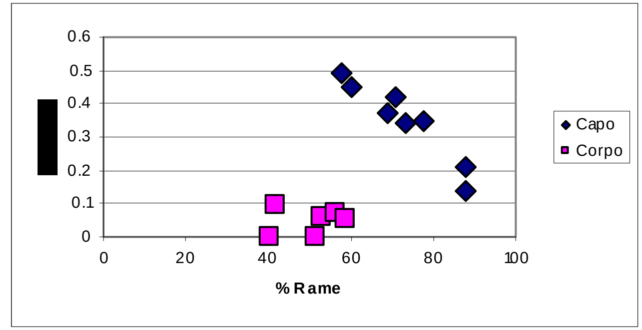

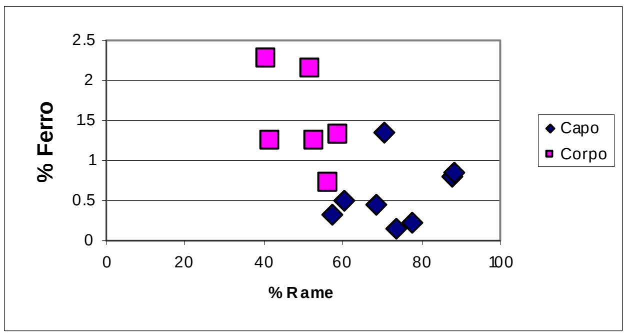

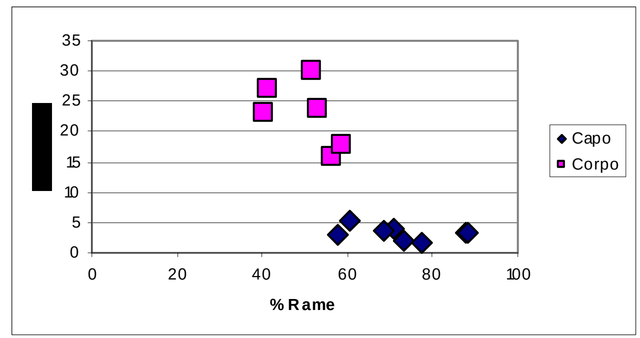

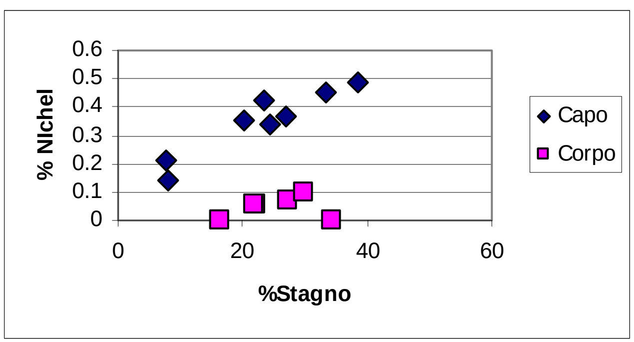

Correlation diagrams of the bronze composition of several points of the head and of the body of the sculpture, showing that the two parts have been produced with different fusion (maybe in a different historical period). The last diagram shows that Ni has been probably introduced as impurity of Sn.

Analysis of an Egyptian Linen (Antinopolis, III century A.C.)

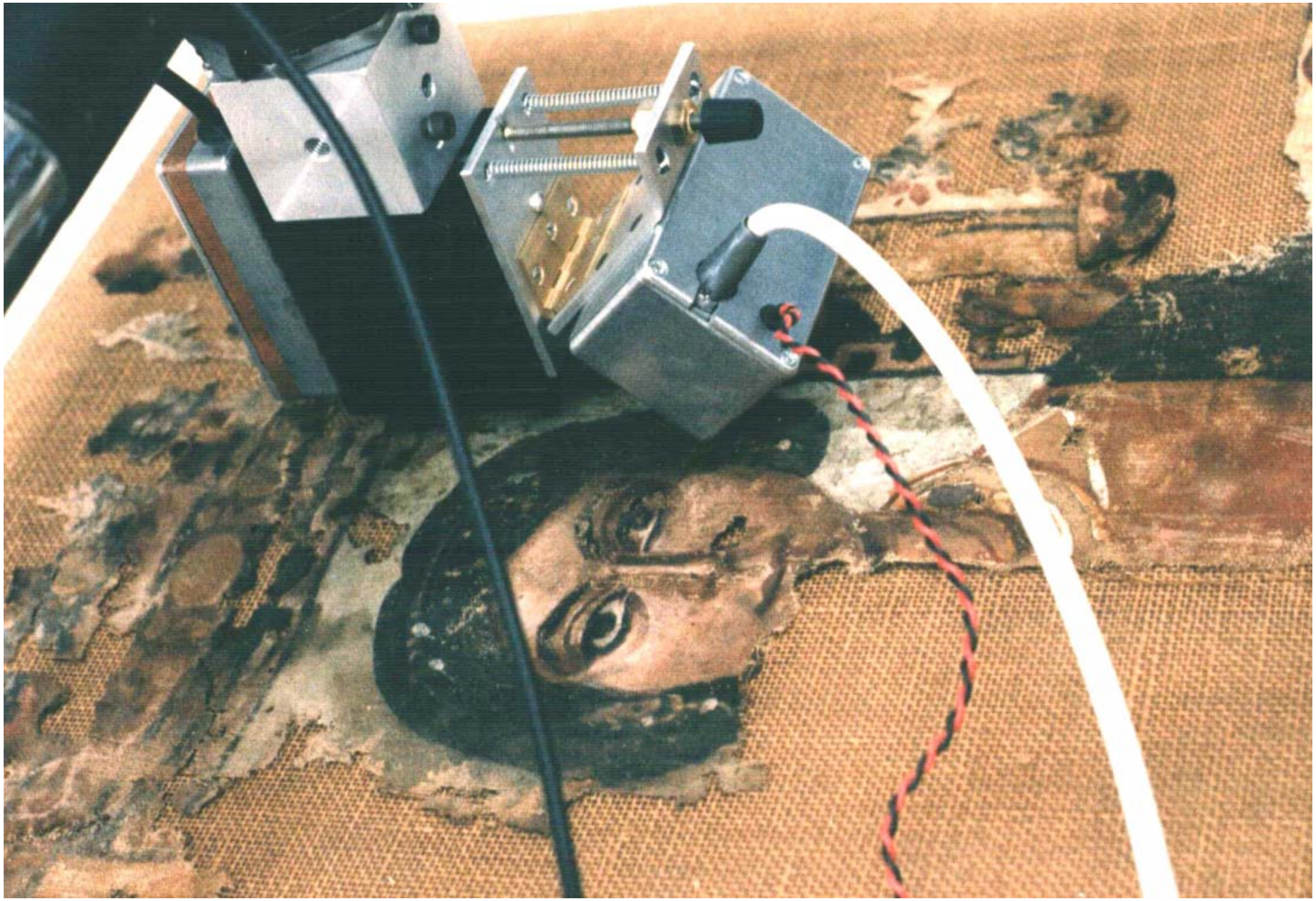

Museo Vaticano, Roma

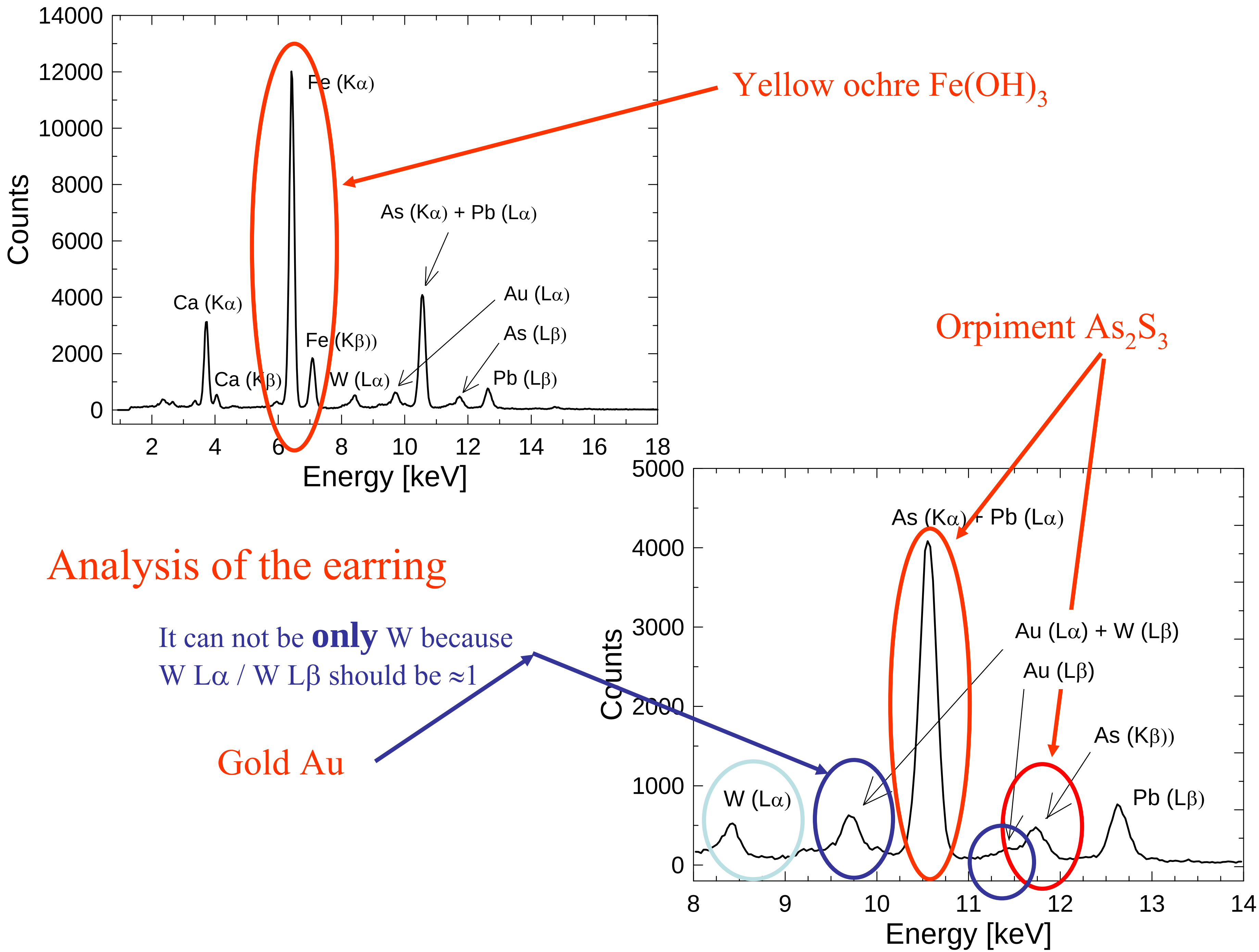

Analysis of the earring
Yellow ochre $Fe(OH)_3$
Orpiment As_2S_3
It can not be **only** W because
W Lα / W Lβ should be ≈1
Gold Au
Counts
Energy [keV]
14000
12000
10000
8000
6000
4000
2000
0
2
4
6
8
10
12
14
16
18
Fe (Kα)
Ca (Kα)
Ca (Kβ)
Fe (Kβ))
W (Lα)
As (Kα) + Pb (Lα)
Au (Lα)
As (Lβ)
Pb (Lβ)
Counts
Energy [keV]
5000
4000
3000
2000
1000
0
8
9
10
11
12
13
14
As (Kα) + Pb (Lα)
Au (Lα) + W (Lβ)
Au (Lβ)
As (Kβ))
W (Lα)
Pb (Lβ)

Authenticity verification

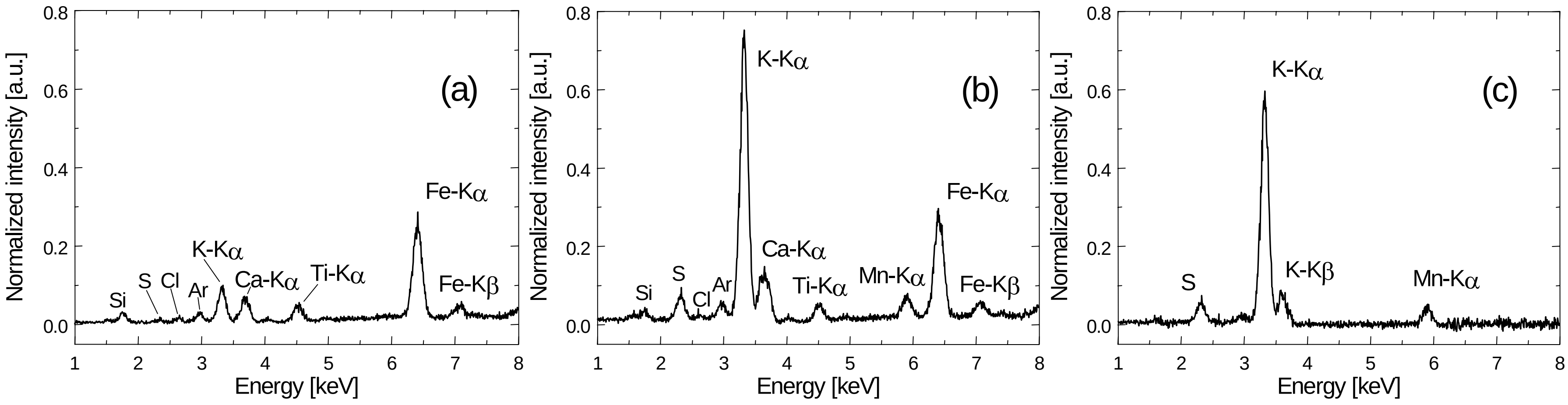

Fluorescence spectra of a document in a reference point (a) and in a point where stain remover was supposed to be applied (b) (the spectra are normalized with respect to the Ti-K_α line).
In (c) the difference between the two spectra (a) and (b) is reported, revealing a probable application of a conventional stain remover containing S, K, and Mn.

Multi-element SDDs

The 12-element SDD detector

"Front" Side
collecting anode,
JFET,
Basing electrodes

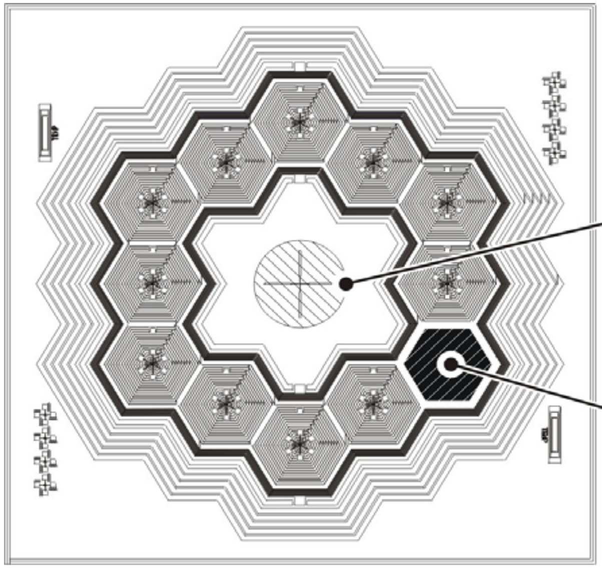

Detector thickness 300 µm

"Back" Side
non-structured
radiation
entrance window.

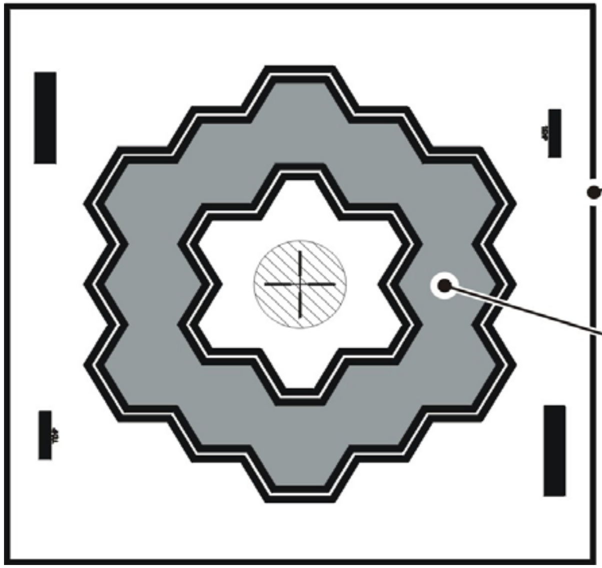

The 12-element SDD detector

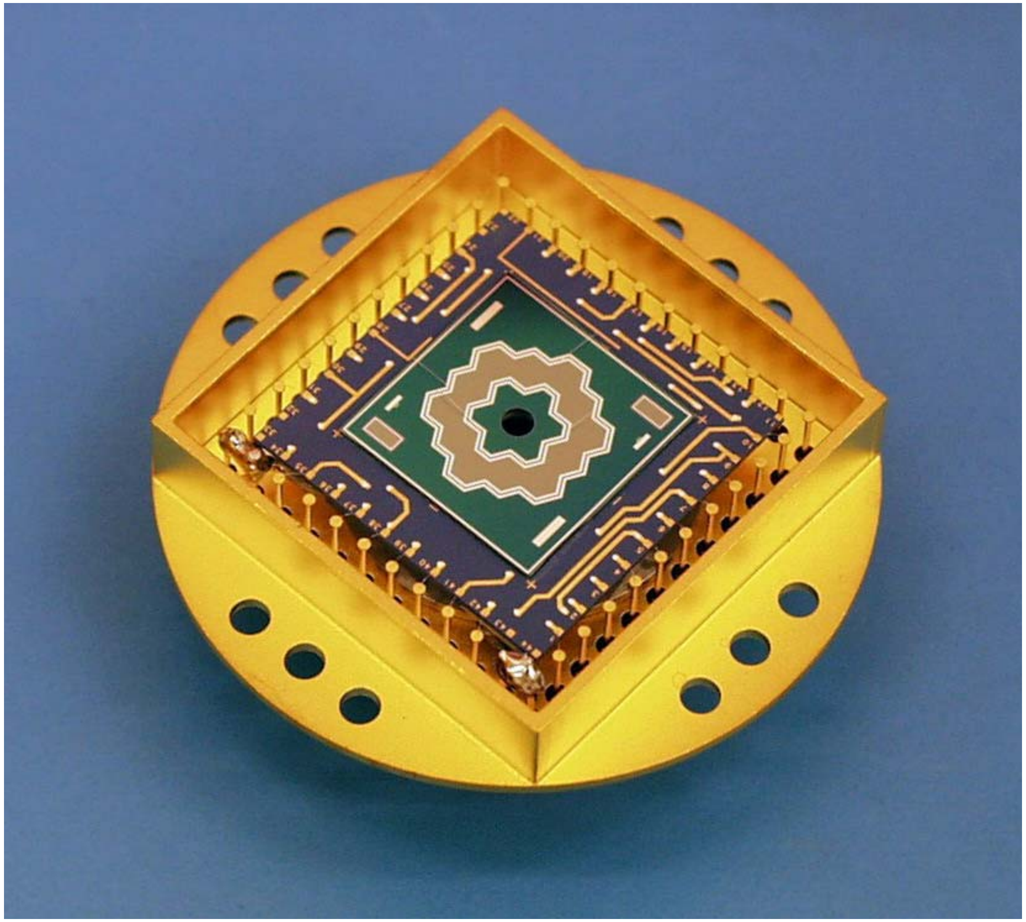

Detector performances

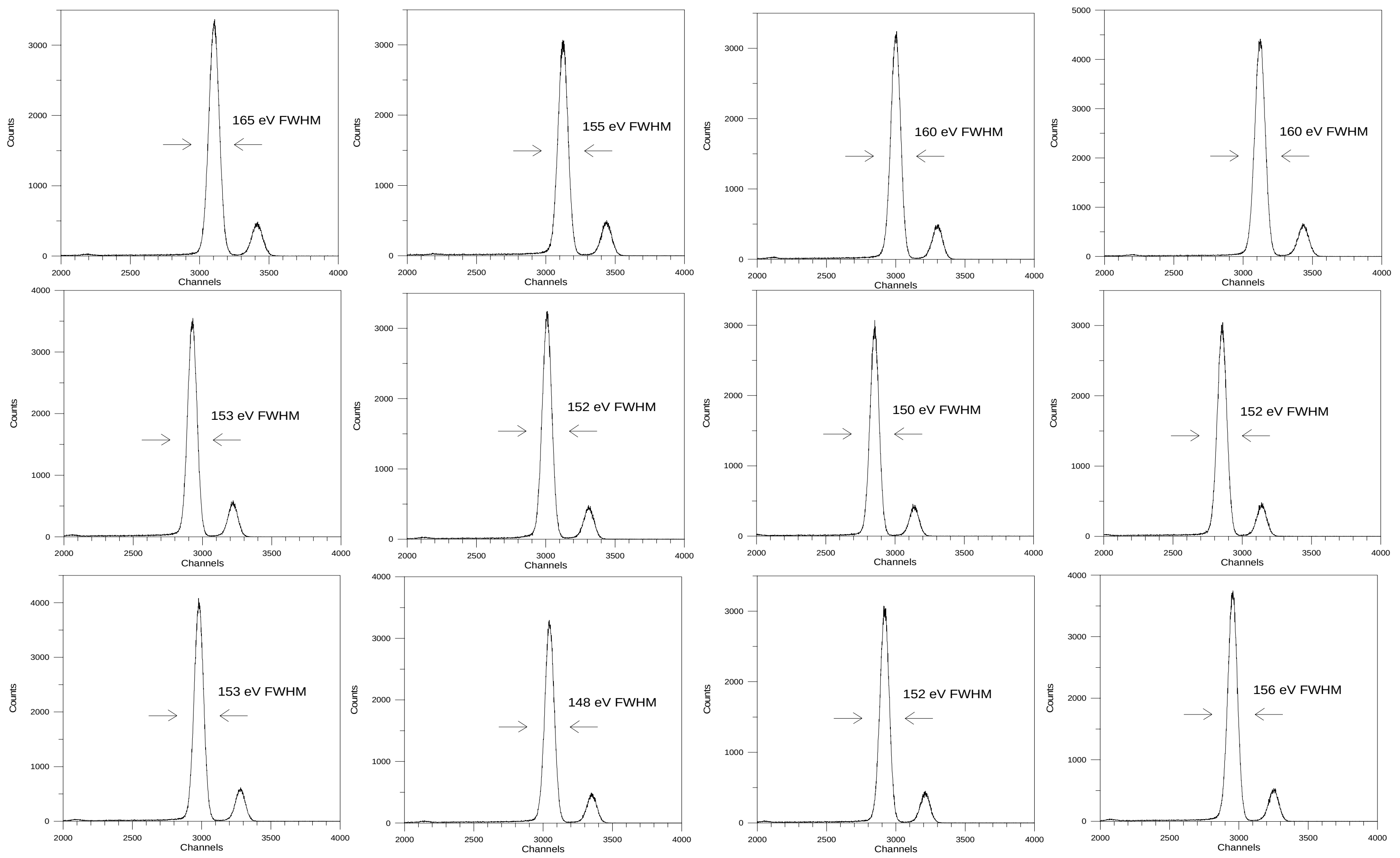

^{55}Fe radioactive source – T = -10 °C – Tennelec TC244 gaussian shaping amplifier $\tau_{sh} = 0.5$ µs
Count rate ≈ 10 kcps / channel. Average FWHM: 154.7 eV

A new multi-element Semiconductor Srift Detector optimized for XRF Elemental Mapping

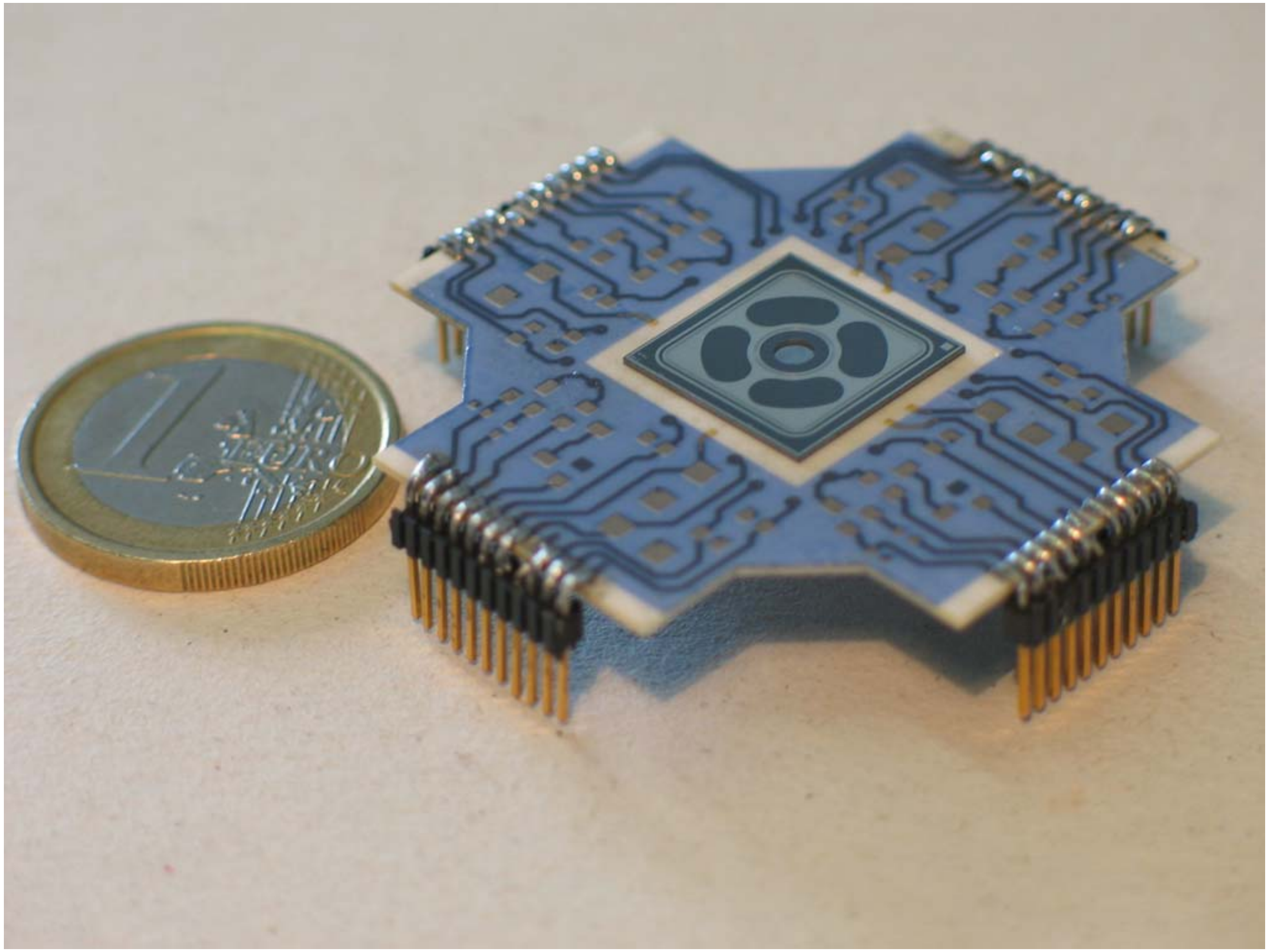

Project FELIX INFN Gr.5 2003-04

A new multi-element Semiconductor Srift Detector optimized for XRF Elemental Mapping

14 mm

Thickness 450 μm

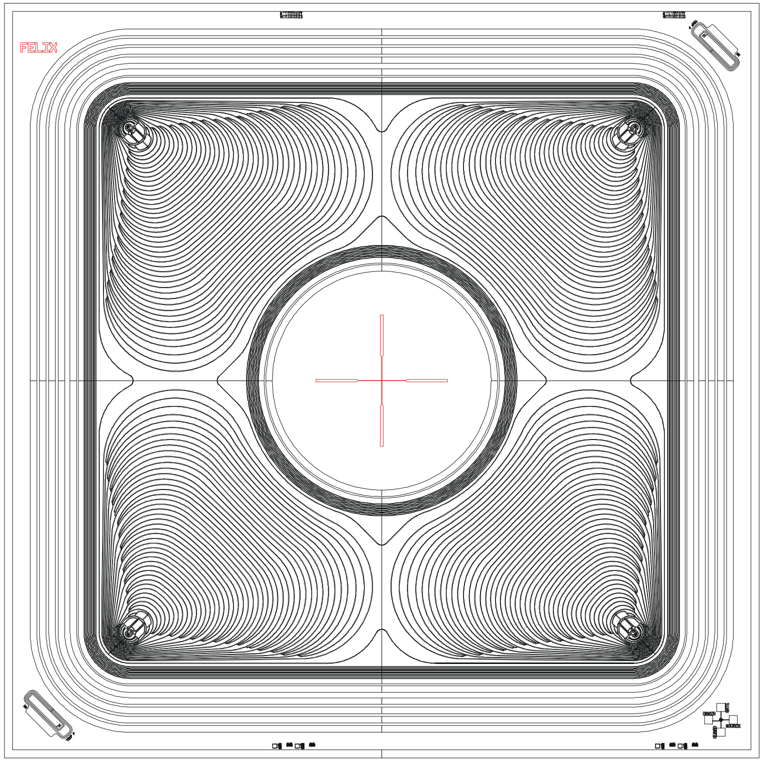

Front side

Collecting anode and transistor

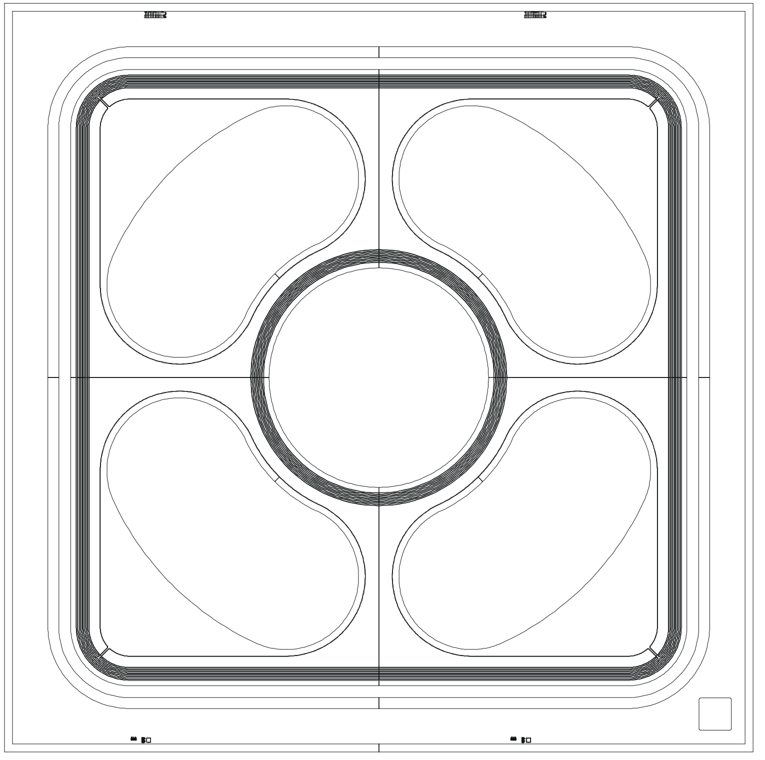

Back side

Radiation entrance window

SDD4 collimator

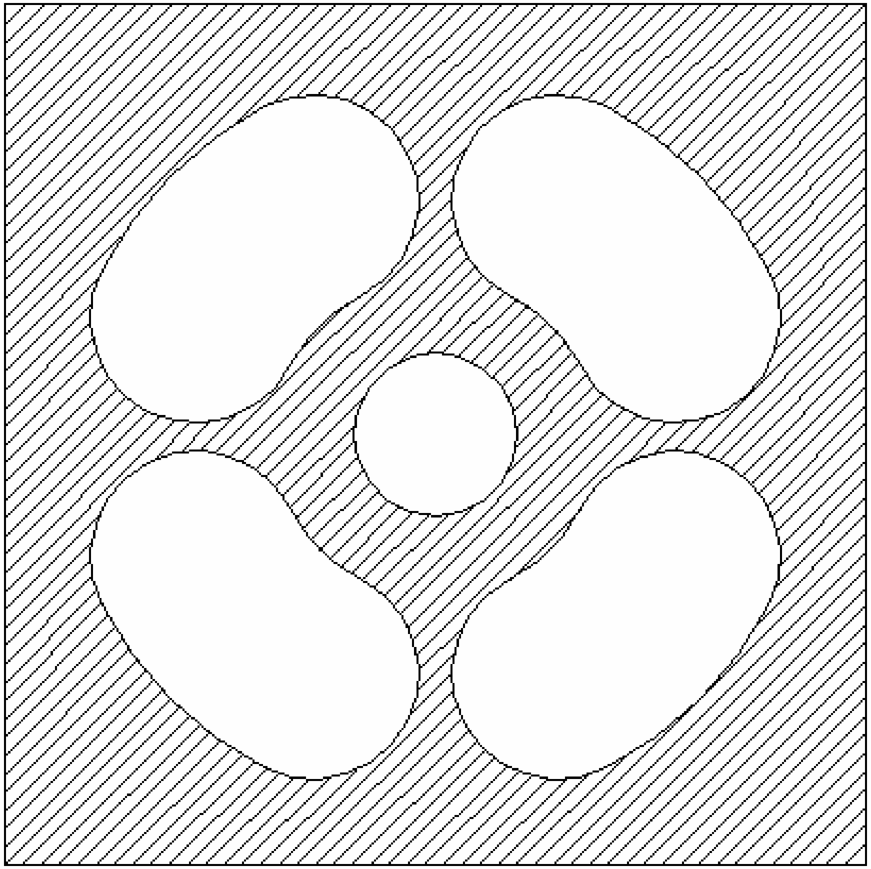

Collimated area ≈ 4 x 15 mm^2

SDD4: collecting region

Collecting anode and input JFET

Ultra-low Detector + JFET capacitance: Cd+Cg ≈ 120 fF

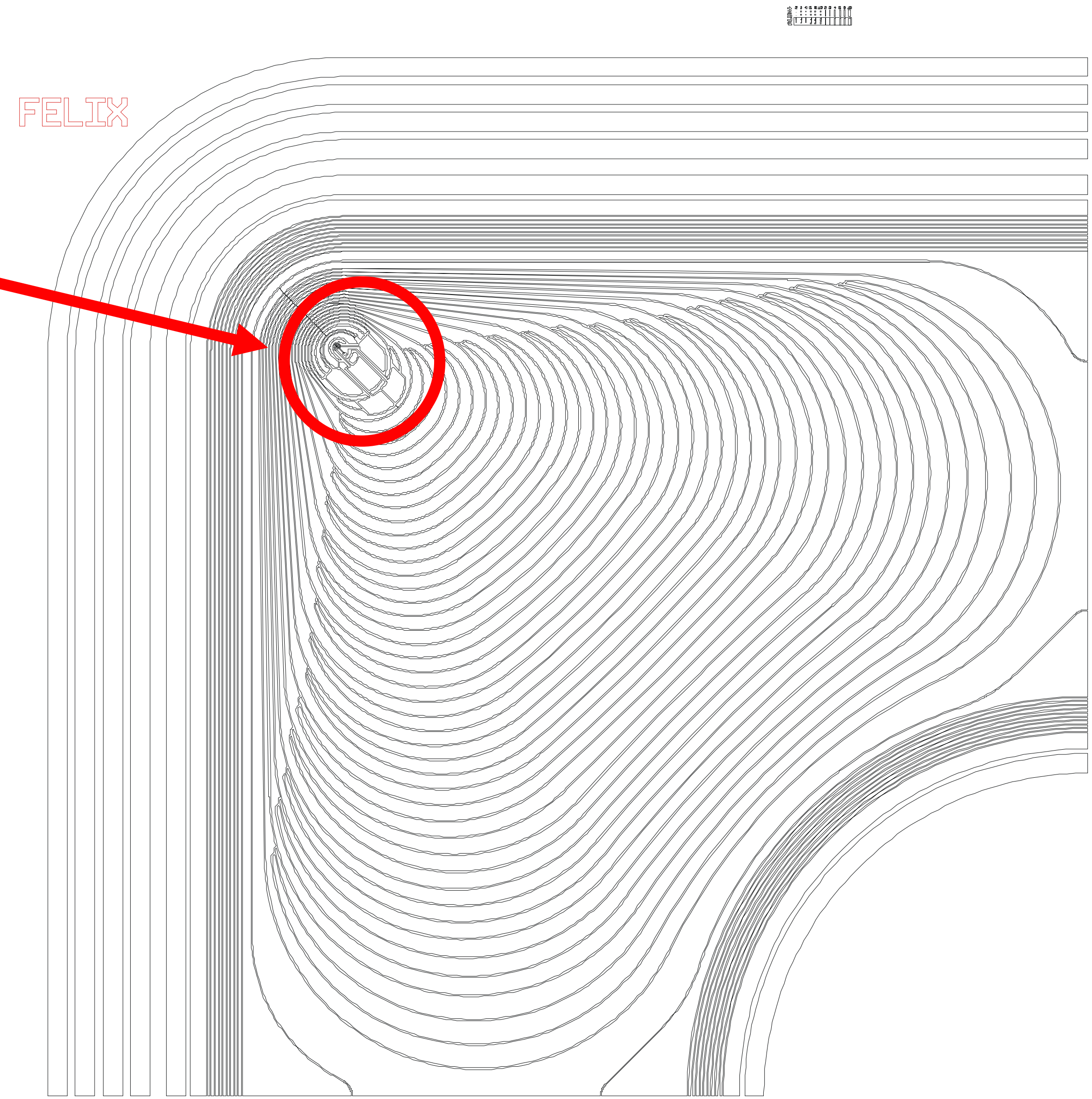

SDD4 potential energy

Radiation entrance window

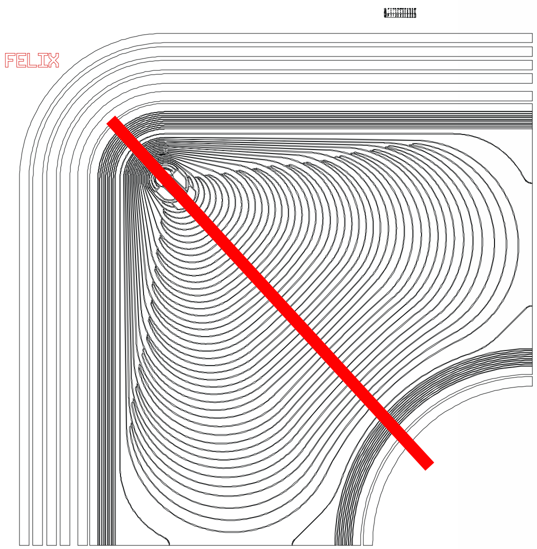

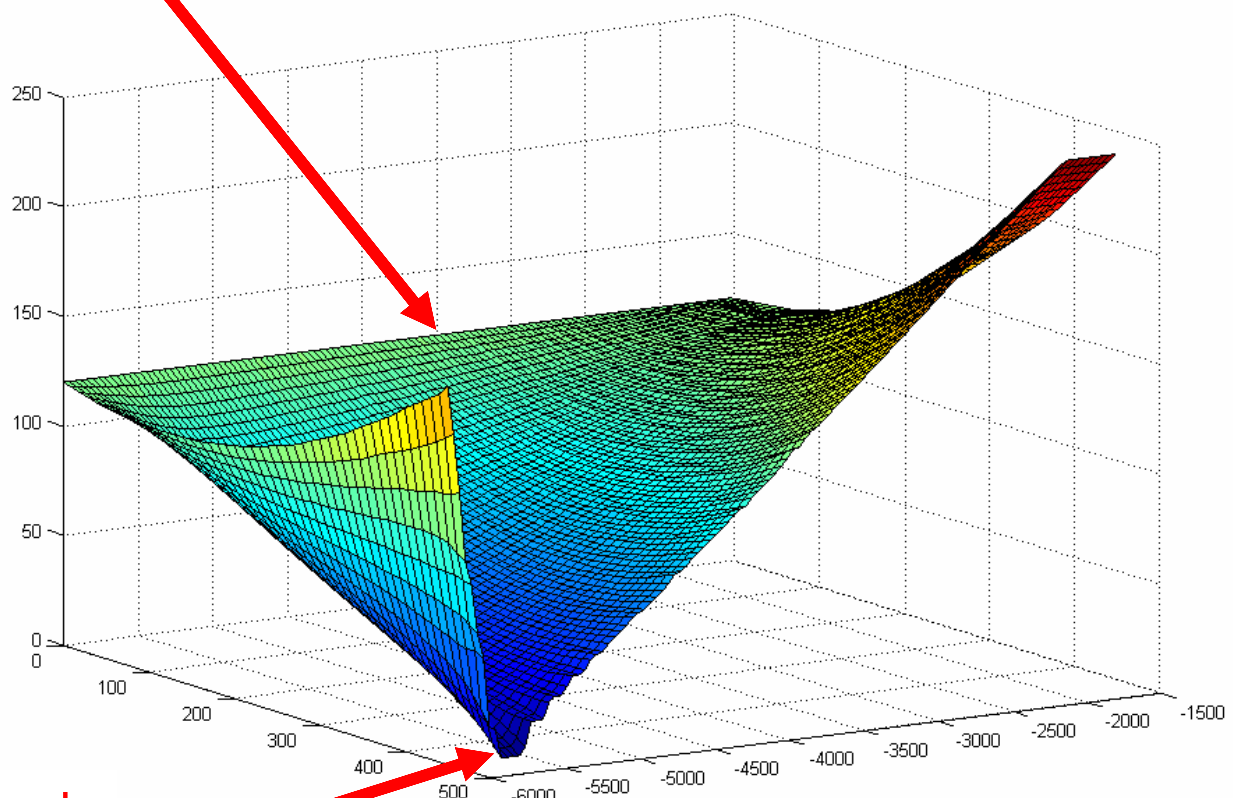

Collecting anode and input JFET

$$C_{DET}+C_{JFET} \approx 120fF$$

SDD4 preliminary results

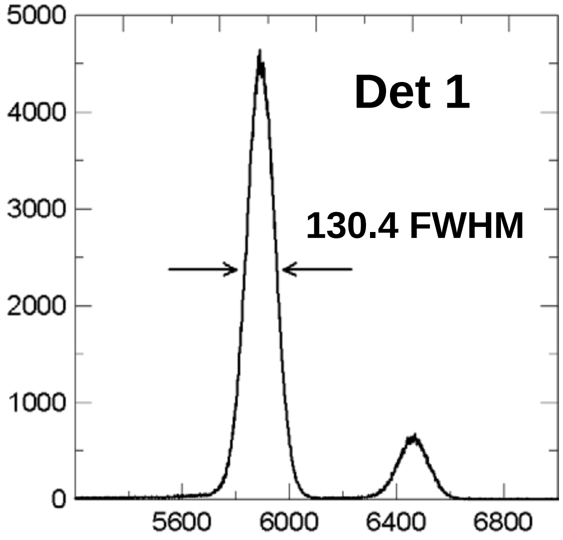

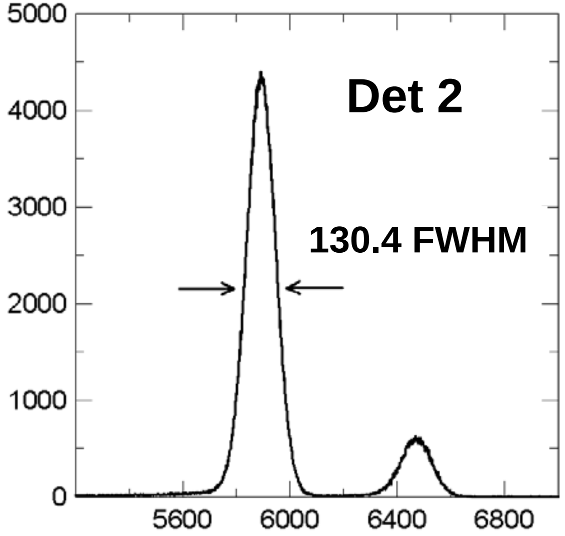

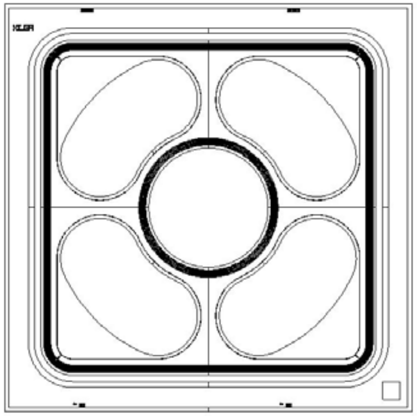

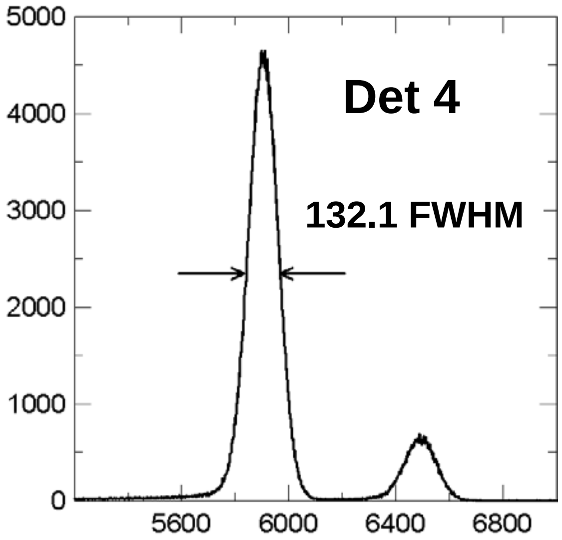

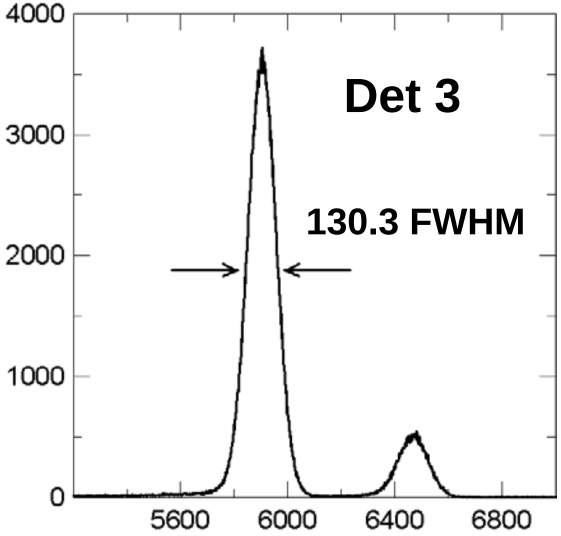

Radiation source: ^{55}Fe
Count rate ≈ 2 kcps / channel
τ_{sh}=1.5μs   NO collimation

SDD4 preliminary results

Peak to valley ratio

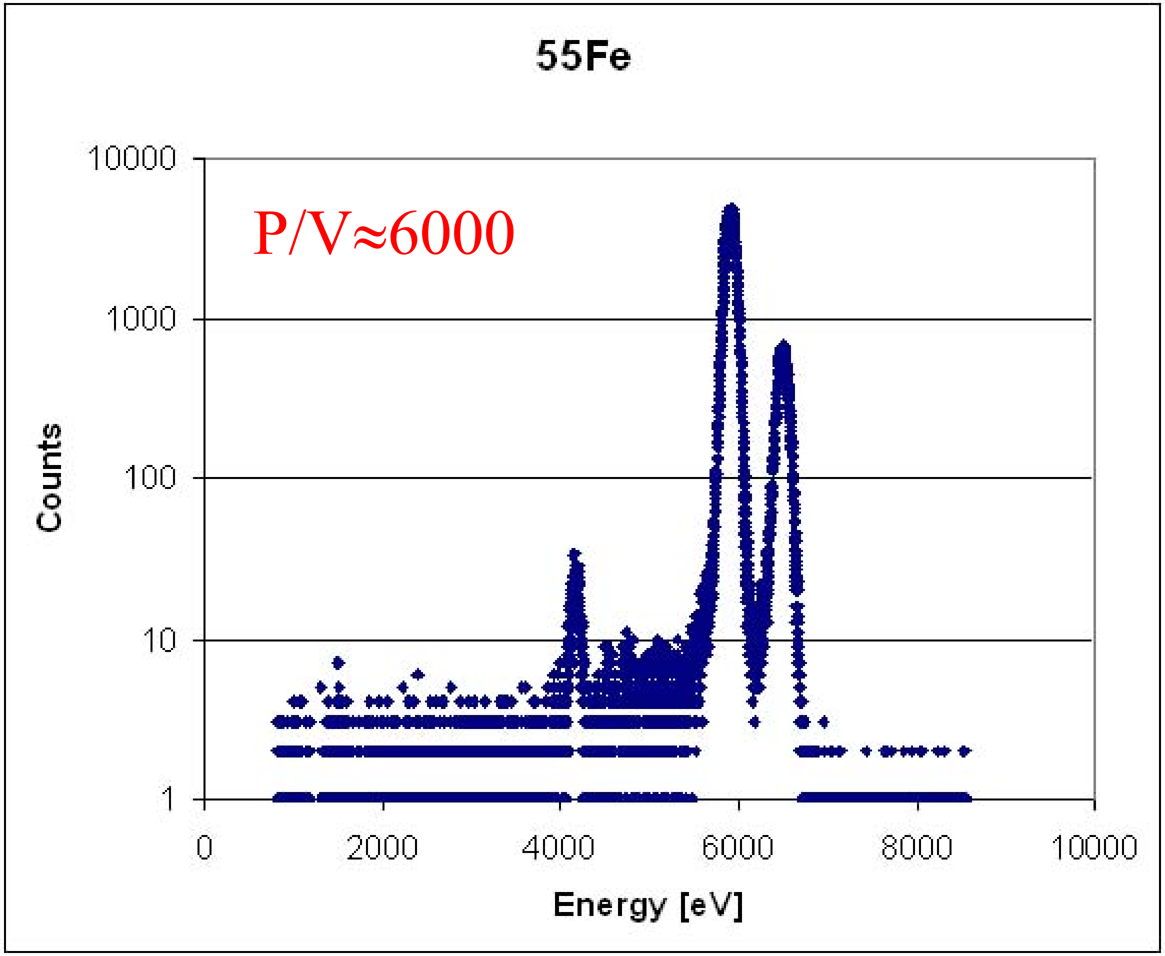

Tsh=500ns   Beam collimated: ∅≈500μm

SDD4 preliminary results

Resolution vs count rate

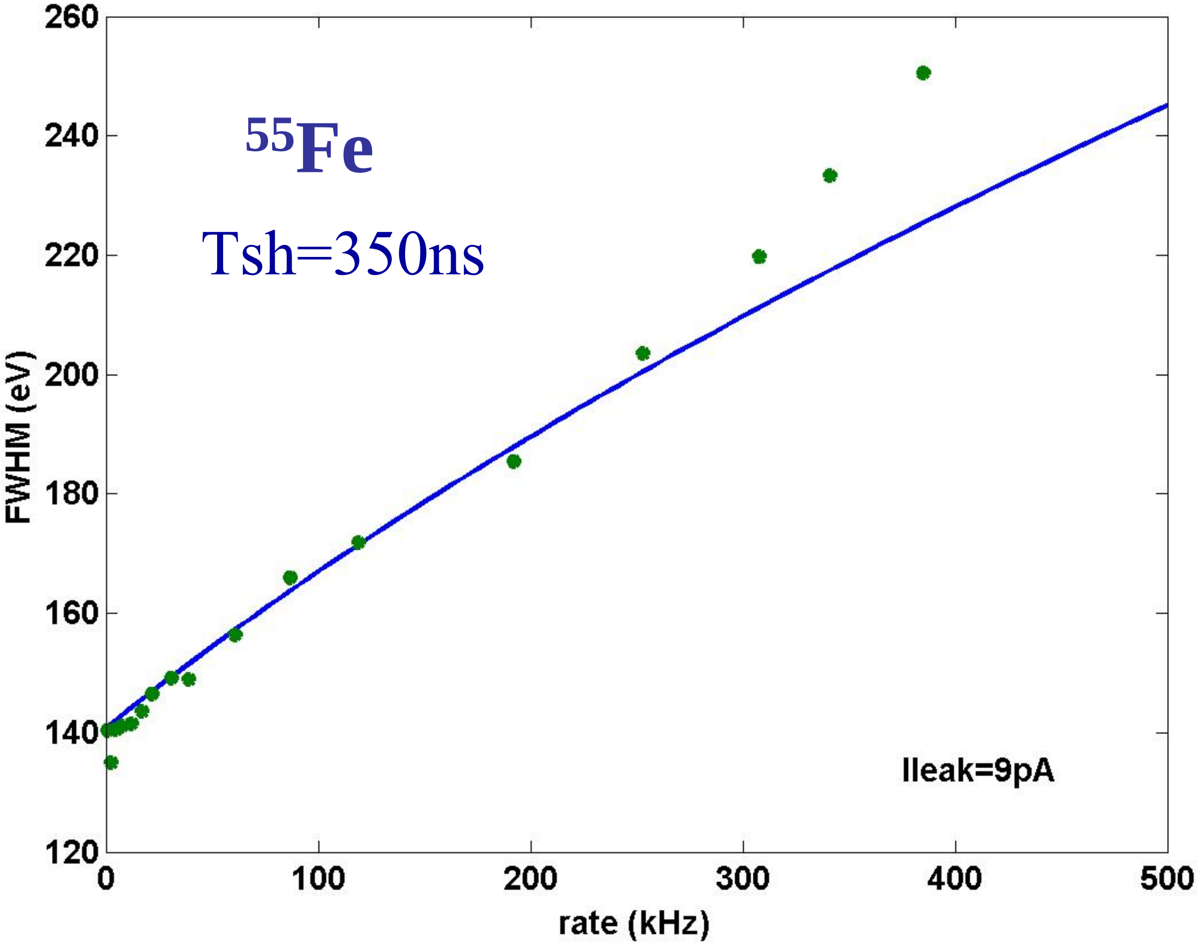

Counts per channel

SDD4 measurement head setup

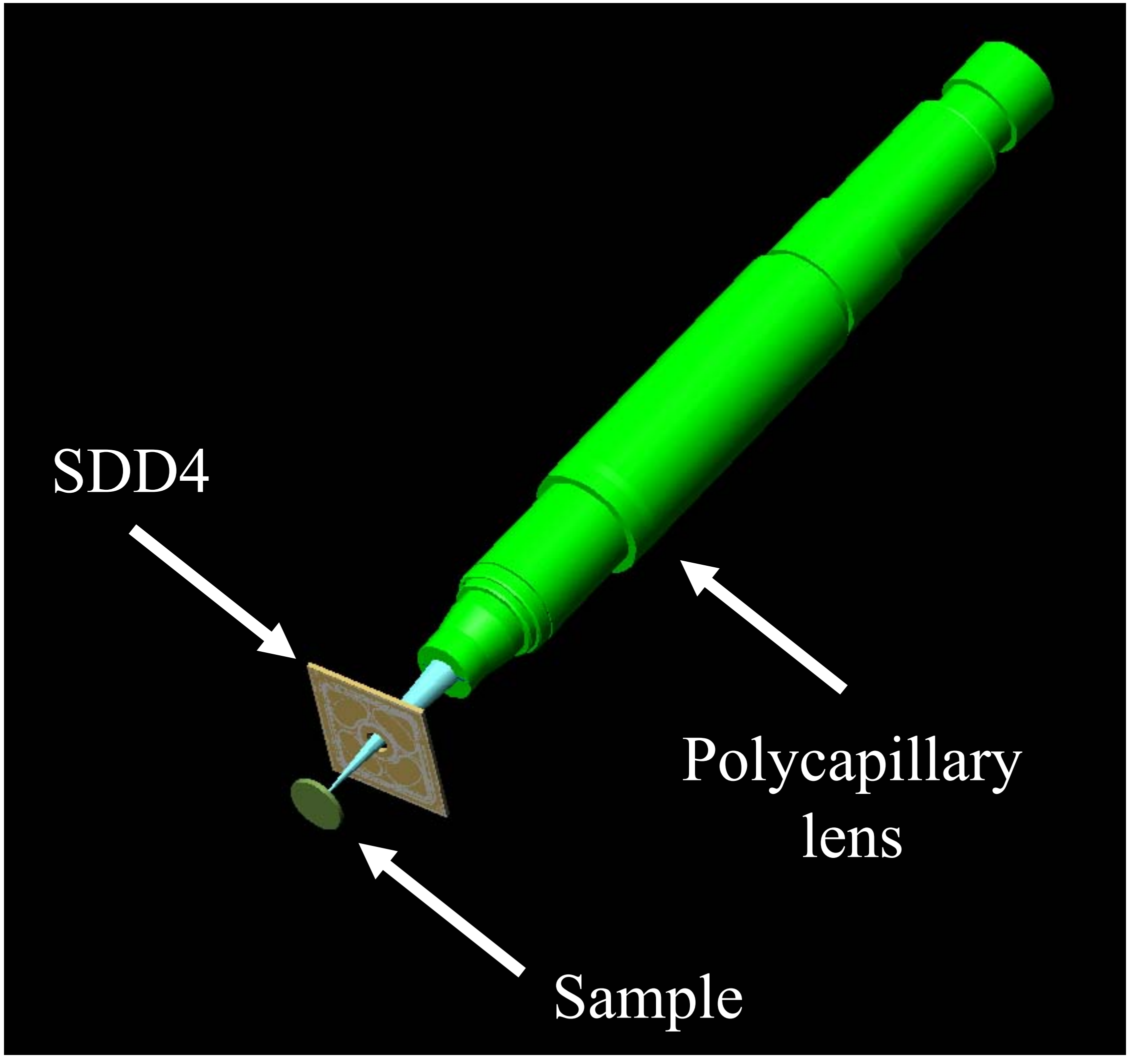

The ceramic board with electronic components

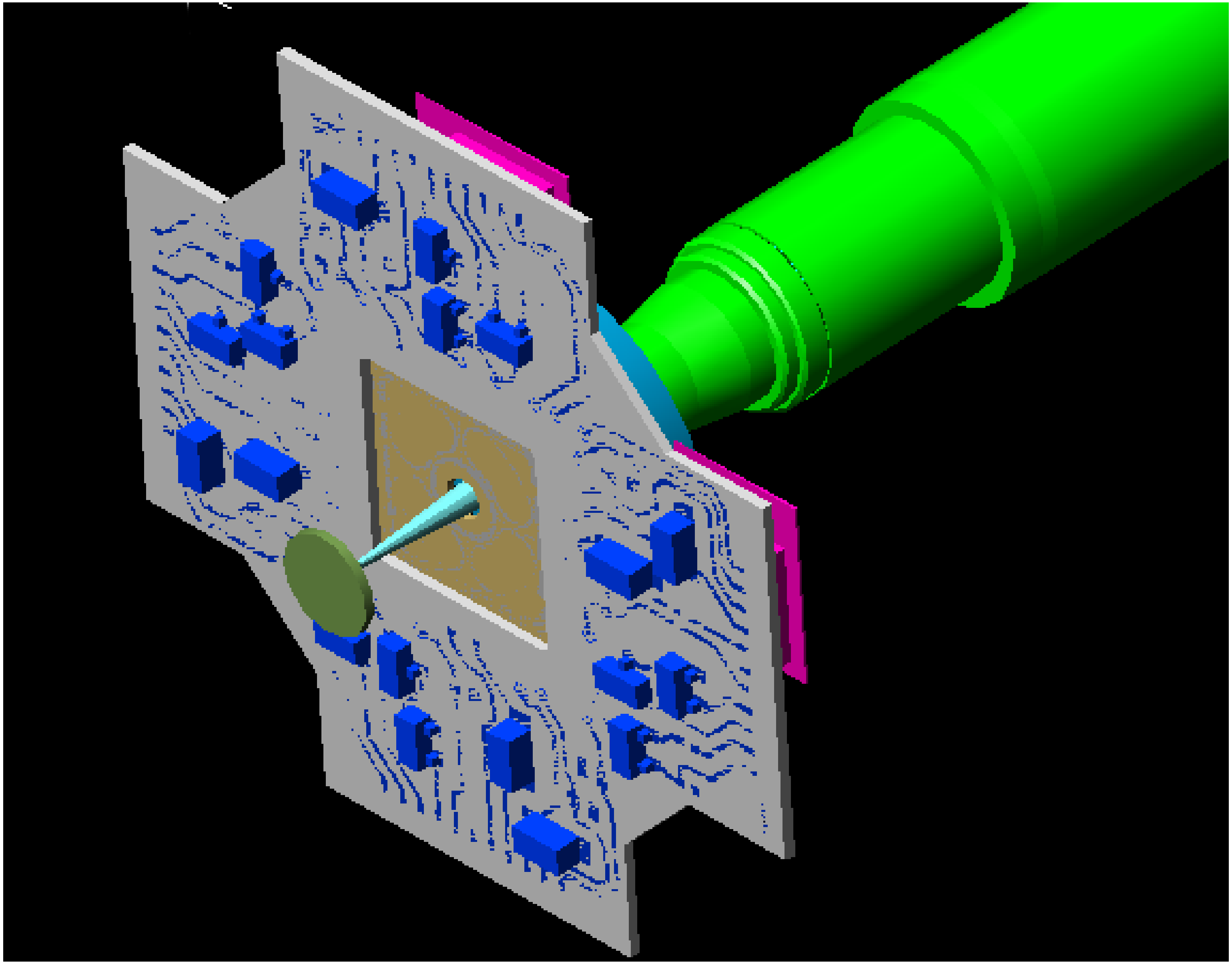

The collimator

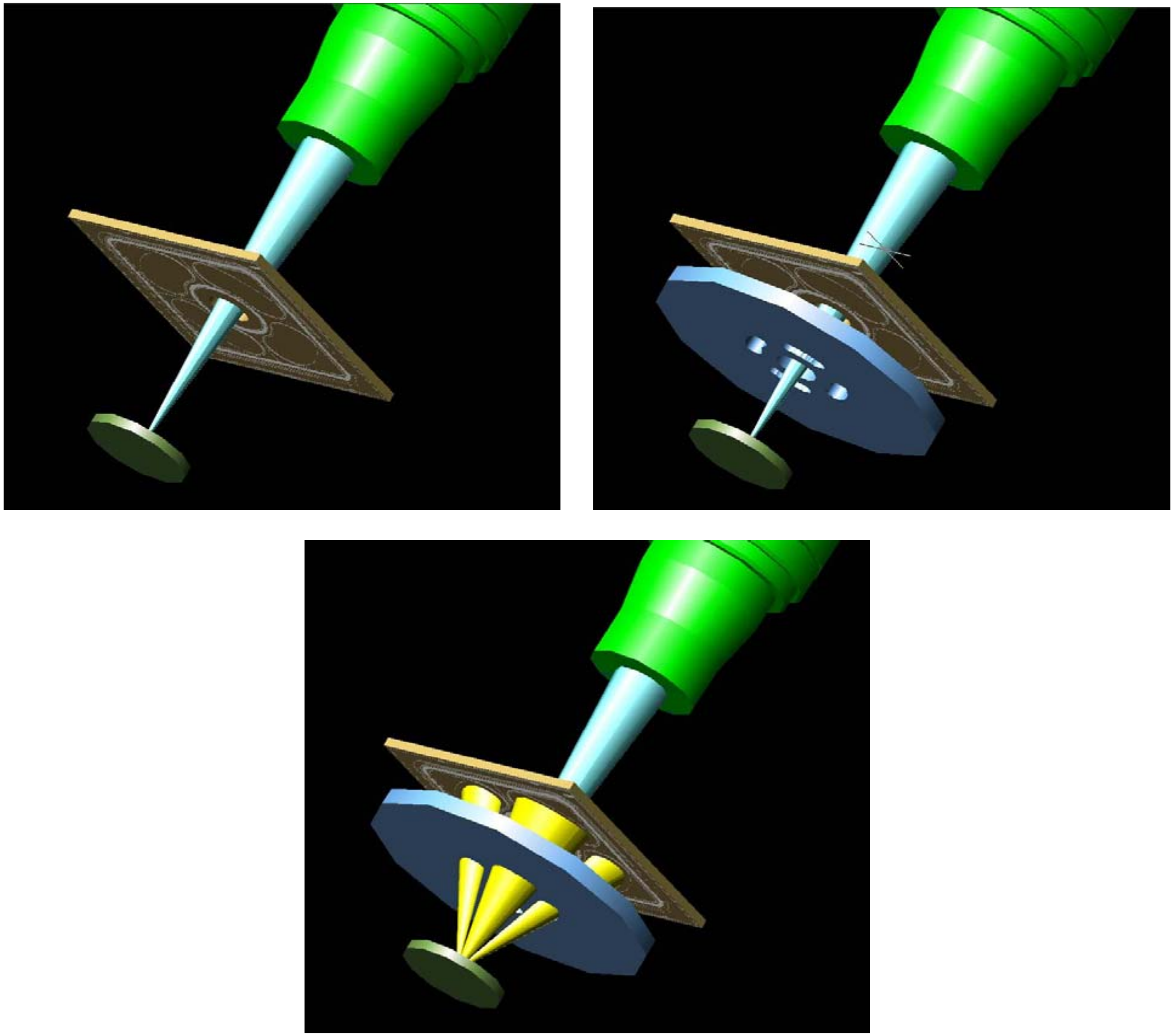

The Peltier refrigerators and the Be windows

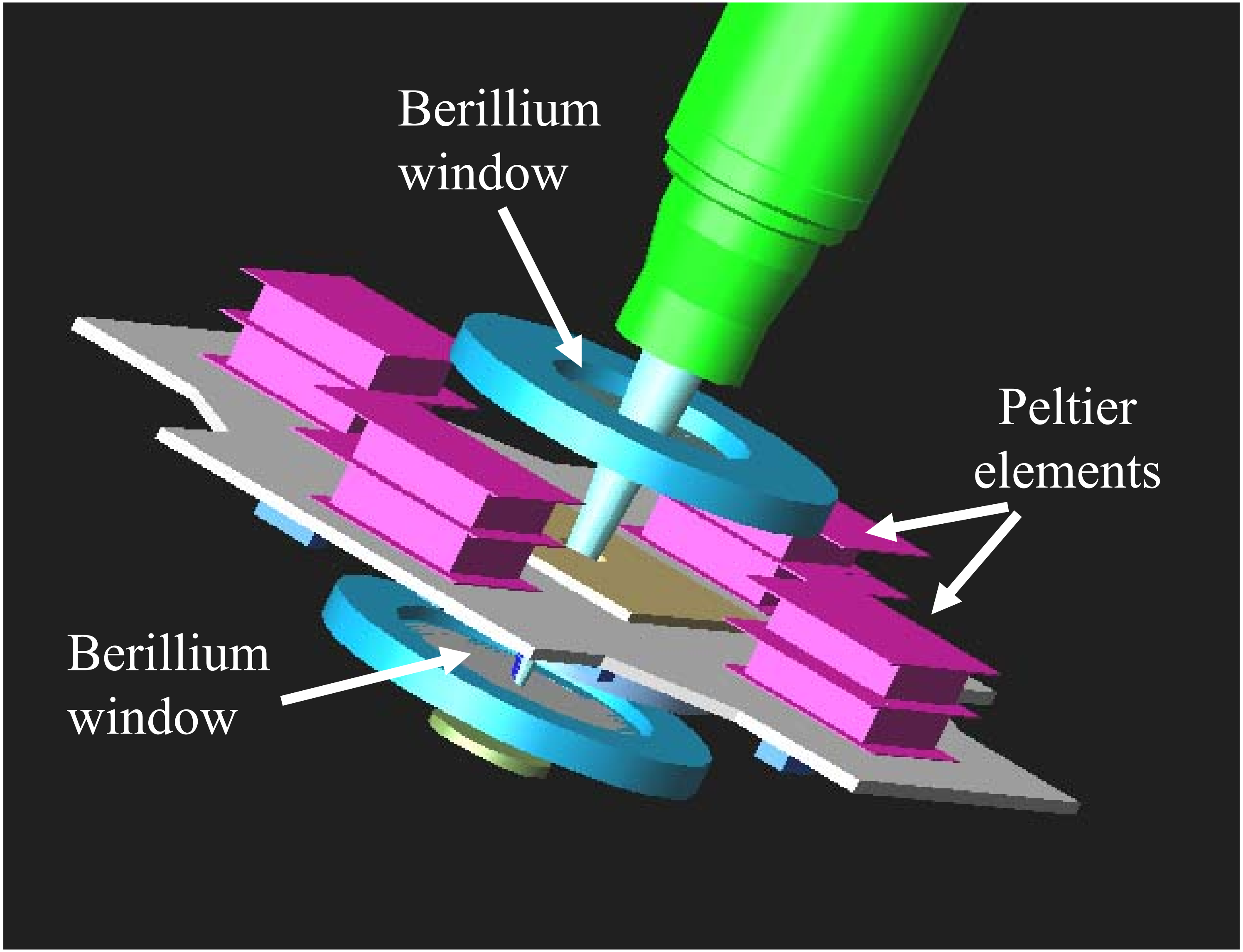

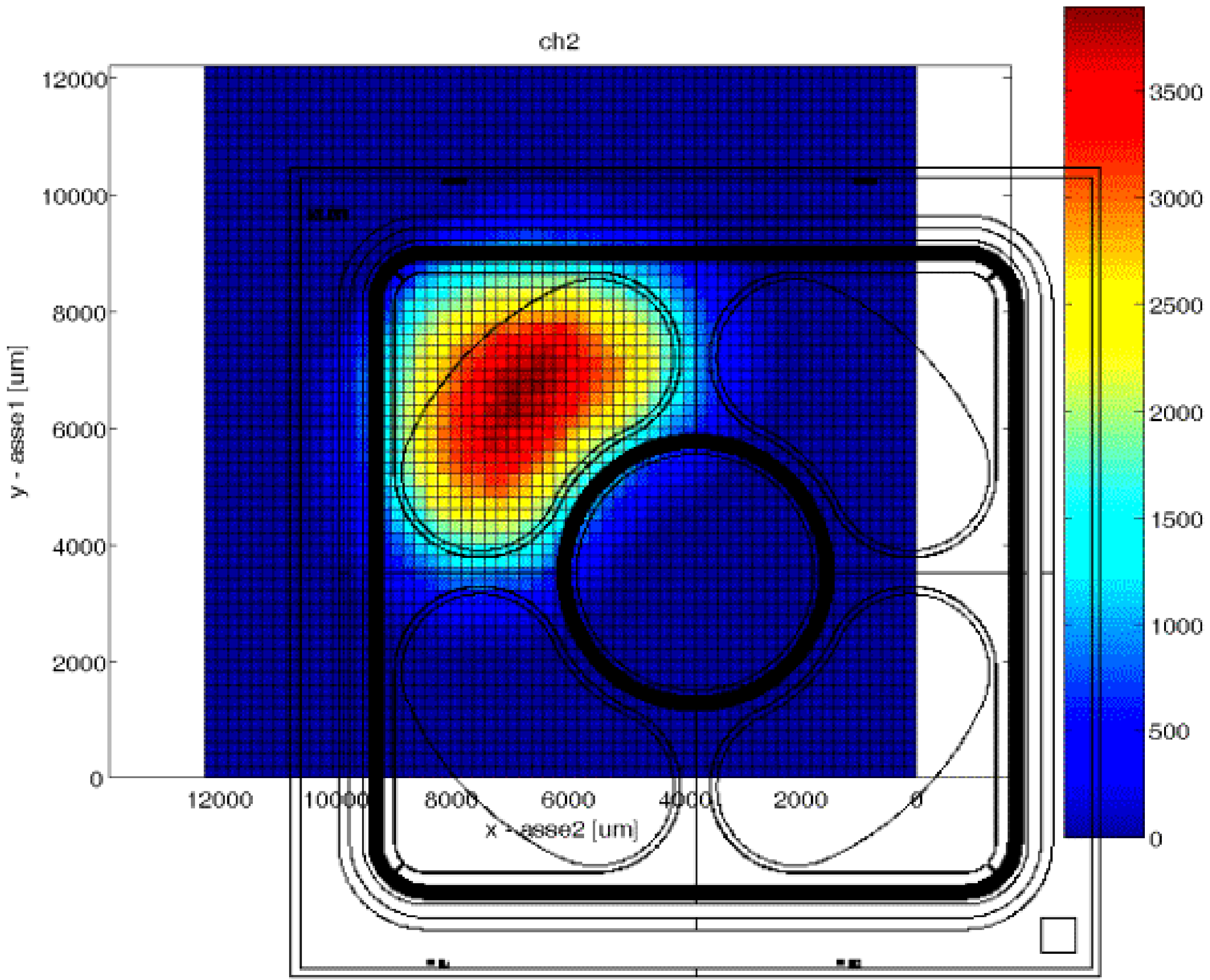
ch2
12000
10000
8000
6000
4000
2000
0
y - asse1 [um]
12000
10000
8000
6000
4000
2000
0
x - asse2 [um]
3500
3000
2500
2000
1500
1000
500
0

Readout electronics + Data acquisition system for the SDD4

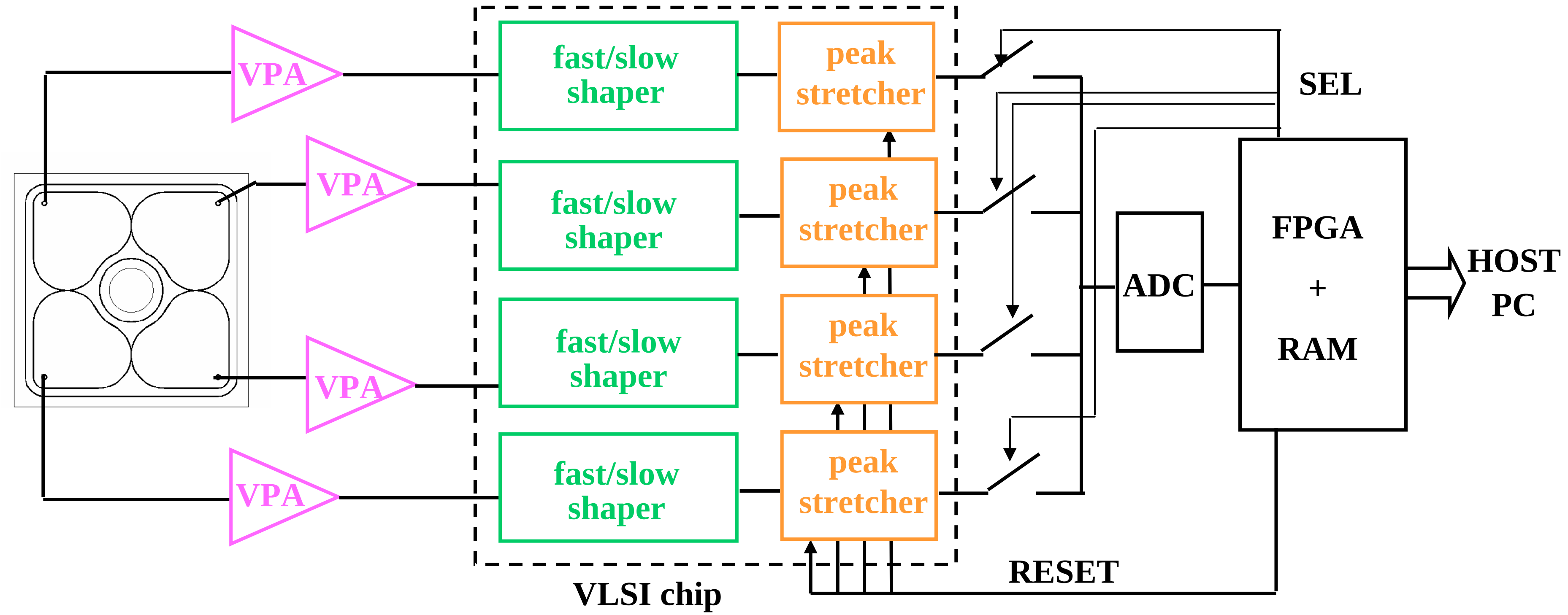

Scheme of principle of the new fast acquisition system presently under development (the histogram is made 'on board')

Researchers involved: A.Longoni, C.Guazzoni, S.Buzzetti

PRESTAZIONI DEL NUOVO SISTEMA DI ACQUISIZIONE

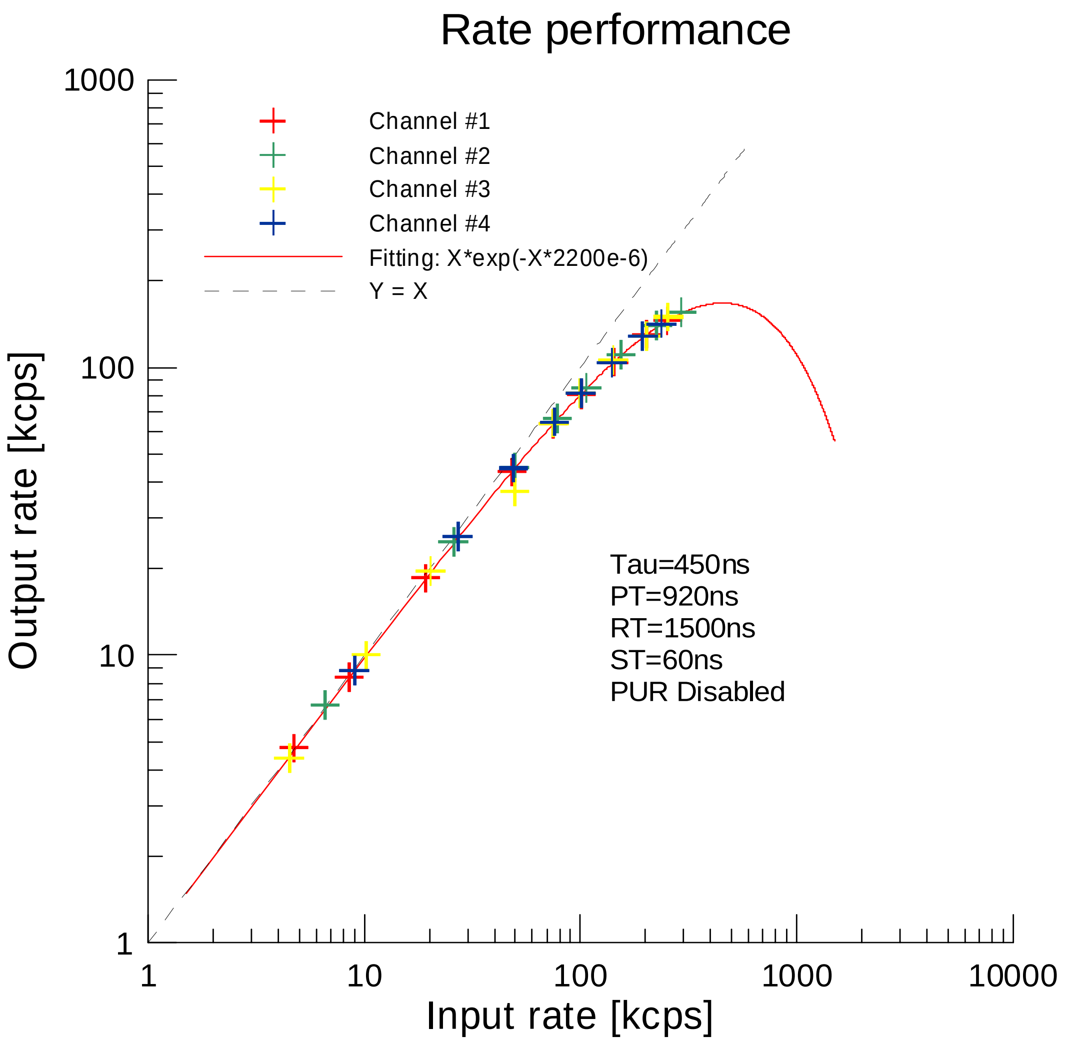

Some applications of the multi-element SDDs

The concept of the multi-element spectrometer for XRF elemental mapping

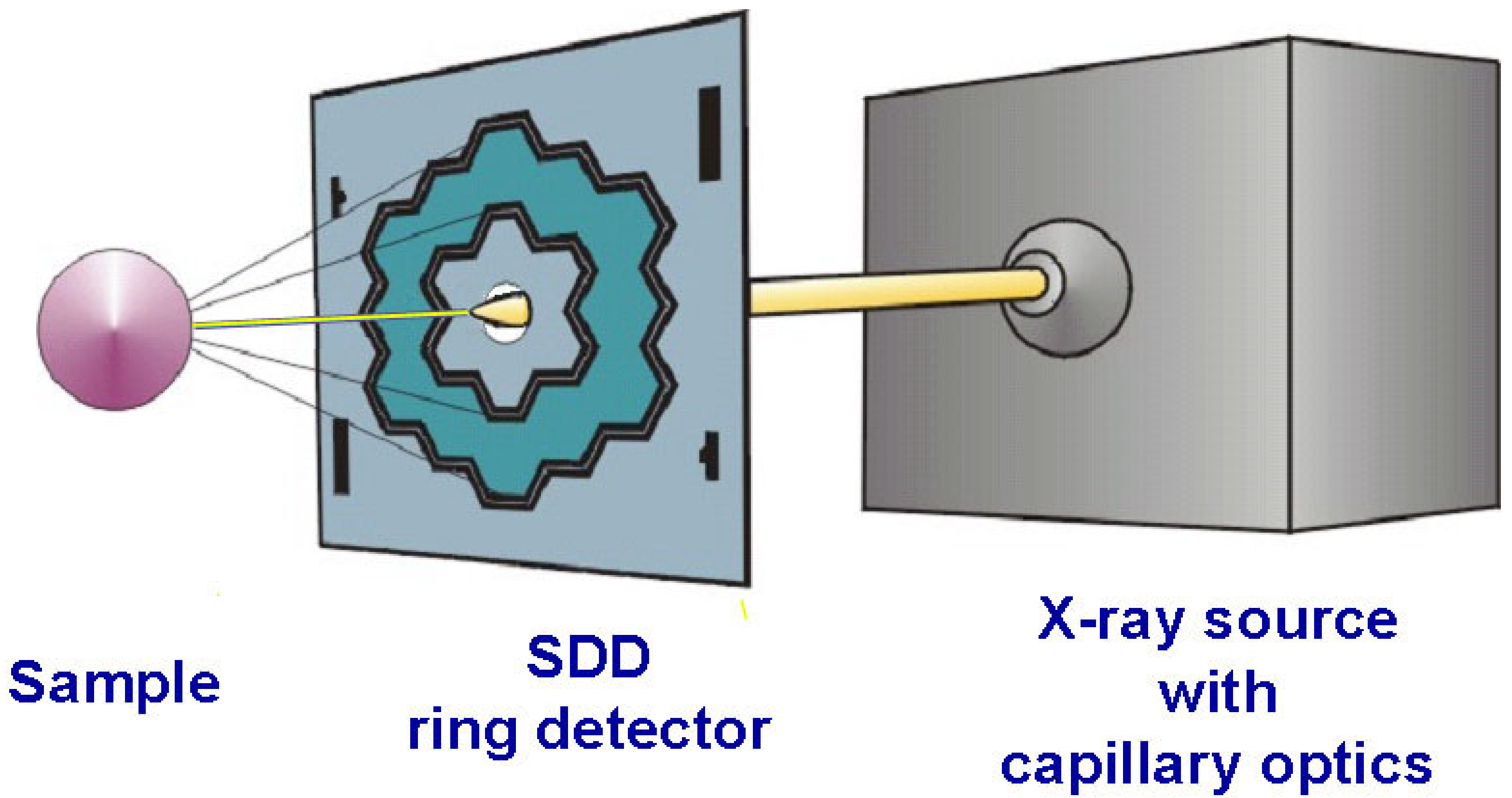

Researchers involved: A.Longoni, C.Fiorini

A polycapillary X-ray lens allows:

an higher photon flux in a small excitation spot

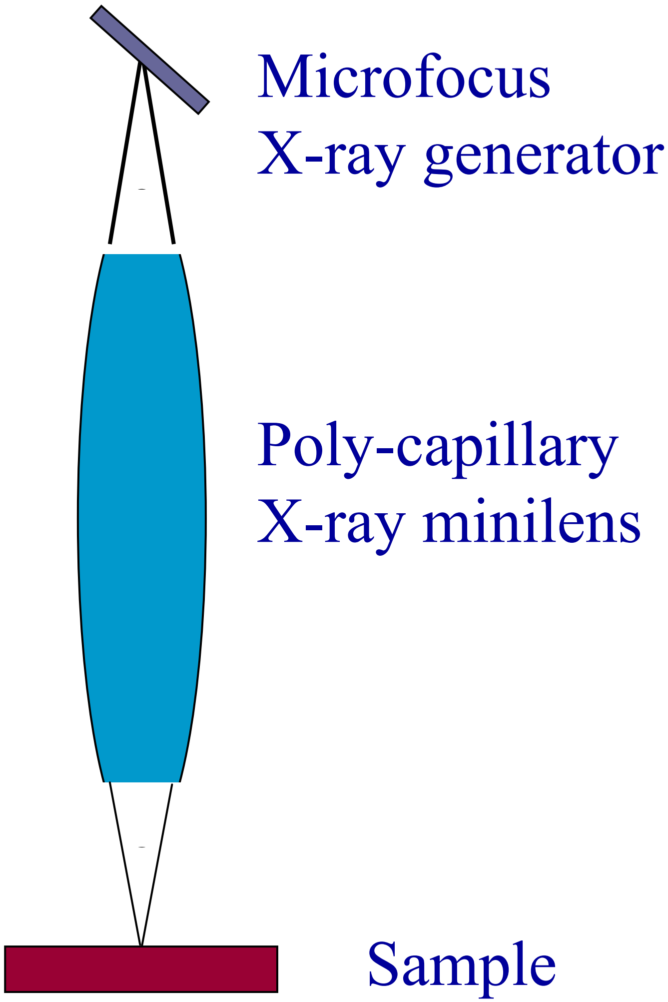

A ring detector centered on the excitation beam allows

•a larger collection angle of the fluorescence

•an higher detection efficiency at low energy

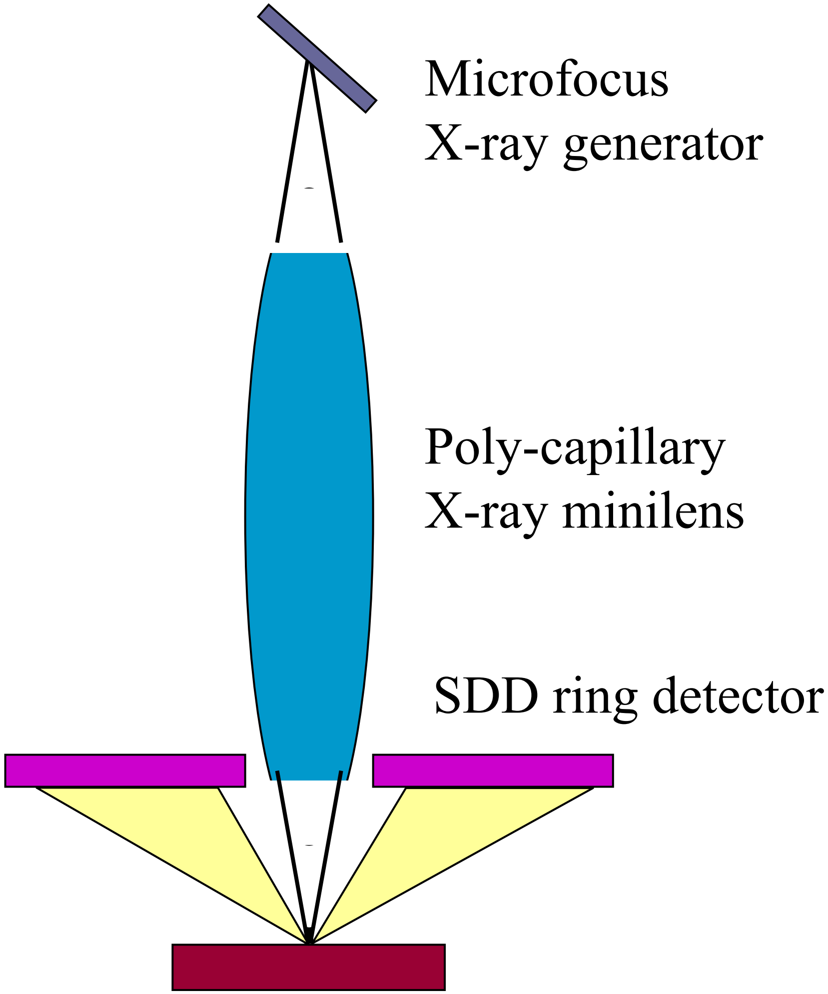

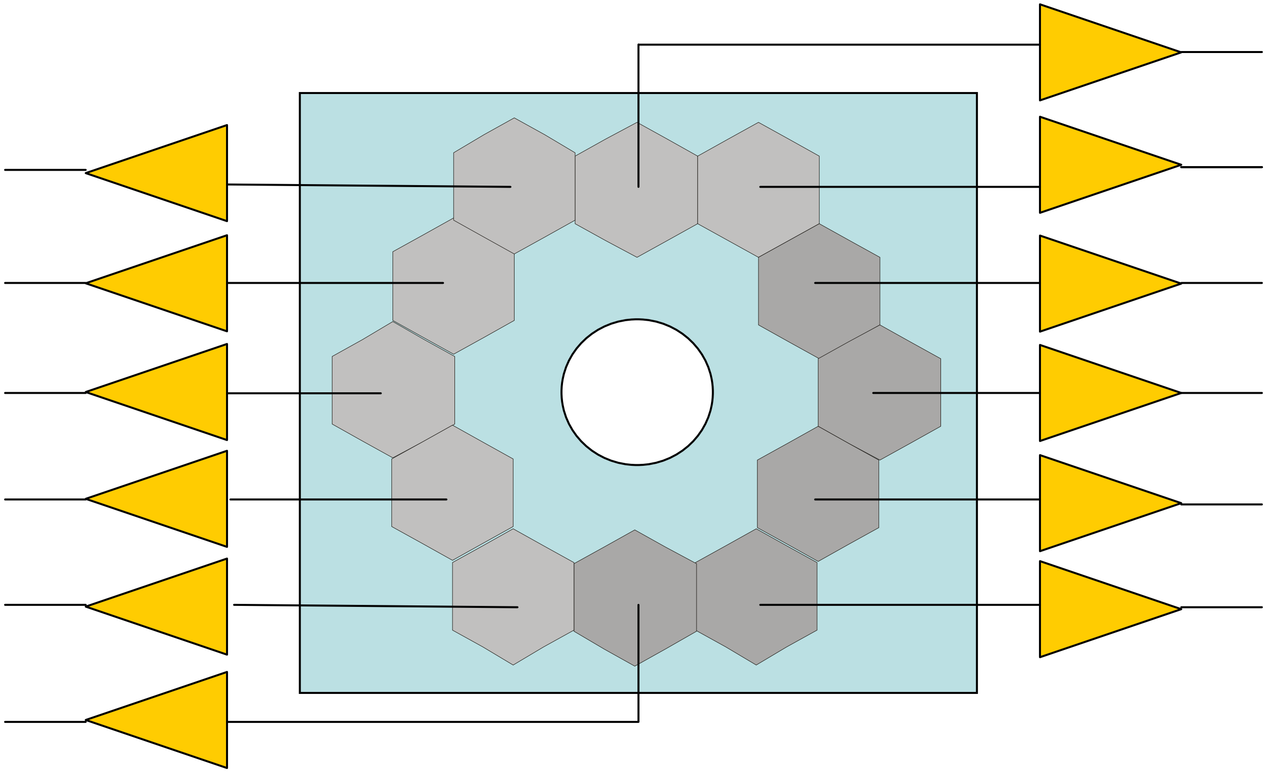

A multi-element detector allows:

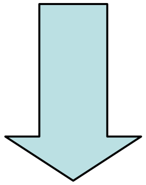

•an higher detection rate for the same total active area

The excitation-detection unit

Microfocus X-ray generator * W anode
50 kV max DC voltage, 30 W max anode load

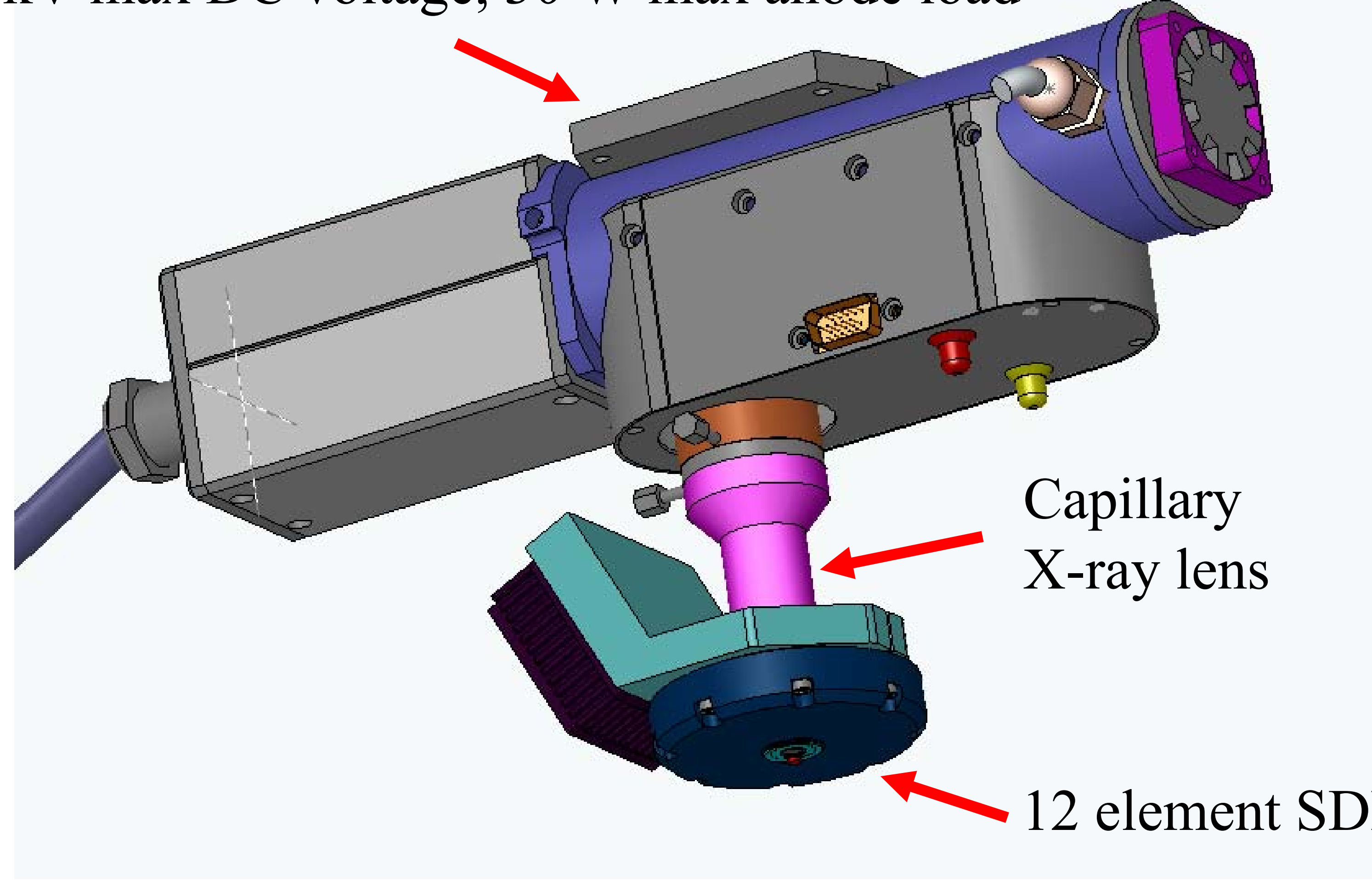

Capillary
X-ray lens

12 element SDD

The X-ray mini-lens parameters

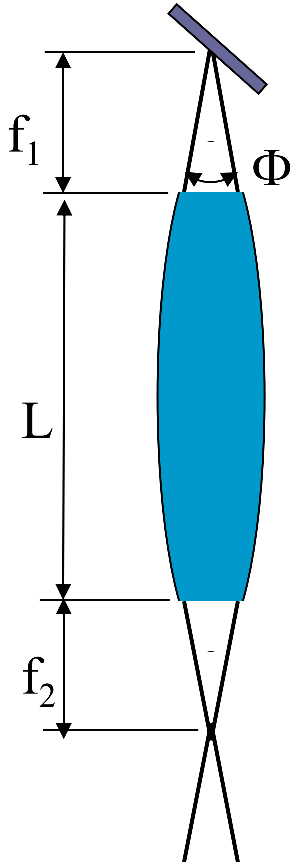

f1=40 mm
f2=20 mm
L=77 mm
Φ=0.094 rad

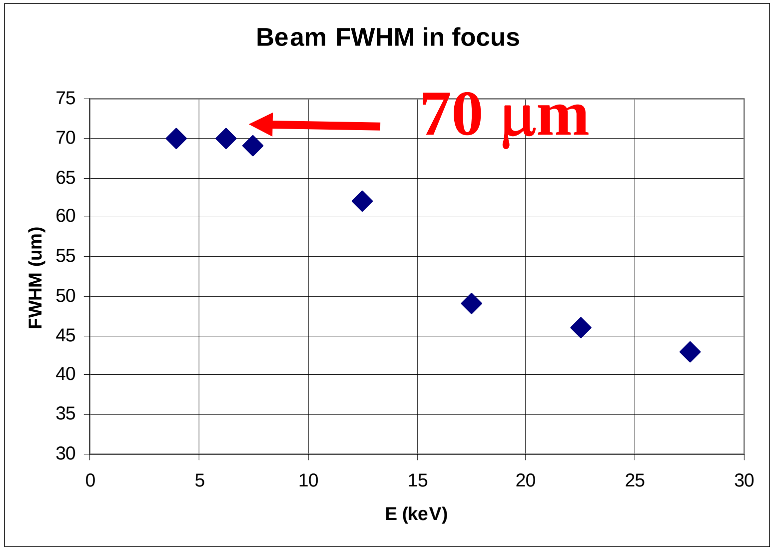

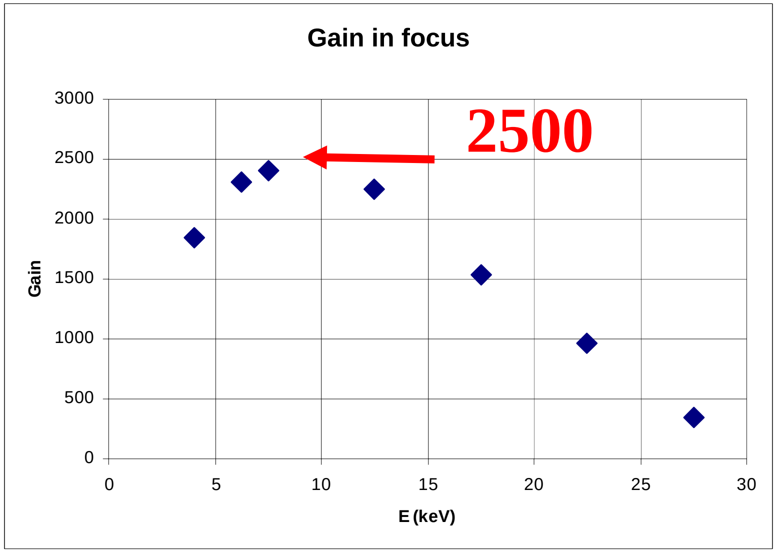

Measured with 15 μm pinhole

The spatial resolution of the spectrometer - 1

Knife-edge test

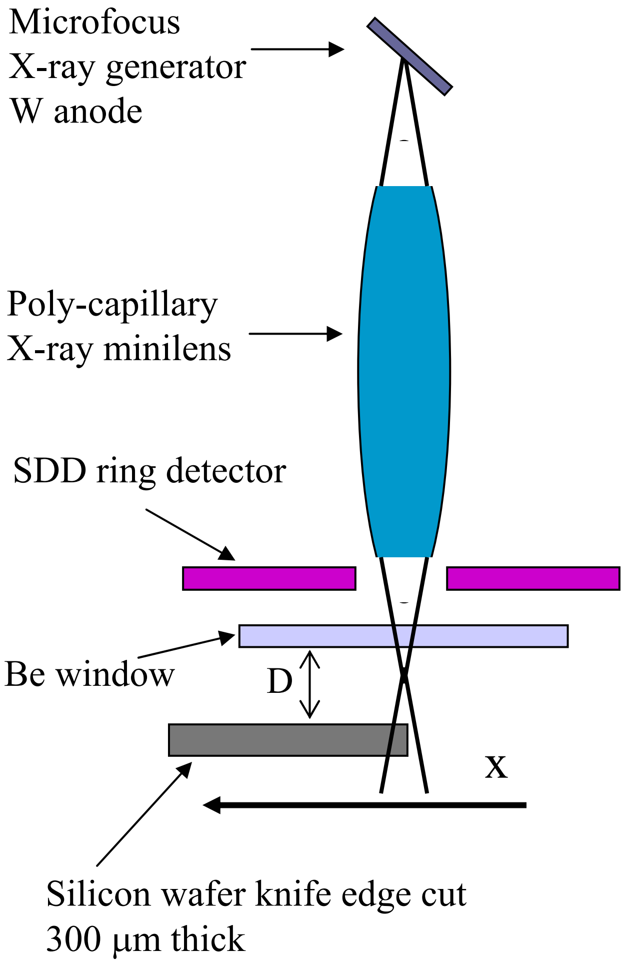

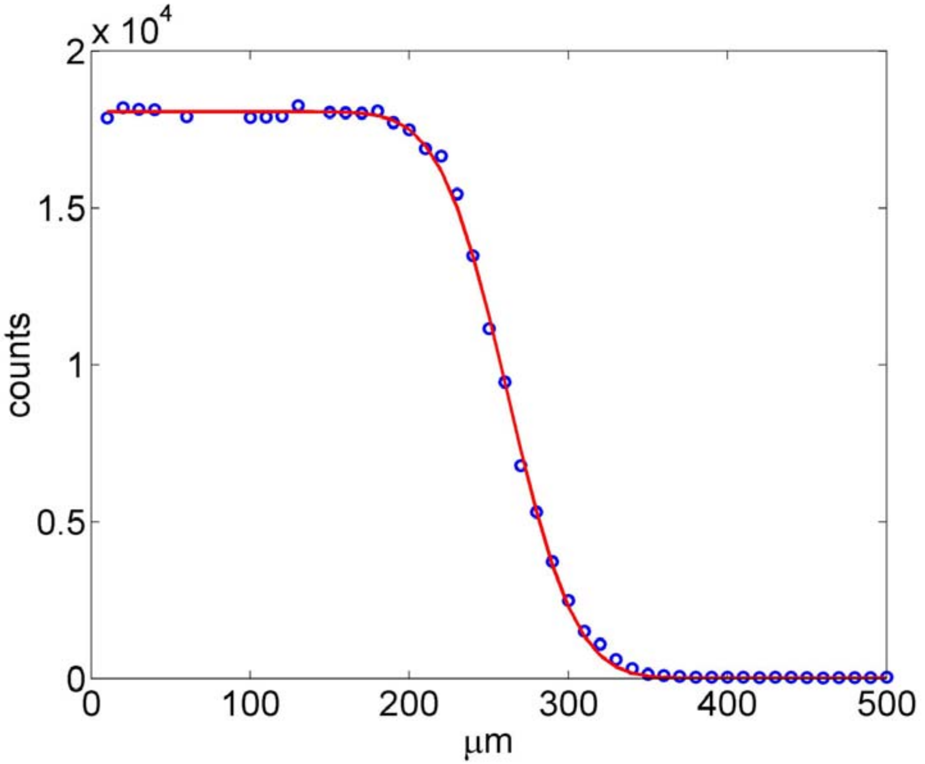

D=1mm FWHM=78μm
(slightly out of focus)

Geology

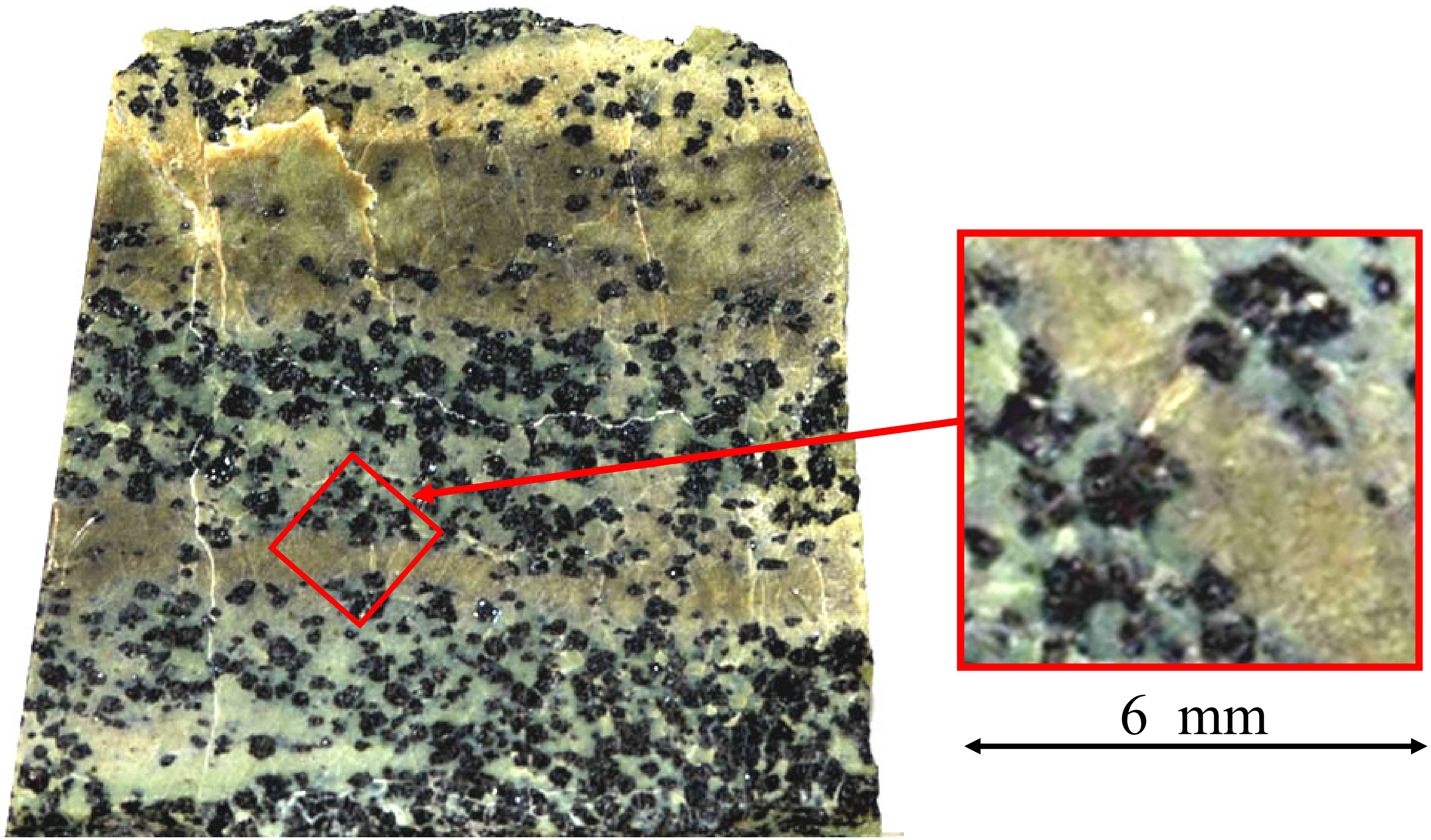

Chromite

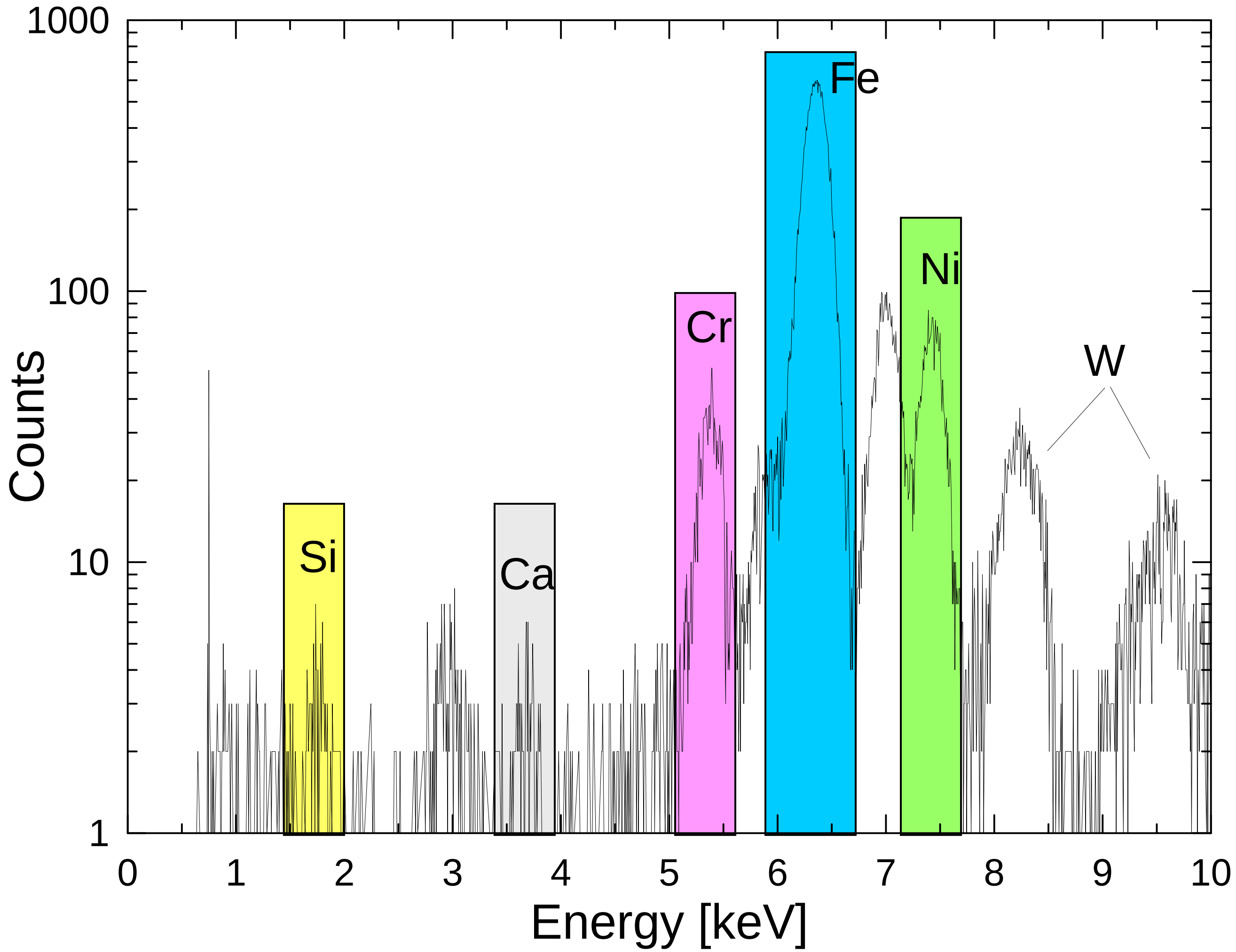

1000
100
10
1
0
1
2
3
4
5
6
7
8
9
10
Counts
Energy [keV]
Si
Ca
Cr
Fe
Ni
W

Chromite: main elements

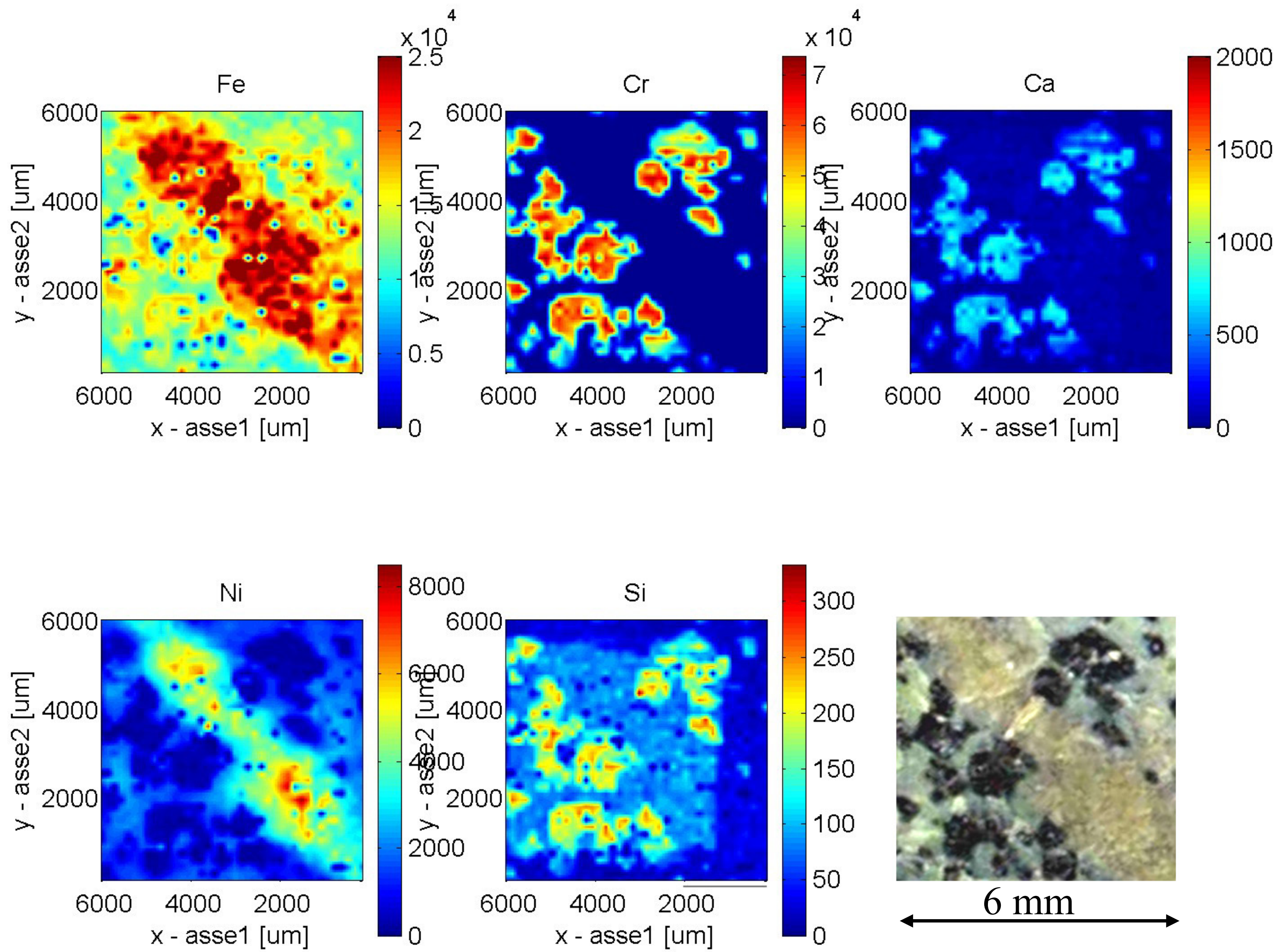

Lombard buckle – inlaid work (agemina)
Second quarter of VII century A.C.
Trezzo d'Adda, Italy

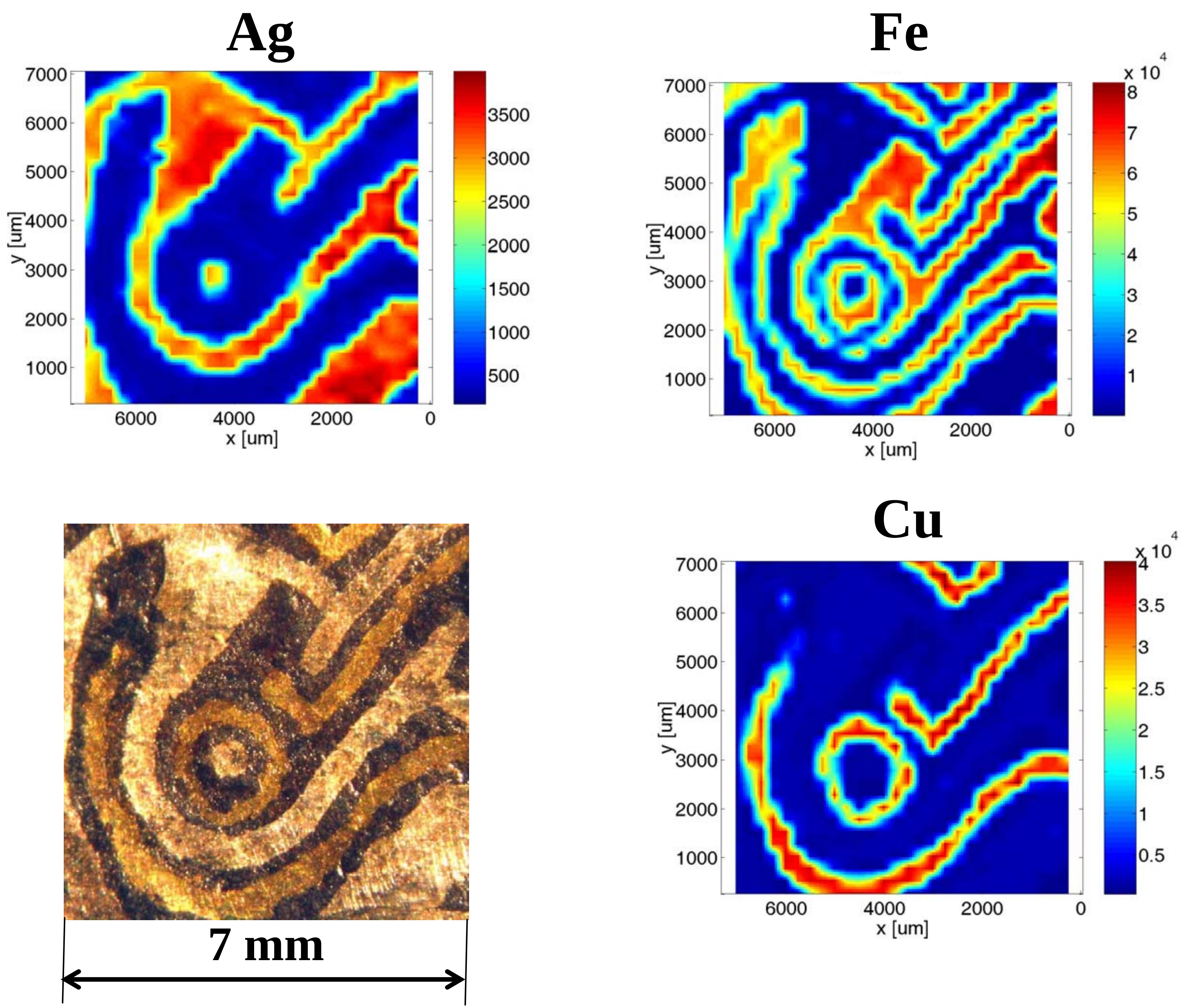

Ag
Fe
Cu
7 mm
x [um]
y [um]
3500
3000
2500
2000
1500
1000
500
x 10^4

Roman (?) ring

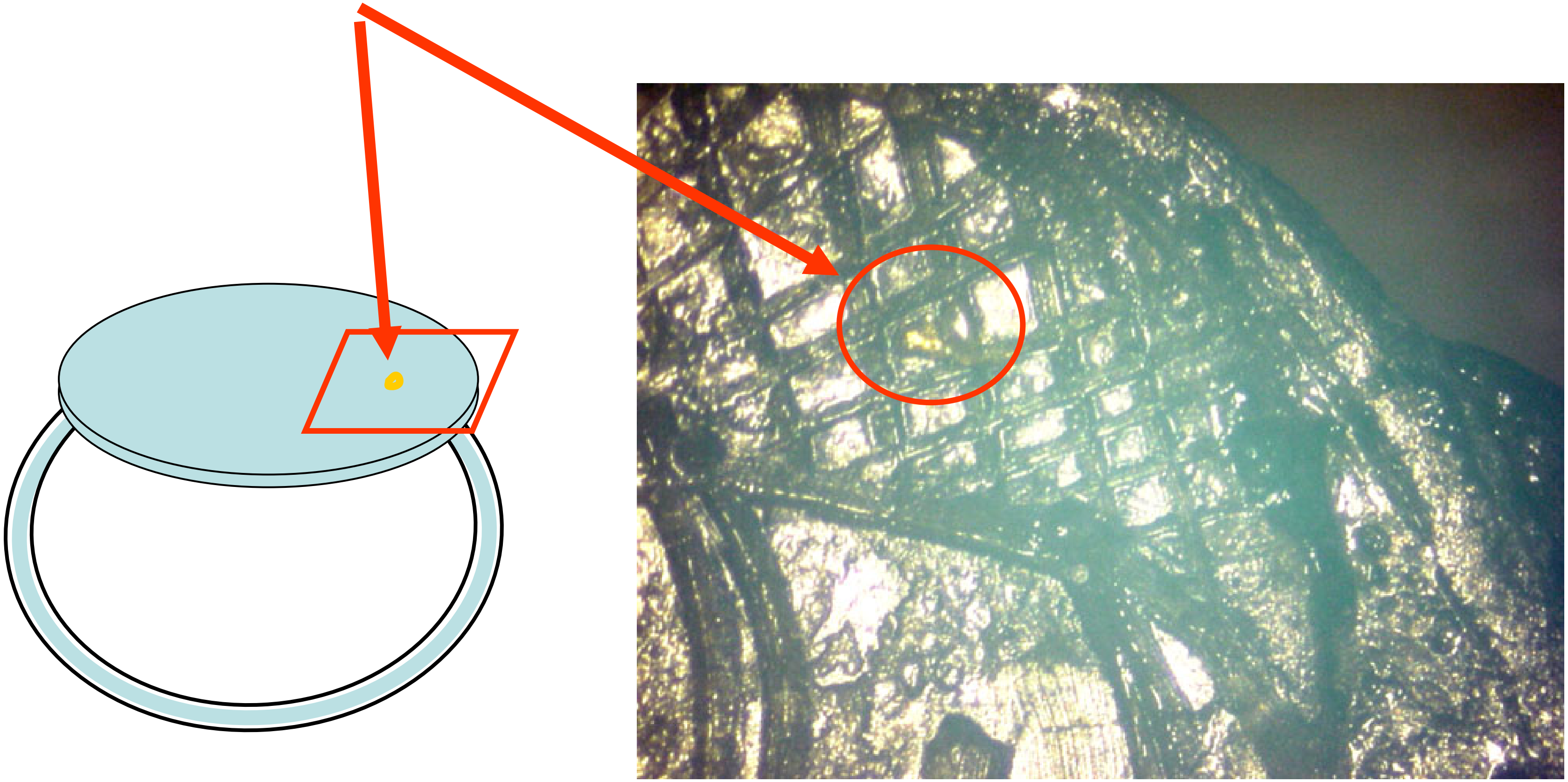

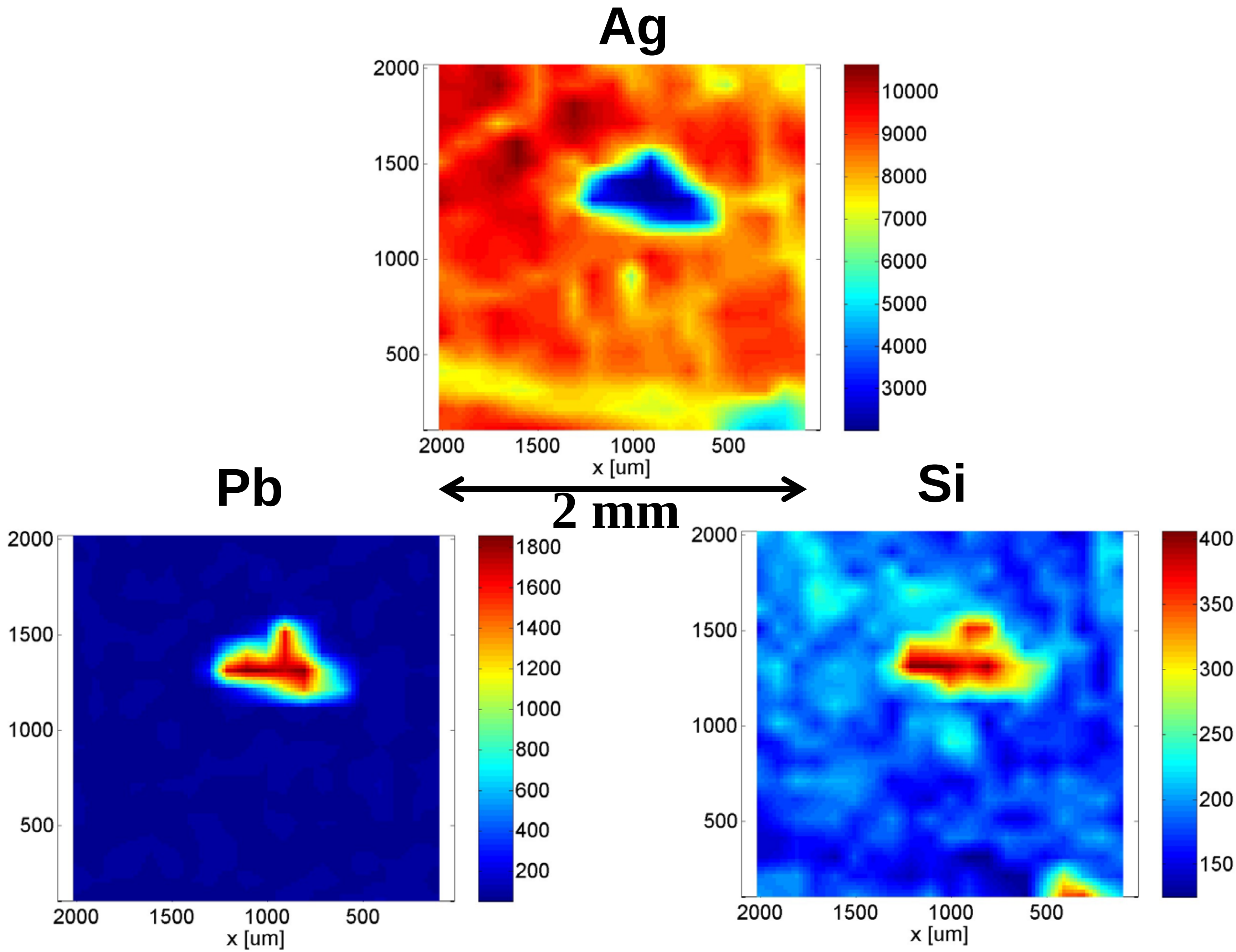
Ag
2000
1500
1000
500
10000
9000
8000
7000
6000
5000
4000
3000
2000
1500
1000
500
x [um]
Pb
2 mm
Si
2000
1500
1000
500
1800
1600
1400
1200
1000
800
600
400
200
2000
1500
1000
500
x [um]
2000
1500
1000
500
400
350
300
250
200
150
2000
1500
1000
500
x [um]

Mretallurgy: study of an Iron-Nichel alloy

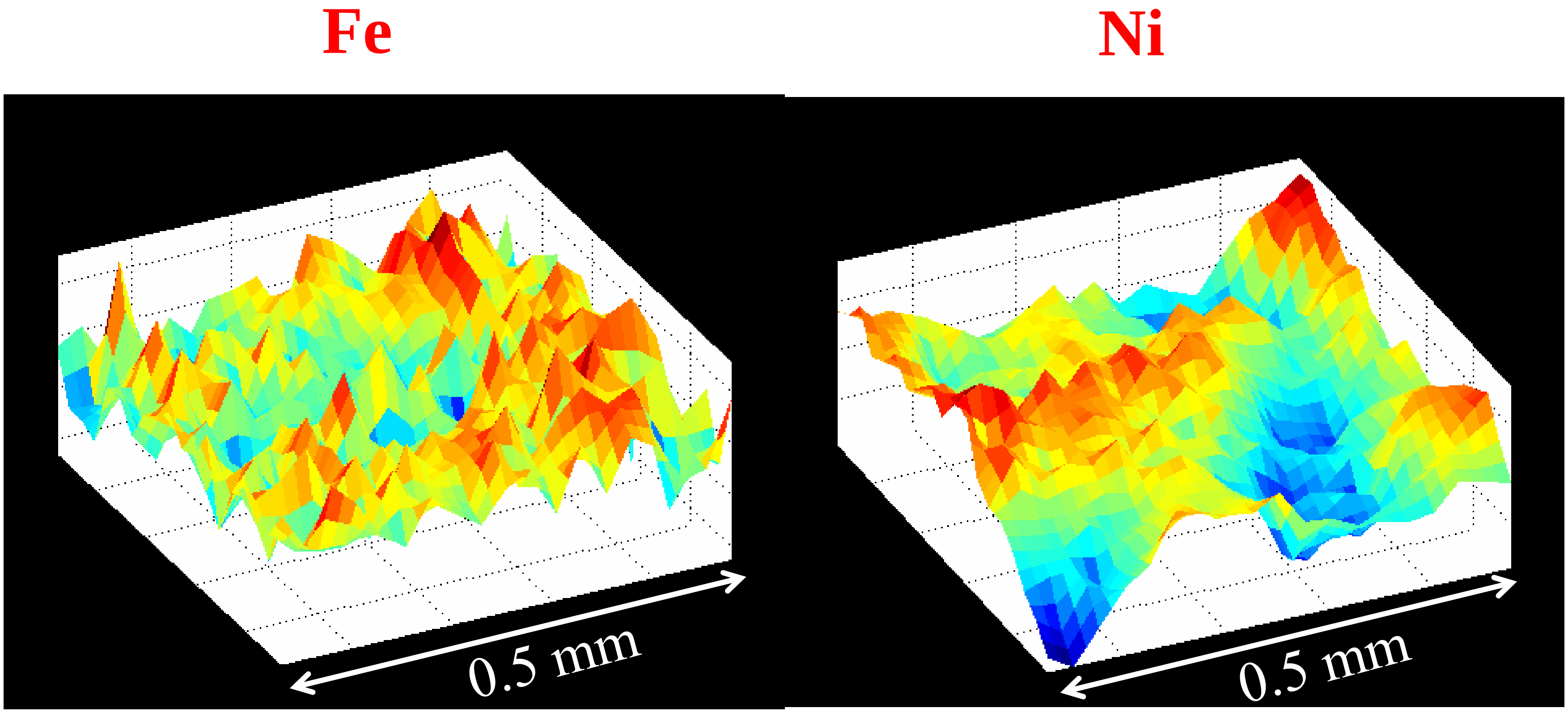

Iron powder with Nickel grains partially diffused on the Iron surface during the syntherization process at 1120 C

Biolology

A leaf feed with a fertilizer

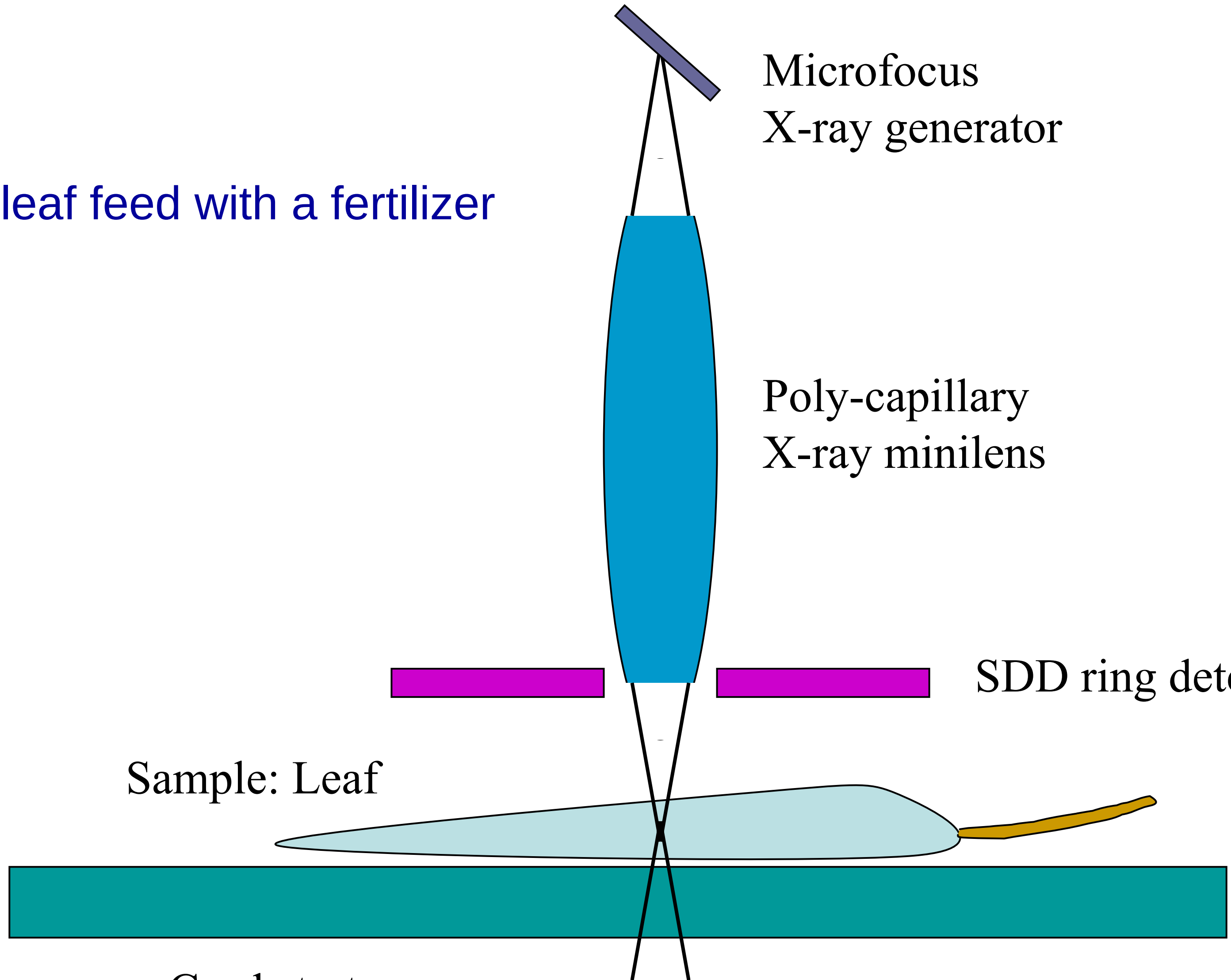

Leaf ‘fluorescence’ (detail)

K

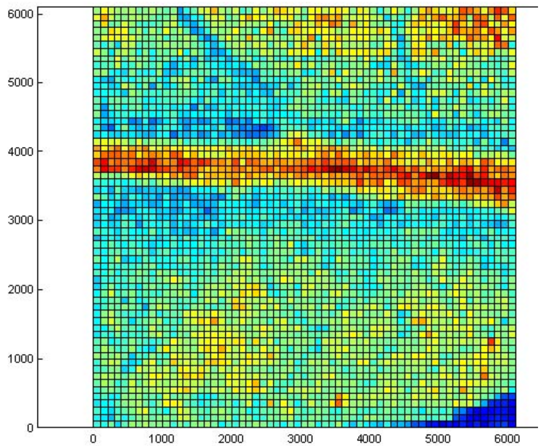

Ca

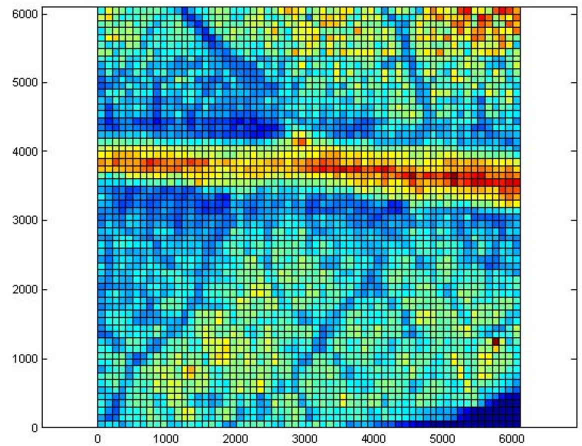

Mn

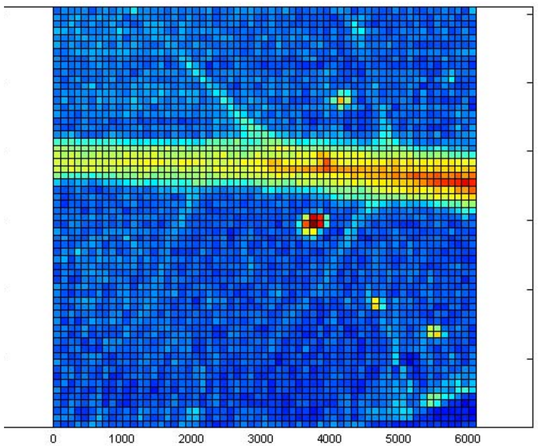

Fe

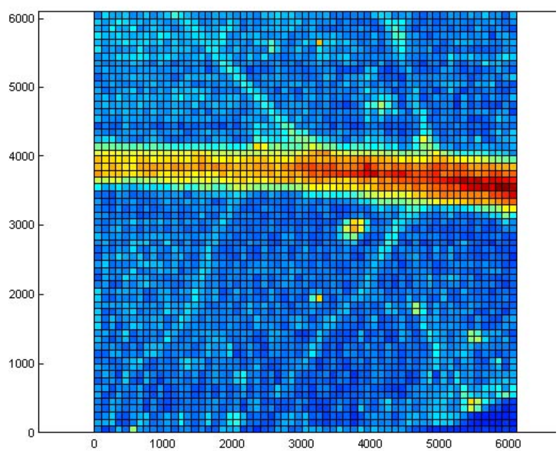

Cu

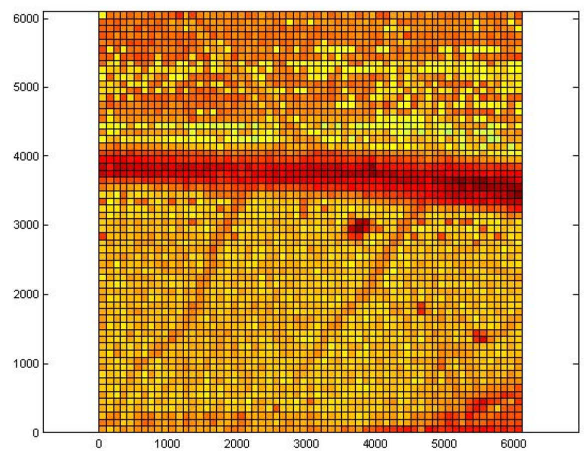

Scanned area 6x6 mm, 61x61 points, 100µm x 100µm pitch, 0.5s meas time per point, 6 SDD active

Max counts/pixel: K 406 Ca 2386 Mn 1902 Fe 3822 Cu 6874

Leaf ‘radiography’ (detail)

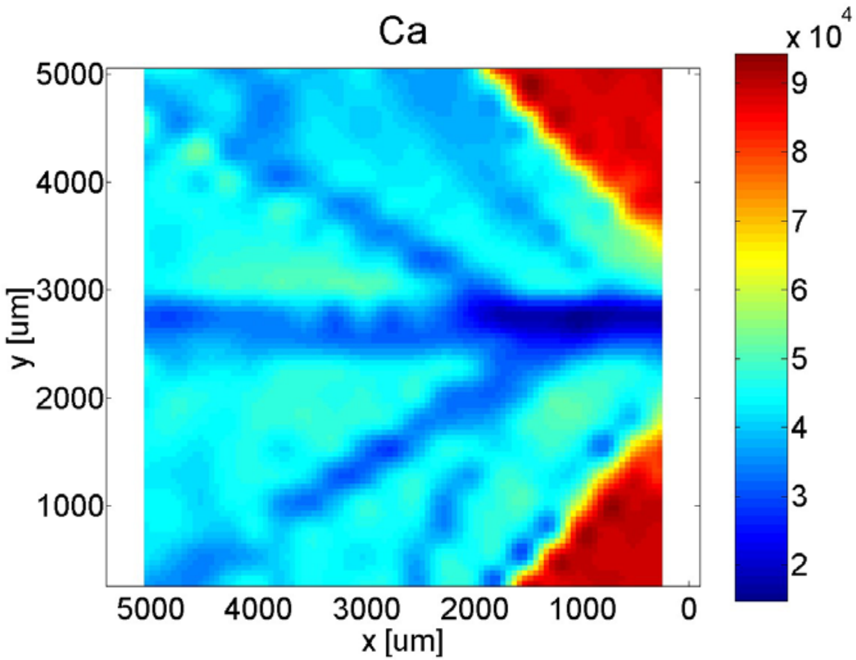

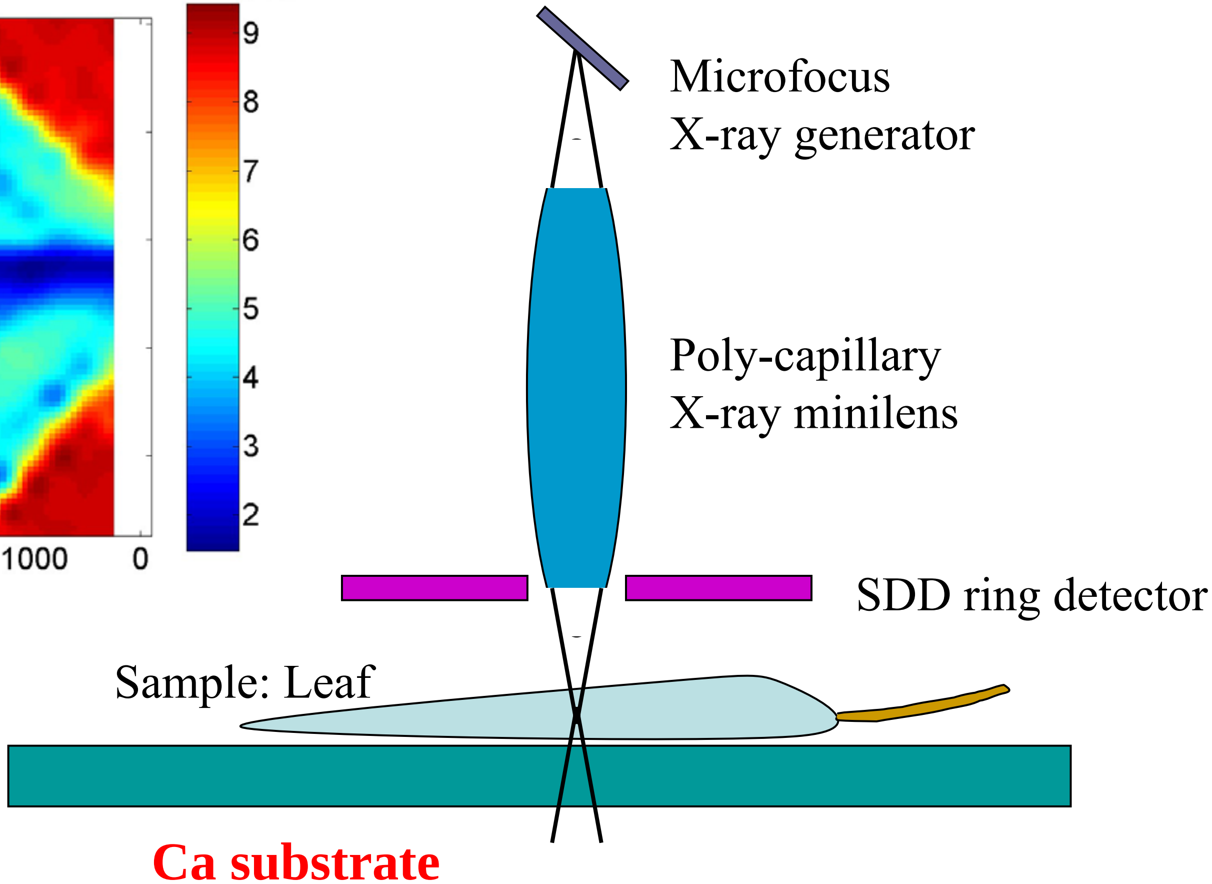

Absorption of Kα Ca line (3.69 keV)

Scan: 21x21points, 250 μm x 250 μm steps, measurement time 1s/point

Technology

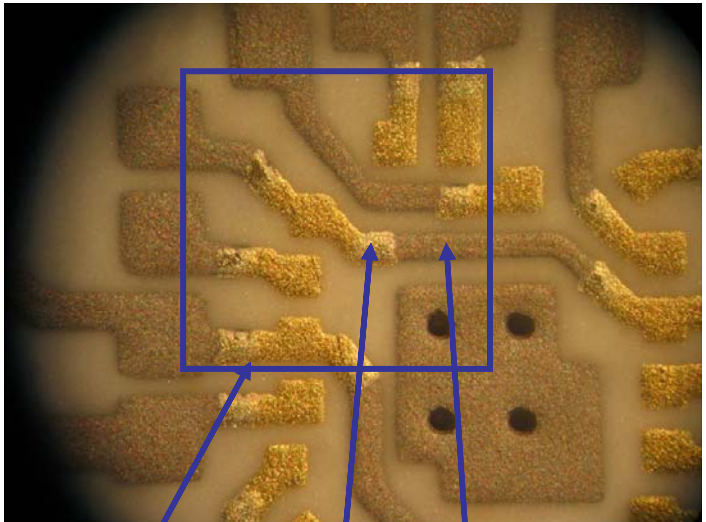

Alumina board for electronic circuits

41x41 sampled points
100x100 μm steps
1 s measurement time per point

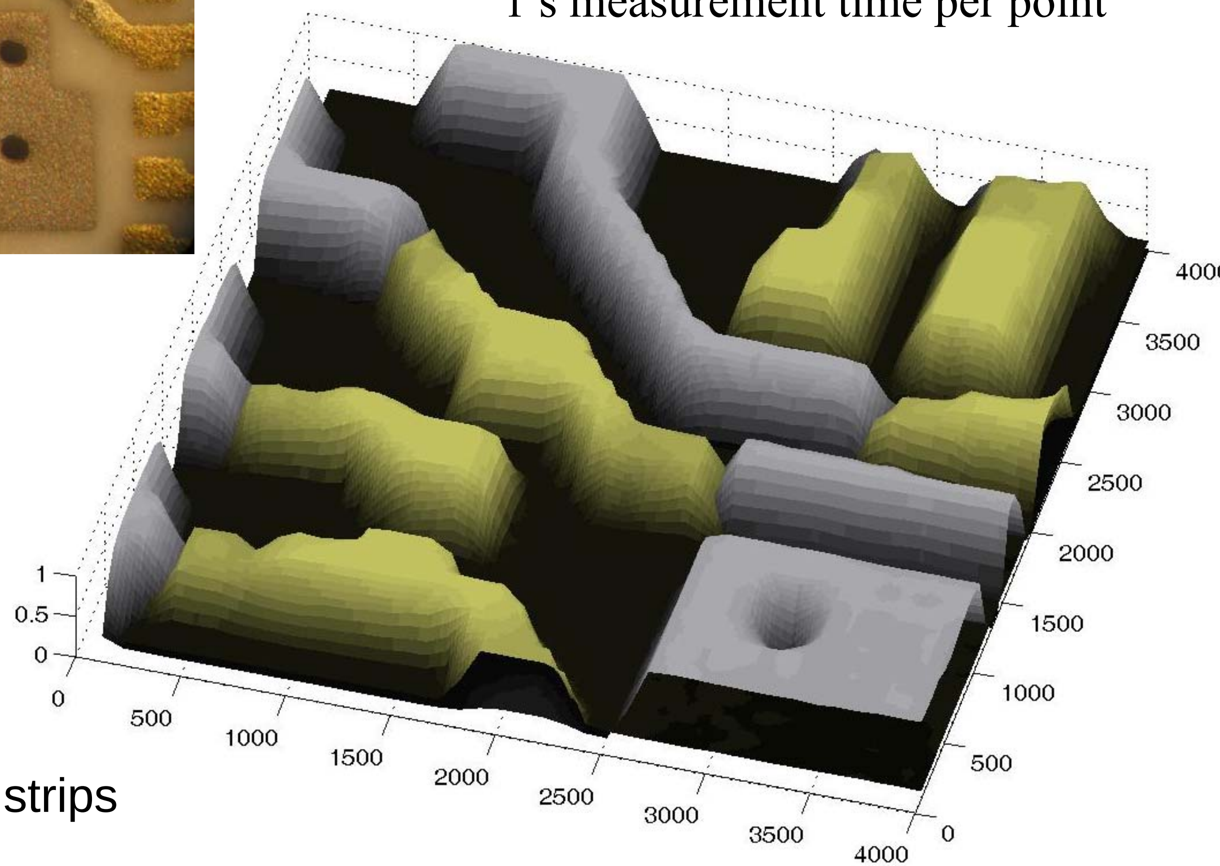

Scanned area
$4x4mm^2$

Gold coating

Silver strips

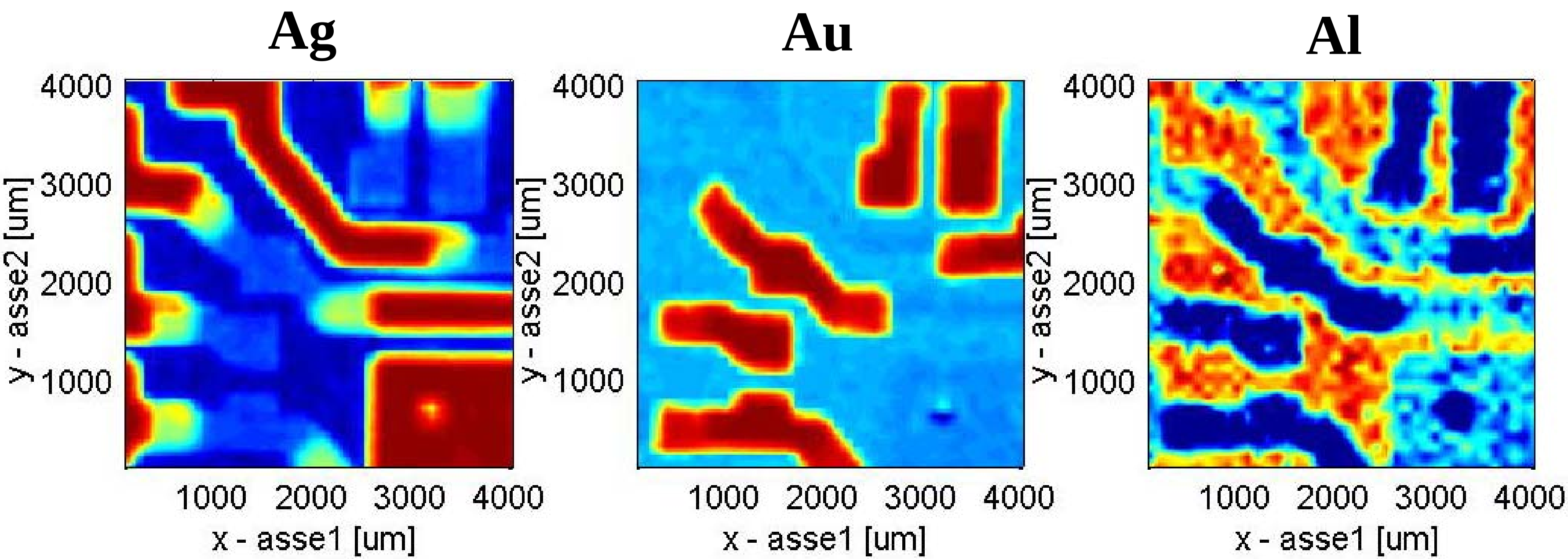
Ag
Au
Al
4000
3000
2000
1000
1000
2000
3000
4000
y - asse2 [um]
x - asse1 [um]

The Gamma ray imaging detectors

SDD arrays coupled with a scintillator crystal

Development of a small Anger Camera for high position resolution γ-ray imaging

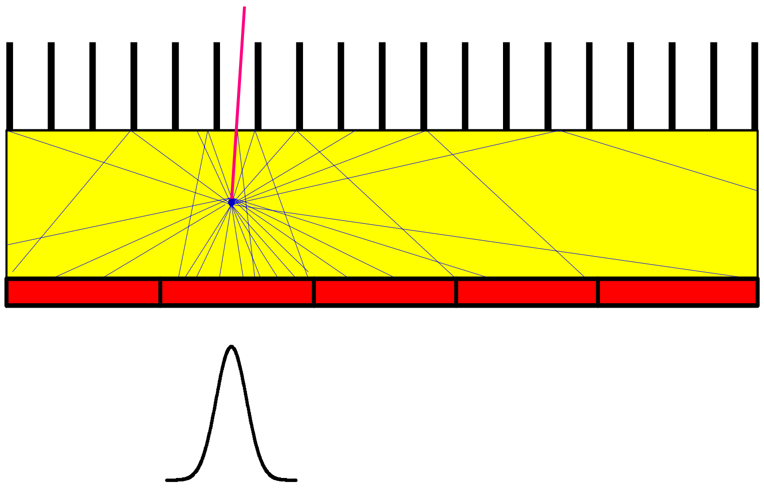

Applications in Medical Imaging:

- compact diagnostic systems for human imaging (thyroid gland diagnostic, brain imaging, breast imaging..)

- small animal imaging systems with < 0.5 mm position resolution

The first prototype of SDD - CsI(Tl) Anger camera

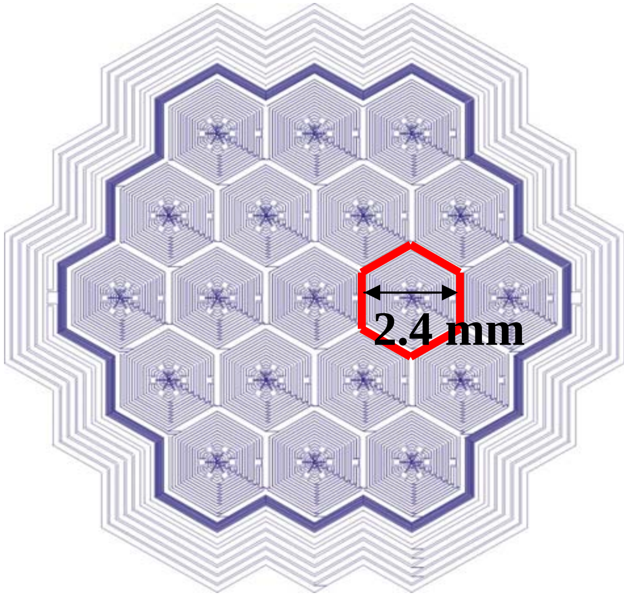

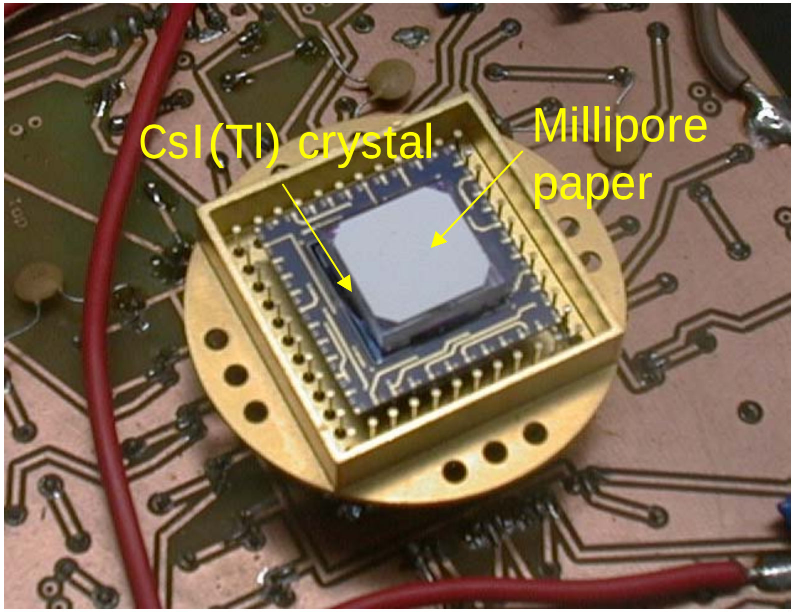

Total area = 5 mm^2×19 ~ 1cm^2

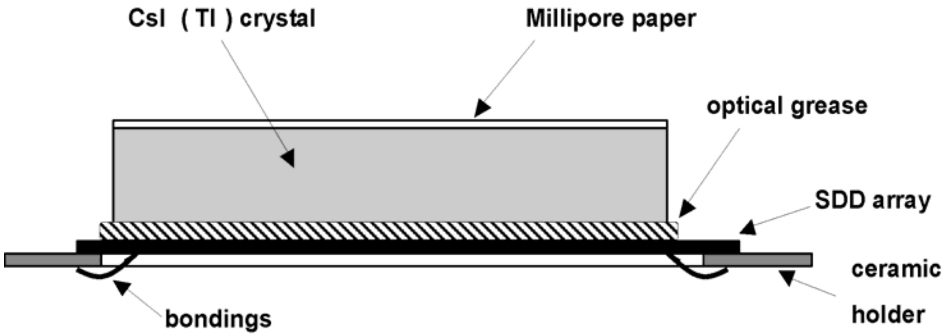

CsI(Tl) thickness = 3 mm

T = -10°C

E = 122 keV (^{57}Co)

C.Fiorini, et al., *Nucl. Instr. Meth.*, Vol. A512, 2003.

SDD - CsI(Tl) Anger camera: final results

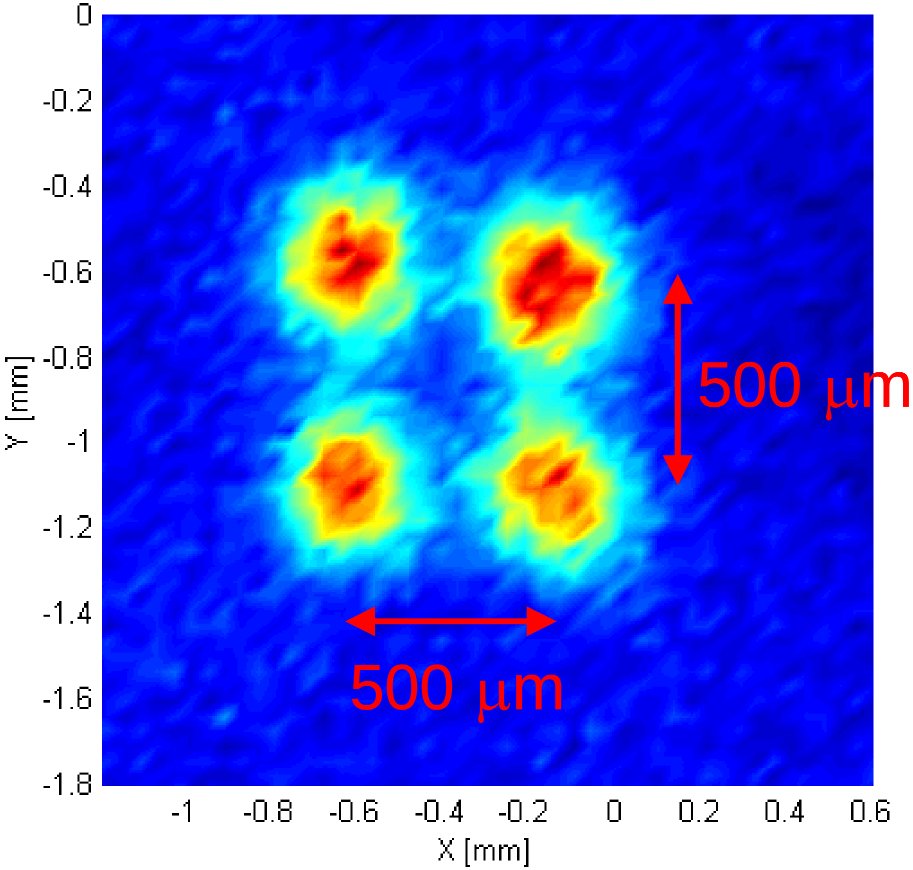

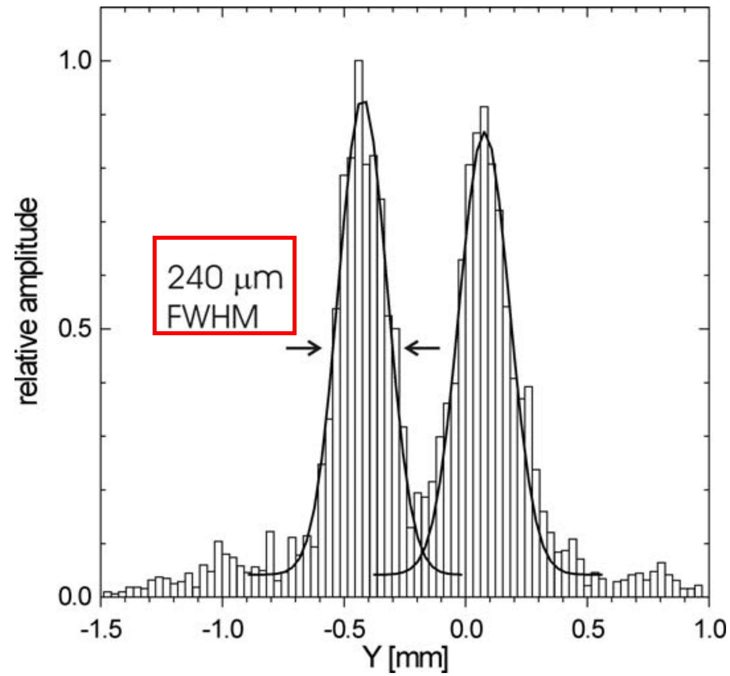

⇒ intrinsic resolution ~ 160 μm

E=122keV (^{57}Co)

ø $_{collimator}$ ~ 180 μm

⇒ factor 10 better than conventional Anger Cameras

^{57}Co position scan

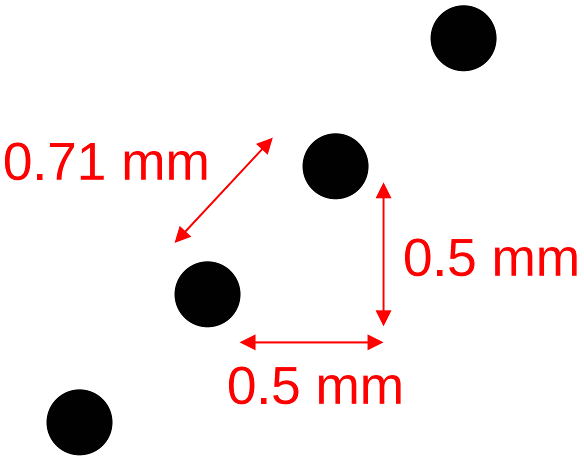

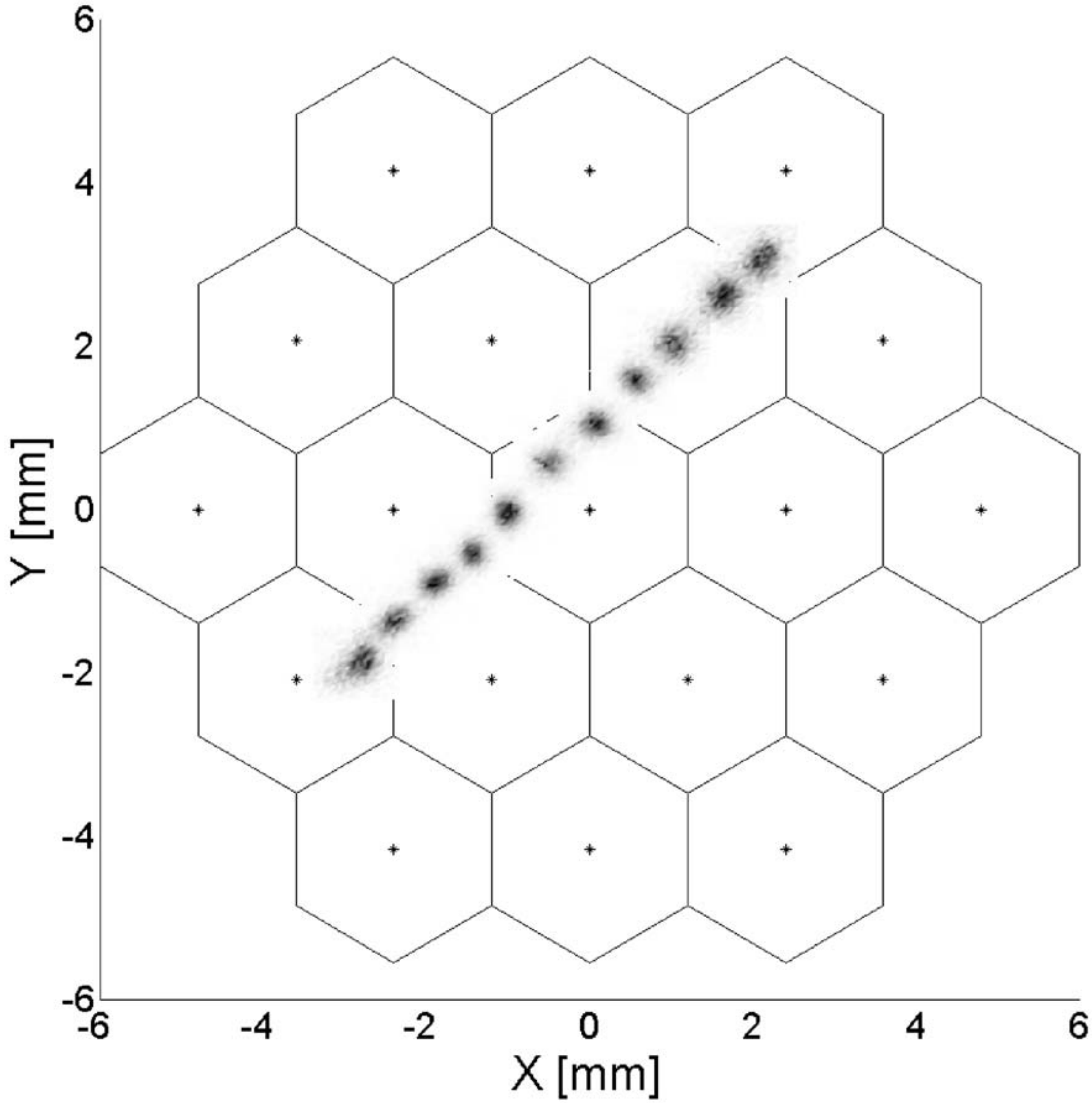

γ-ray Imaging

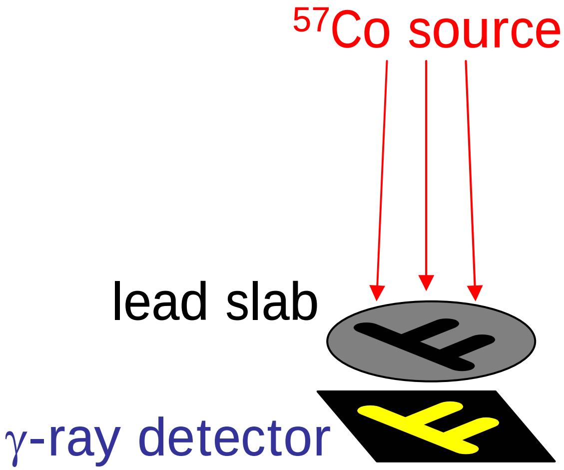

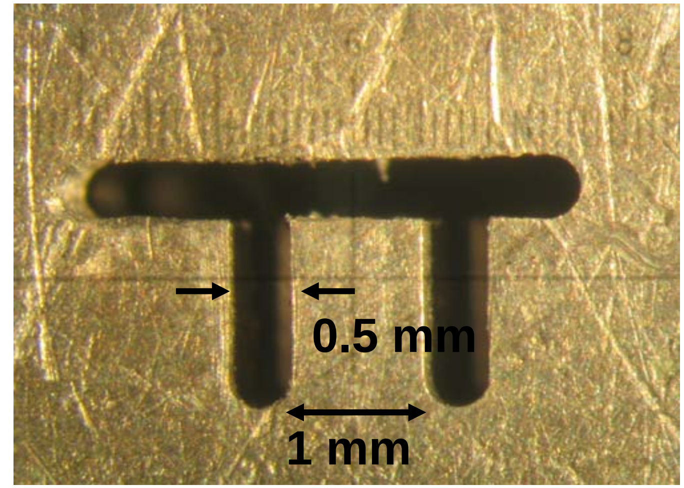

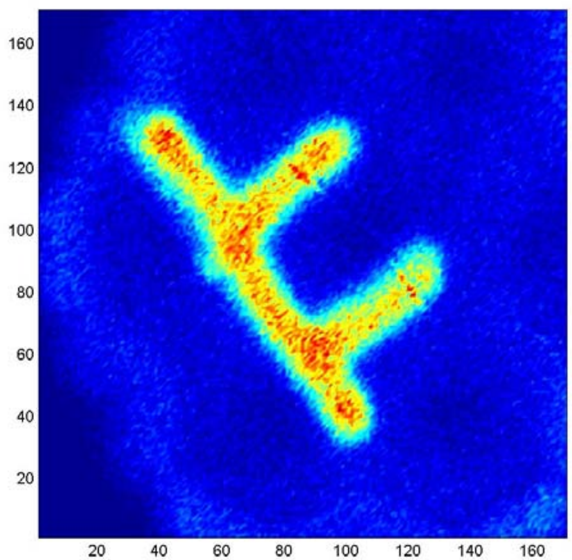

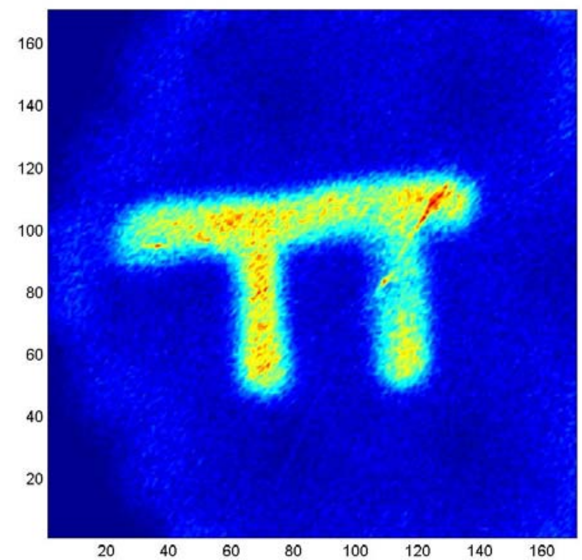

The monolithic array of 77 SDDs: front side

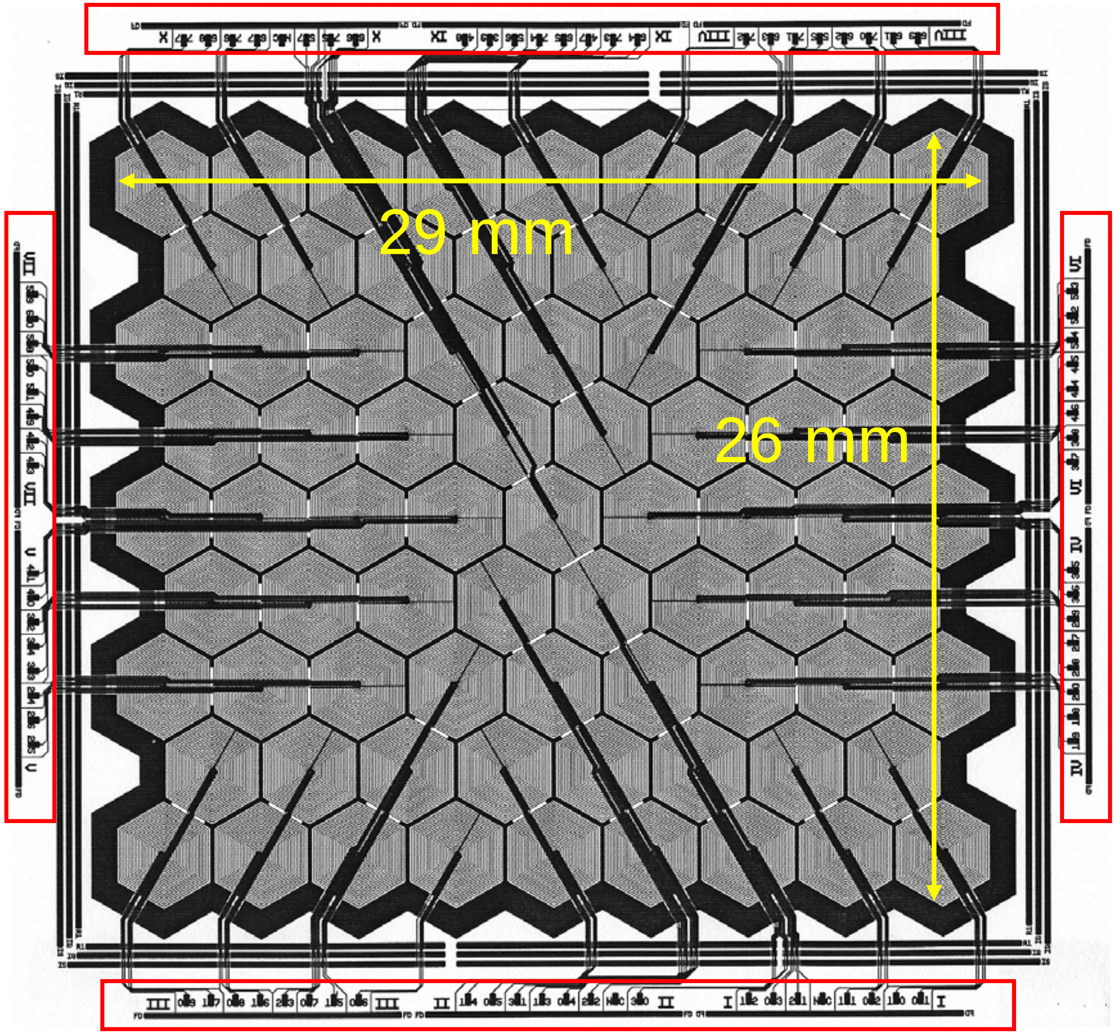

- 77 units, 8.7 mm^2 each

$\Rightarrow$ active area = 6.7 cm^2

- active area: 29 $\times$ 26 mm^2
- two interconnection layers available (polysilicon, Al)
- output pads for bias/signals placed outside the active area

Detector back side

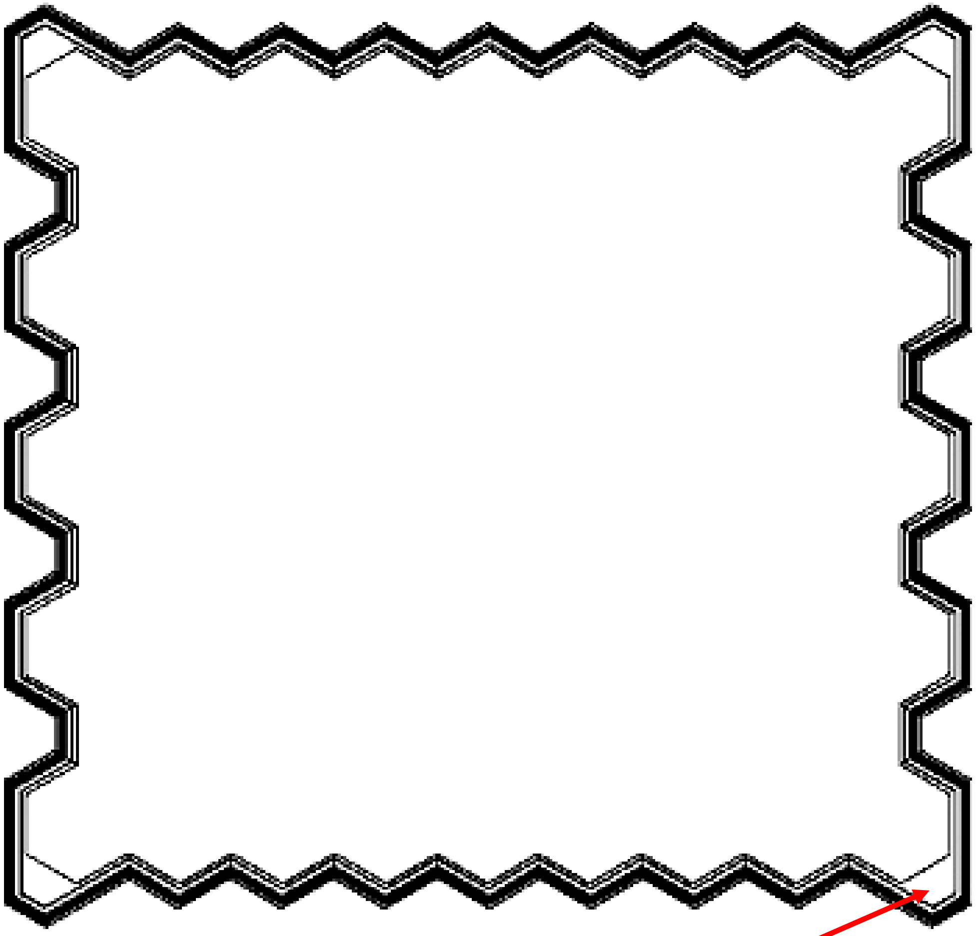

bonding pads

Anti-reflective coatings implemented
Expected QE > 80%

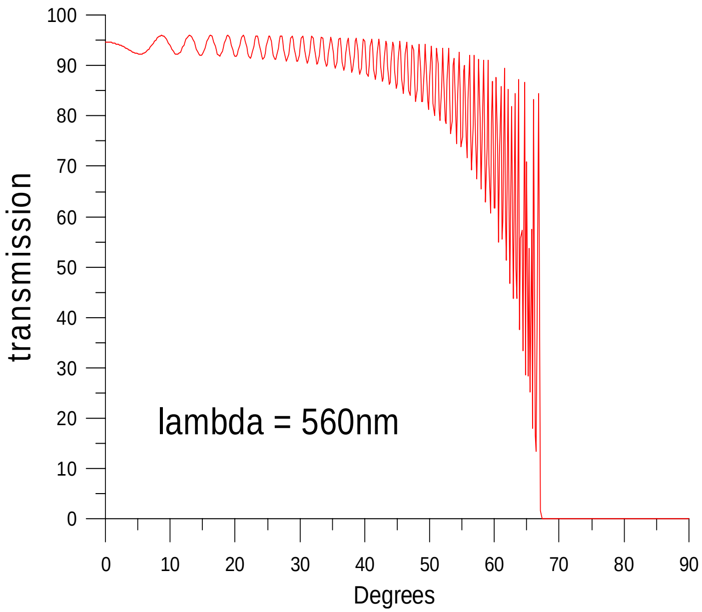

Preliminary caracterization of the whole array:
^{55}Fe spectra measured with bias optimized for each unit

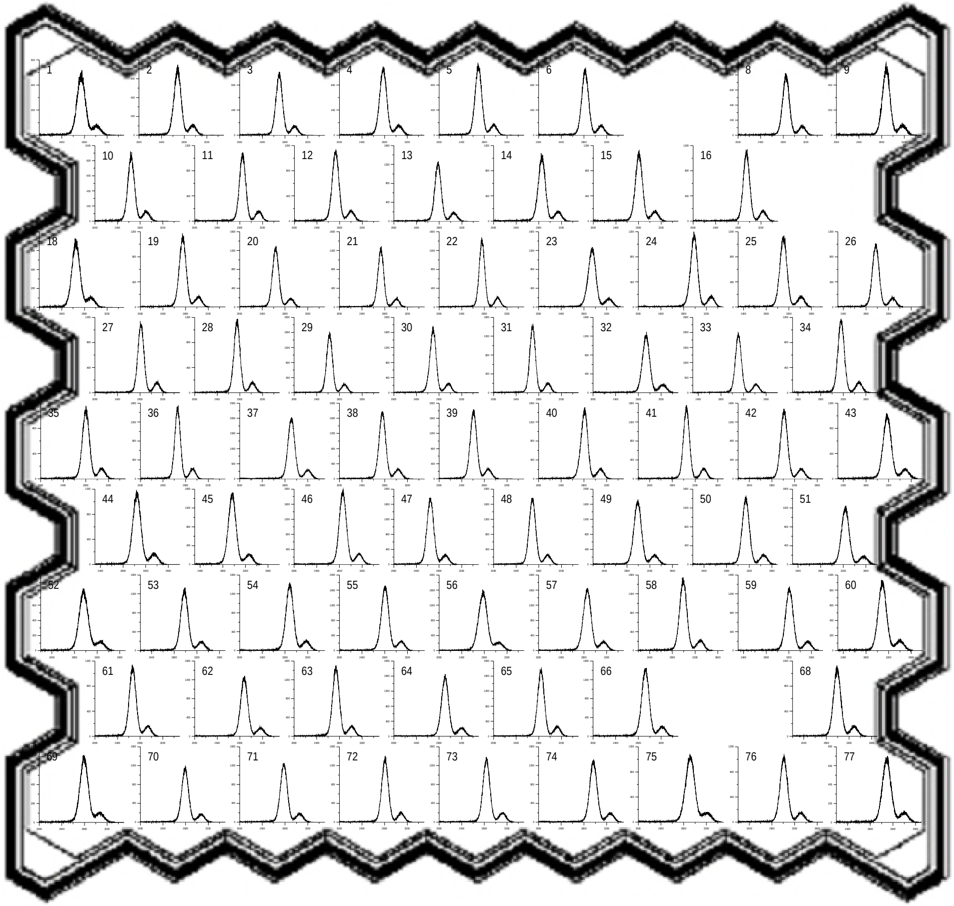

room T

$\tau_{shaping}$ = 0.25μs

V_{BACK} optimized for each unit: -76V ÷ -94V

(alternatively R#1 can be optimized for each unit, with the same results)

noise is good and uniform among all units

(3 units are not working)

The DRAGO project *

(DRift detector Array-based Gamma camera for Oncology)

Purpose:
development of a compact Anger Camera for γ-ray imaging with sub-millimeter resolution

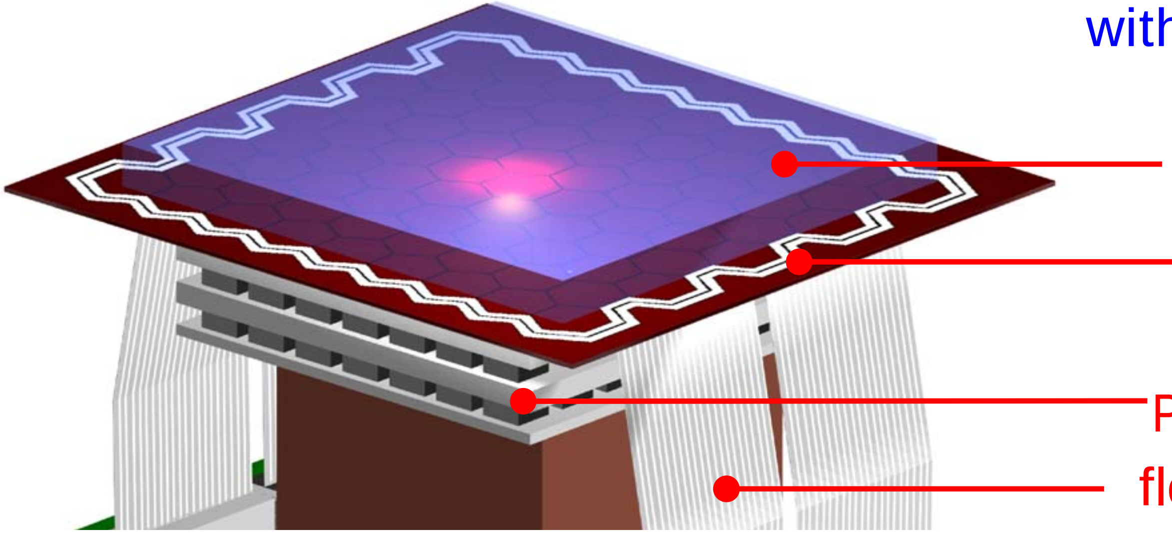

* Project INFN Gr.5 2003-05

The large-area SDDs

SDD 1cm^2 x 3 for the experiment SIDDHARTA

INFN – EU 6° program

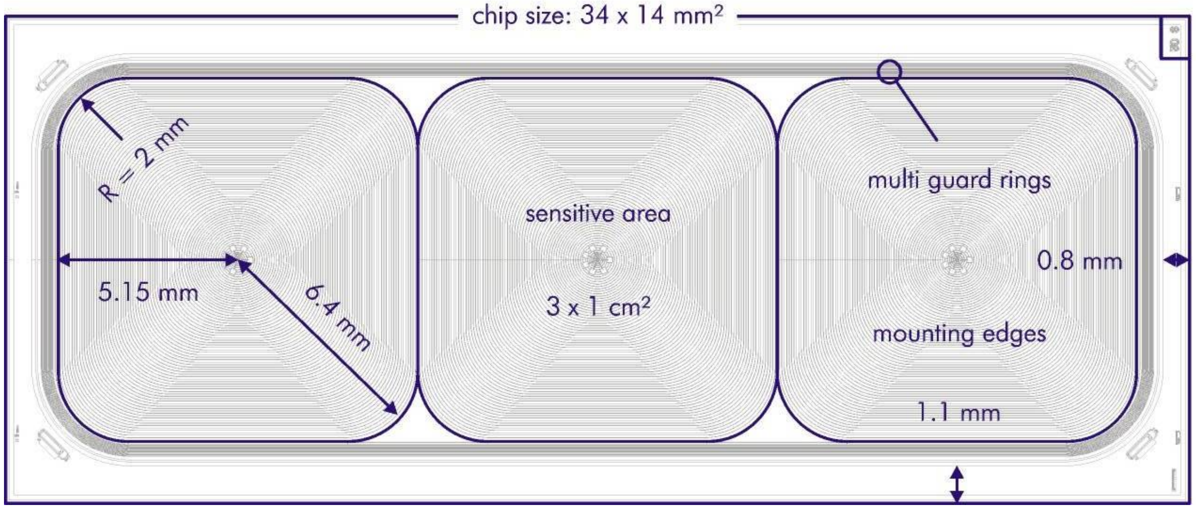

Structured side

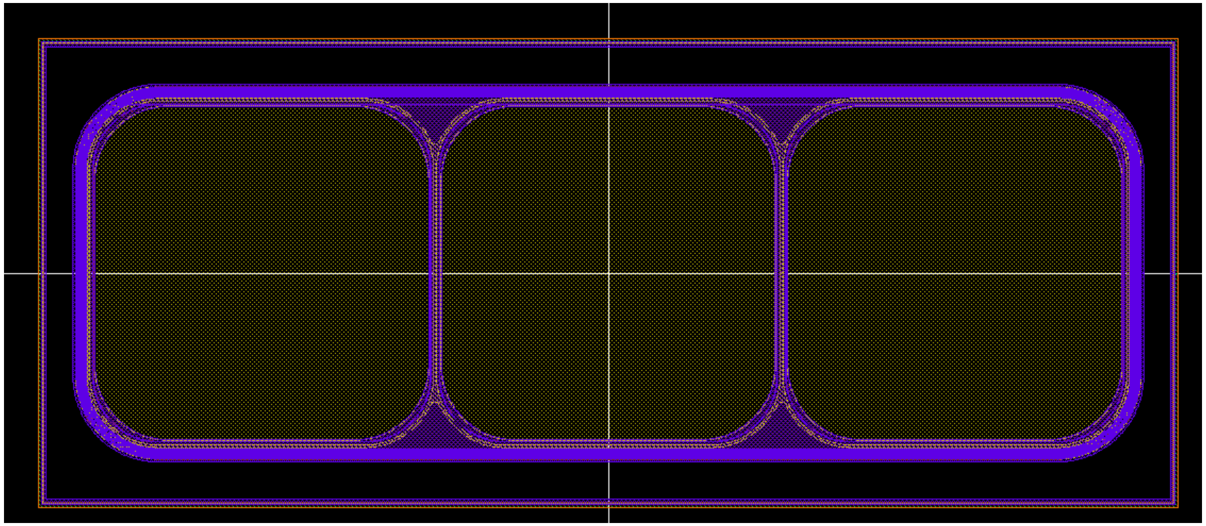

Radiation entrance window

Unstructured side

horizontal/vertical centerline

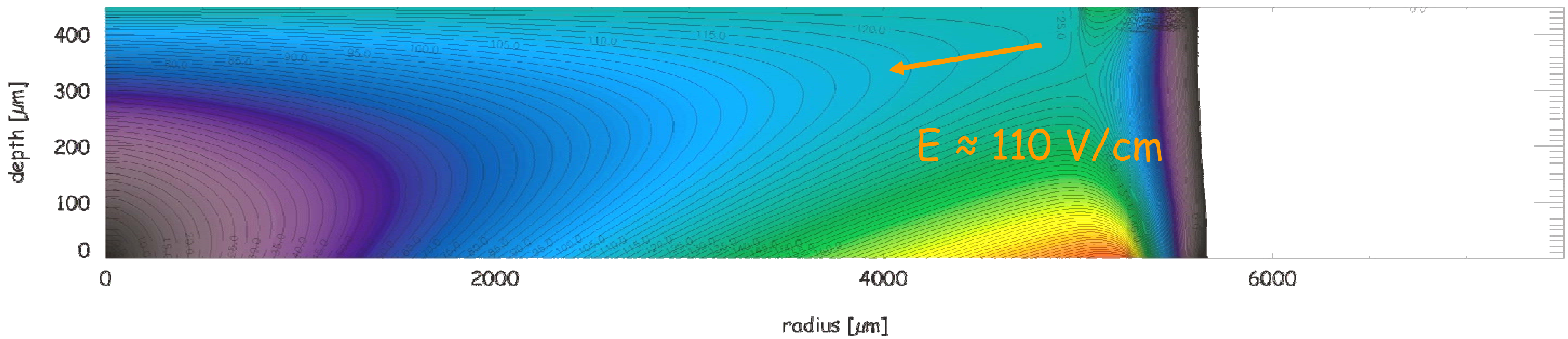

diagonal

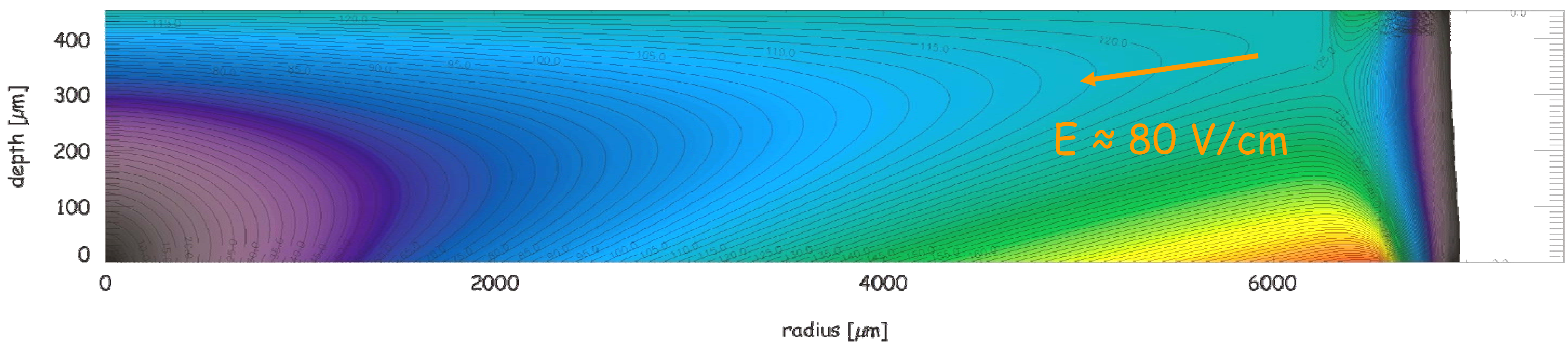

Detector Setup

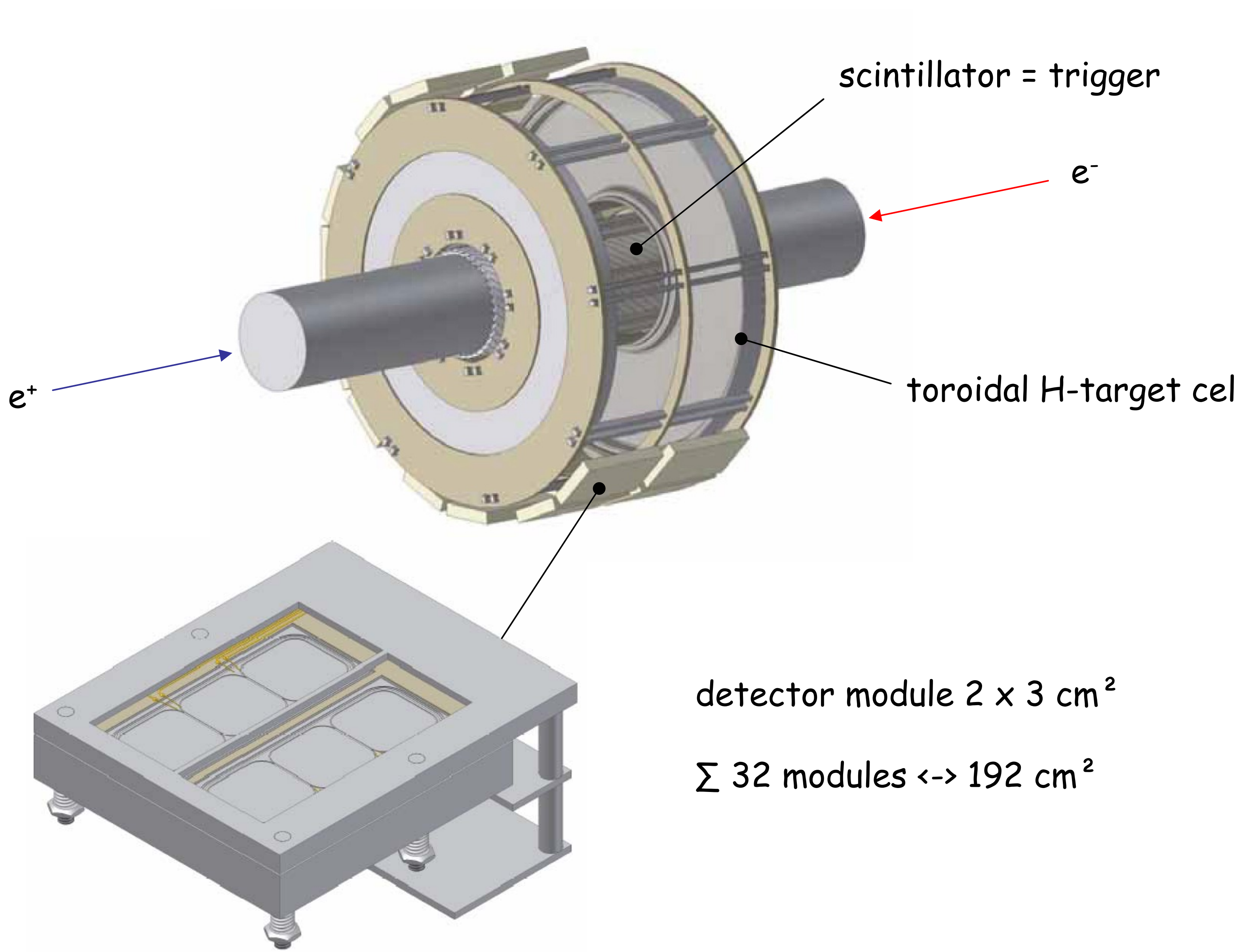

detector module 2 x 3 cm^2

∑ 32 modules <-> 192 cm^2

Conclusions

The Dectors here presented are today the best results of the “nearly old” idea of the the SDDs (E. Gatti and P. Rehak, 1983).

SDDs (under different commercial names) are nowadays widely used in several applications (SEMs, Synchrotrons, Portable XRF spectrometers, Mars exploration, …).
Other devices derived from the original idea of Gatti and Rehak, the “fully depleted” PN-CCDs, are flying in a satellite for X-ray astronomy (XMM mission).
New devices, similarly derived from the original idea, are on the way: CDDs, DEPMOS pixel arrays, avalanche SDDs, ….

The INFN has believed in SDDs and has supported their development, in cooperation with the MPI Halblaiterlabor, from the very beginning of these devices.